UNIVERSITY OF BIRMINGHAM

Investigating the Effect of Perhexiline and FPER-1 in Pulmonary Arterial Hypertension

[redacted]

[redacted]

A thesis submitted to the University of Birmingham for the degree of MSc by Research Cardiovascular Science

Institute of Cardiovascular Sciences
College of Medical and Dental Sciences
University of Birmingham
January 2024

Abstract

Pulmonay arterial hypertension (PAH) is a vascular remodelling disease whereby proliferation of pulmonary artery smooth muscle cells (PASMCs) is increased. The pathophysiology of the disease is not fully understood, but there is a growing body of evidence in the literature that supports the notion that PAH PASMCs exhibit a similar metabolic phenotype to that of cancer cells. Previous studies have shown that PAH PASMCs reprogram their energy metabolism to utilise glycolysis over oxidative phosphorylation for ATP production due to a reduction in pyruvate dehydrogenase (PDH) activity. In the present study, we hypothesised that by increasing PDH activity, perhexiline and the novel fluorinated perhexiline (FPER-1), both carnitine palmitoyltransferase 1 (CPT1) inhibitors, would restore PDH flux and hence increase oxidative phosphorylation, and attenuate PASMCs proliferation. Utilising cultured PASMCs from healthy and PAH patient donors, we showed that perhexiline and FPER-1 effectively attenuates the increased rate of proliferation of PASMCs from PAH donors, whilst maintaining cell viability. We futher propose a novel mechanism of action of perhexiline/FPER-1 in PAH PASMCs whereby both perhexiline and FPER-1 reduces PAH PASMC proliferation by suppressing the activation of the AKT pathway (reduced phosphorylation of AKT^{ser473}) and activating PDH (dephosphorylation of PDH-E1α ^{ser293}). Our findings demonstrate that both perhexiline and FPER-1 show promise as a novel therapeutic agent for reversing the increased PASMC proliferation apparent in PAH, but additional studies regarding the safety of FPER-1 as a therapy are required.

Acknowledgements

I would like to thank both Professor Melanie Madhani and Dr Kayleigh Griffiths, for all the help and guidance throughout this project, both during my time in the lab and also during my time writing up. I have learned so much during my time with the research group, both laboratory and academic writing skills and I am grateful for the opportunity to have been part of the research group. I would also like to thank Professor Nicholas Morrell (University of Cambridge) for kindly providing us with the PASMCs used in this project and Dr Iain Grieg (Aberdeen University) for synthesing FPER-1. Finally, I would like to thank my friends and family for supporting me throughout the project.

Manuscript

This work is part of a paper which is currently under review at the Vascular Pharmacology. The reference is as follows:

Fluorinated Perhexiline Derivative Attenuates Vascular Proliferation in Pulmonary Arterial Hypertension Smooth Muscle Cells. Kayleigh Griffiths, Roger J Grand, Ian Horan, Michelangelo Certo, **Ross C Keeler**, Claudio Mauro, Chih-Chung Tseng, Iain Grieg,Nicholas W Morrell, Matteo Zanda, Michael P Frenneaux, Melanie Madhani. *Manuscript currently re-submitted to Vascular Pharmacology*.

Contents

Tables and Figures

Abbreviations

^{18}FDG	Fluorine-18–labeled 2-fluoro-2-deoxyglucose
α-KG	α-ketoglutarate
ADP	Adenosine diphosphate
AKT	Protein kinase B
ALK1	Activin-like kinase-type I
APS	Ammonium persulfate
ATP	Adenosine triphosphate
BCAA	Branched chain amino acid
BCATs	Branched-chain amino acid transaminases
BCKAs	Branched-chain α-keto acids
BCKDH	Branched-chain α-keto acid dehydrogenase
BDH1	D-β-hydroxybutyrate dehydrogenase
BMPR2	Bone morphogenetic protein receptor 2
BSA	Bovine serum albumin
cAMP	Cyclic adenosine monophosphate
CAPE	Caffeic acid phenethyl ester
cGMP	Cyclic guanosine monophosphate
CPT1	Carnitine palmitoyltransferase 1
CYP2D6	Cytochrome P450 2D6
DAG	Diacylglycerol
DCA	Dichloroacetate
ECL	Enhanced chemiluminescence
ENG	Endoglin
eNOS	Endothelial nitric oxide synthase
ERA	Endothelin-receptor antagonist
ERK	Extracellular-signal regulated kinase
ET	Endothelin
$FADH_2$	Flavin adenine dinucleotide
FAO	Fatty acid oxidation
FAS	Fatty acid synthase
FPER-1	Fluorinated derivative of perhexilline
GLUT1	Glucose transporter 1
GTP	Guanosine triphosphate
HIF-1α	Hypoxia Inducible Factor 1 subunit α
HIV	Human immunodeficiency virus
HK-2	Hexokinase-2
HMGB1	High-mobility group box-1
HPV	Hypoxic pulmonary constriction
IP_3	Inositol trisphosphate
LATs	L-type amino acid transporters
LCFA	Long chain fatty acid
LDH	Lactate dehydrogenase

MCD	Malonyl-CoA decarboxylase
MCT	Monocrotaline
MELAS	Mitochondrial myopathy, encephalopathy, lactic acidosis, and stroke-like episodes
MLCK	Myosin light chain kinase
mmHg	Millimetres of mecury
mPAP	Mean pulmonary arterial pressure
NADH	Nicotinamide adenine dinucleotide
NO	Nitric oxide
NOS	Nitric oxide synthase
NYHA	New York heart association
PAEC	Pulmonary arterial endothelial cell
PAfib	Pulmonary arterial fibroblast
PAH	Pulmonary arterial hypertension
PASMC	Pulmonary arterial smooth muscle cell
PAWP	Pulmonary arterial wedge pressure
PDE5	Phosphodiesterase type 5
PDGF	Platelet-derived growth factor
PDH	Pyruvate dehydrogenase
PDK1	Pyruvate dehydrogenase kinase 1
PET	Positron emission tomography
PFK-1	6-phosphofructo-1-kinase
PHX	Perhexiline
Pi	Inorganic phosphate
PI3K	Phosphoinositide 3-Kinase
PIP_2	Phosphatidylinositol 4,5-bisphosphate
PKA	Protein kinase A
PKC	Protein kinase C
PKG	Protein kinase G
PLC	Phospholipase C
PVDF	Polyvinylidene fluoride
PVR	Pulmonary vascular resistance
RVSP	Right ventricular systolic pressure
SCOT	Succinyl-CoA:3-oxoacid-CoA transferase
SDS	Sodium dodecyl-sulfate
sGC	Soluble guanylate cyclase
SNPs	Single-nucleotide polymorphisms
TCA	Tricarboxylic acid cycle
TEMED	Tetramethyl ethylenediamine
TX_{a2}	Thromboxane
UCP2	Uncoupling protein 2
VSMC	Vascular smooth muscle
WHO	World health organisation

1. Introduction

1.1. Pulmonary Arterial Hypertension

1.1.1. What is PAH?

Pulmonary arterial hypertension (PAH) is a rare, complex disease which is characterised by elevated pulmonary arterial pressure (PAP) and pulmonary vascular resistance (PVR) due to pulmonary arterial smooth muscle cell (PASMC) proliferation and vascular remodelling (1). PAH is defined as an elevation in mean pulmonary arterial pressure (mPAP) above 20mmHg, a pulmonary artery wedge pressure (PAWP) of less than 15mmHg, and a PVR of more than 3 Wood units (2). Increased PAP and PVR leads to increased right ventricular afterload, leading to right ventricular hypertrophy, which reduces right ventricular function, resulting in right ventricular failure and death (3). Symptoms of PAH include breathlessness, fatigue, angina, heart palpitations and oedema in the legs, ankles, feet, and/or abdomen (4).

According to the British Heart Foundation, PAH affects between 10 and 57 people per million worldwide (5). Interestingly, PAH has a higher prevalence in females than in males (6). In a recent retrospective database study of 2527 PAH patients in England, it was reported that between 2013 and 2017 the economic burden of PAH on the NHS was £43.2M (7).

1.1.2. Pathogenesis of PAH

PAH patients are split into the following subtypes of PAH: (i) idiopathic, (ii) heritable, (iii) drug and toxin-induced and (iv) associated with other conditions (8).

i) **Idiopathic PAH** is a subtype of PAH, which is not associated with other diseases, genetic mutations or exposure to drugs or toxins. However, the patients still present with the haemodynamic criteria for PAH mentioned previously (2).

ii) **Heritable PAH** is usually caused by mutations in the bone morphogenetic protein receptor 2 (BMPR2) gene, with BMPR2 identified as the gene responsible for almost 75% of heritable PAH cases (9–12). However, mutations in other members of the transforming growth factor-beta family such as activin-like kinase-type I (ALK1) and Endoglin (ENG), have also been associated with heritable PAH, although they are less common (13,14).

iii) **Drug and toxin-induced PAH** is associated with the exposure to certain drugs and toxins such as methamphetamine, dasatinib or fenfluramine (2). Between 2003 and 2015, Zamanian et al (15) performed a prospective cohort study of patients with methamphetamine-associated PAH and idiopathic PAH to investigate how the clinical phenotype and long-term outcomes between the two patient groups compared. It was found that patients with

methamphetamine-associated PAH had a worse prognosis compared to patients with idiopathic PAH (15).

iv) **PAH associated with other conditions** is another subset of PAH that is linked with another condition or disease such as connective tissue disease, HIV, portal hypertension, congenital heart disease and schistosomiasis (16).

Connective Tissue Disease-associated PAH

The most common connective tissue disease associated with PAH is scleroderma, with PAH affecting 8-14% of scleroderma patients (17,18). However, other connective diseases such as systemic lupus erythematosus, mixed connective tissue disease, sjorgen syndrome and rheumatoid arthritis are also associated with PAH (6,19,20).

HIV-associated PAH

PAH is a comorbidity of HIV characterised by chronic inflammation and dysfunctional fibrosis (3). A prospective study performed in HIV-positive adults found that HIV-associated PAH had a prevalence of 0.46%, with 35 PAH cases out of 7648 HIV-positive patients, compared with around 10 cases per million in a HIV-negative population (21).

Portal Hypertension-associated PAH

Portal hypertension due to portal vein thrombosis, cirrhosis, periportal fibrosis without cirrhosis or hepatic vein sclerosis are associated with the development of PAH, with portal hypertension due to cirrhosis having the worst prognosis (22). The link between portal hypertension and PAH is not fully understood, however in a prospective study assessing patients who had undergone a liver transplant, 5% of the patients were diagnosed with portal hypertension-associated PAH (23).

Congenital Heart Disease-associated PAH

Congenital heart disease is the name of a range of heart defects that are present since birth. There are 4 sub-groups of congenital heart disease-associated PAH: Eisenmenger syndrome, PAH with small cardiac defects (small atrial or ventricular septum defects), PAH associated with systemic-to-pulmonary shunts and PAH after cardiac defect correction (24). In patients with congenital heart disease-associated PAH, 10-year survival rates were 89% for those with Eisenmenger syndrome, 93% for those with systemic-to-pulmonary shunts, 88% for those with small cardiac defects and 65% for those with cardiac defect correction compared to 46% in those with idiopathic PAH. Therefore the prognosis of patients diagnosed with congenital heart disease-associated PAH is more favourable (25).

Schistosomiasis-associated PAH

Schistosomiasis is an infection that damages the bladder, kidneys and liver and is caused by a parasitic worm found in fresh water in tropical regions such as Africa, the Caribbean and parts of Asia (26). Schistosomiasis is more common in countries living in poverty due to socio-economic factors hindering the use of successful prevention and treatment strategies (27). In countries where schistosomiasis is common, schistosomiasis-associated PAH is the main cause of PAH with 5-8% of patients with severe schistosomal liver disease developing schistosomiasis-associated PAH (28).

1.1.3. The Physiology of the Pulmonary Circulation

The healthy lung contains several blood vessels which make up the pulmonary circulation to aid efficient gas exchange of the blood supplied from the right hand side of the heart, including the pulmonary arteries. The pulmonary arteries carry deoxygenated blood, pumped by the right ventricle, to the lungs for gas exchange (29). The pulmonary arteries progressively divide into smaller vessels and eventually into the capillaries that surround the alveoli, the site of gas exchange (29). The well-being of the pulmonary circulation can be assessed by measuring the mPAP, PAWP and PVR. Where these assessemnts are measured is depicted in Figure 1.1. mPAP is a measure of the blood pressure within the main pulmonary artery and normal mPAP at rest is defined as 14±3 mmHg (30). PAWP is used to measure left atrial pressure and normal PAWP is between 4-12 mmHg (31). PVR is the resistance against the blood flowing through the pulmonary vasculature towards the left atrium and normal PVR is between 0.25-1.6 Wood units (32).

Within the healthy pulmonary circulation, there is a unique phenomenom named hypoxic pulmonary vasoconstriction (HPV) which describes the constriction of the pulmonary arteries in response to alveolar hypoxia to divert blood to better-oxygenated areas of the lung (33). The mitochondria within the PASMCs are thought to be the oxygen sensors that initiate HPV and induce contraction of the PASMC and therefore the pulmonary arteries in response to hypoxia in healthy individuals (34,35). HPV is unique to the pulmonary circulation since the physiological response to hypoxia in the systemic circulation is vasodilation.

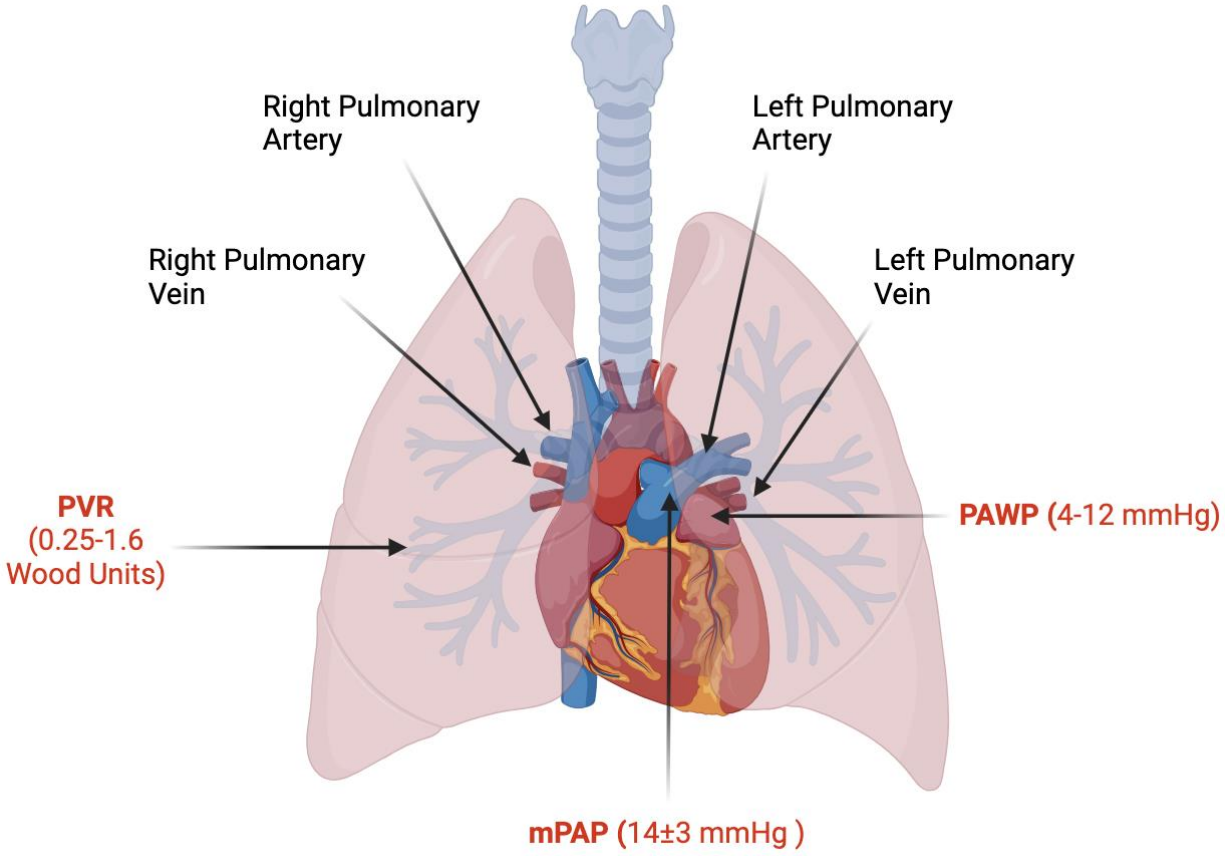

Figure 1.1. A basic illustration of the physiology of the healthy pulmonary circulation. The illustration depicts the physiology of the healthy pulmonary circulation and what PVR, mPAP and PAWP measure. The normal ranges of each assessment of the pulmonary circulation are shown in brackets. PVR measures the resistance against the blood flowing through the pulmonary vasculature. mPAP measures the blood pressure within the main pulmonary artery. PAWP measures left atrial pressure. PVR= pulmonary vascular resistance, mPAP= mean pulmonary arterial pressure, PAWP= pulmonary arterial wedge pressure. This figure was created by using Biorender.com.

1.1.4. The Pathophysiology of PAH

The pulmonary arterial wall is made up of three layers: the intima, media, and adventitia (Figure 1.2). The intima is the inner-most layer and is made up primarily of pulmonary artery endothelial cells (PAECs). The media is the middle layer, which is made up primarily of PASMCs, whilst the adventitia is the outer-most layer and is made up predominantly of pulmonary artery fibroblasts (PAfib). During PAH, there is PAEC dysfunction, increased PASMC proliferation and resistance to apoptosis, thus leading to medial hyperplasia and hypertrophy (Figure 1.2) (36). There is also fibrosis in the adventitia due to increased PAfib proliferation and increased collagen production (Figure 1.2) (36). This vascular remodelling contributes to the increase in PVR and subsequent increase in mPAP (16)(Figure 1.2). A study investigating the haemodynamics and the outcomes of PAH patients, found that in a cohort of 308 PAH patients, the average mPAP was 48.9mmHg, around a 34.9mmHg increase compared to the healthy average mPAP (2,37). In the early stages of PAH, the right ventricle compensates for the increased afterload caused by the elevation in PVR *via* right ventricular hypertrophy, but as the disease progresses, the right ventricle fails, leading to right ventricular failure and death (38).

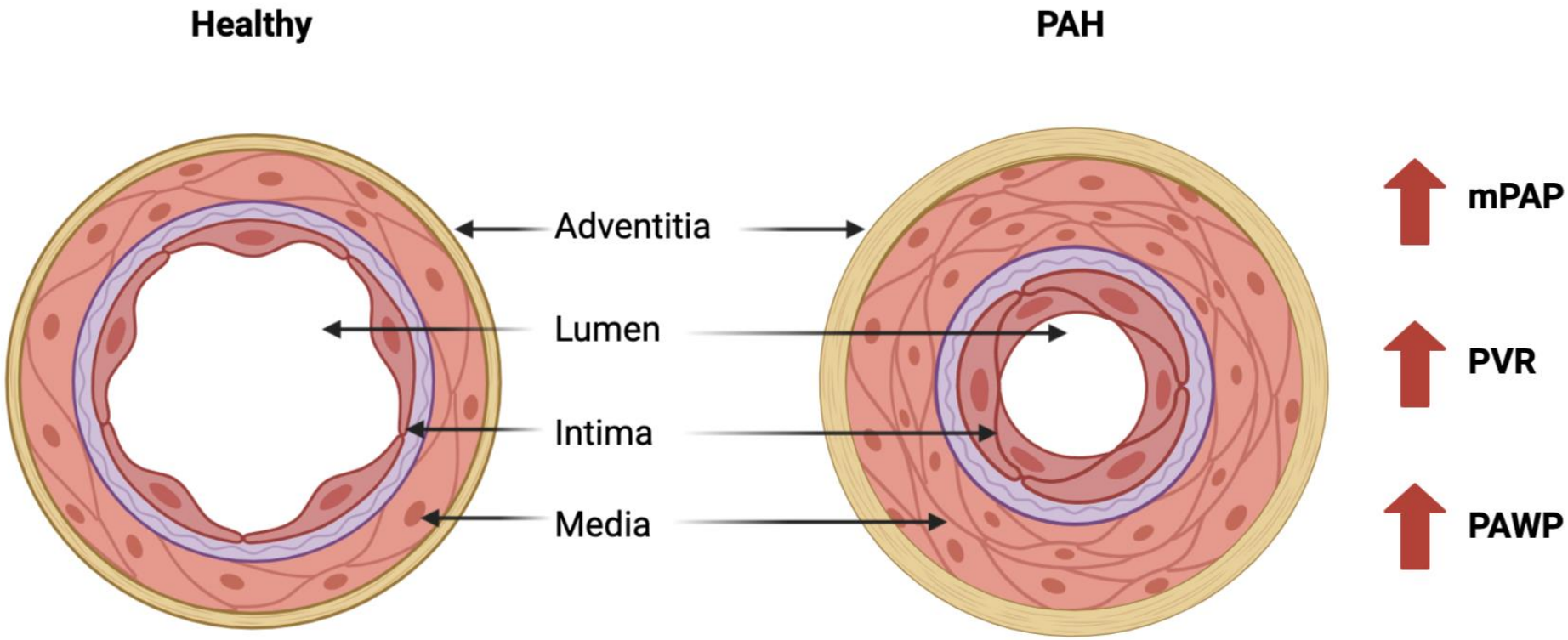

Figure 1.2. An illustration depicting the cross section of a healthy pulmonary artery vs a PAH pulmonary artery. In the PAH vessel, there is PAEC dysfunction, increased proliferation of the PASMCs leading to narrowing of the vessel lumen. There is also fibrosis of the adventitia due to increased proliferation of the PAfib and increased collagen production. The vascular remodelling results in increases in mean pulmonary arterila pressure (mPAP), pulmonary vascular resistance (PVR) and pulmonary arterial wedge pressure (PAWP). This figure was created using Biorender.com.

1.2. Current Treatments for PAH

Unfortunately, there is no known cure for PAH, as such current treatment options only alleviate symptoms and manage the condition, these include diuretics, anticoagulants and oxygen treatment (38,39). Addionally, pharmacological therapies are available that target three main pathways, these include the nitric oxide (NO)-cyclic guanosine monophosphate (cGMP) pathway, the endothelin (ET) receptors ET_A and ET_B and prostacyclin signalling (39,41). These therapies aim to inhibit vasoconstriction and induce vasodilation to reduce the feeling of breathlessness.

1.2.1. Targeting the NO-cGMP pathway to treat PAH

NO is an endogenously produced gas that acts as a signalling molecule in multiple physiological processes such as vasorelaxation, angiogenesis, vascular permeability, hormone secretion and wound healing (42). Nitric oxide synthases (NOS) are a family of enzymes that catalyse the production of NO from L-arginine. Under physiological conditions, NO binds to soluble guanylate cyclase (sGC), which results in the production of cGMP from guanosine triphosphate (GTP). cGMP activates protein kinase G (PKG) which initiates relaxation of the vascular smooth muscle cells (VSMC). Thus, the NO-cGMP pathway can be targeted to induce vasodilation to treat PAH (43–45). The two types of drugs that are used to target the NO-cGMP pathway to treat PAH are phosphodiesterase type 5 (PDE5) inhibitors, such as sildenafil and tadalafil and sGC stimulators such as riociguat (40).

Lamb and rat models of PAH have been shown to have decreased expression of eNOS and increased expression of PDE5 (46,47). Likewise, PAH patients have been reported to have decreased expression of endothelial NOS (eNOS) (48) and increased expression of PDE5 (49). These findings support the notion of targeting the NO-cGMP pathway to induce vasodilation to treat PAH.

PDE5 is the key enzyme responsible for degredation of cGMP to 5'-GMP (50). However, one way of inceasing cGMP concentration in pulmonary vessels is by inhbiting the activity of PDE5, thus resulting in increased vascular smooth muscle relaxation *via* PKG activation (Figure 1.3) (50). Additionally, sGC stimulators directly activate sGC to produce cGMP, independent of NO, again resulting in increased vascular smooth muscle relaxation *via* PKG activation (3). In fact, clinical trials have investigated the effect of PDE5 inhibtors (sildenafil and tadalafil) on PAH patients (43,44). The first trial demonstrated that sildenafil increased 6-minute walk distance from 45m to 50m and improved World Health Organsiation (WHO) functional class by at least 1 class in 28% to 42% of patients (43). Whilst the second trial reported that tadalafil improved 6-minute walk distance by 31m *vs* placebo (44).

Alternatively, riociguat stabilises NO-sGC binding which sensitises sGC to NO and restores the NO-sGC-cGMP pathway resulting in elevated cGMP (45), followed by vascular smooth muscle relaxation. One study reported the effects of a single PAH patient transitioning from sildenafil treatment to riociguat and found not only was it safe but also clinically beneficial (45). The patient reported increased energy and less breathlessness,

but it was noted that the safety of transitioning from the longer-acting PDE5 inhibitor, tadalafil to riociguat is unknown (45).

1.2.2. Targeting the endothelin receptors to treat PAH

ET is a potent vasconstrictor and mitogenic agent and is thought to play an important role in the vascular remodelling apparent in PAH (51,52). There are three isoforms of ET, ET-1, ET-2 and ET-3. ET-1 is the most common isoform found in the cardiovascular system and is synthesized by ET converting enzymes, mainly in endothelial cells, but VSMCs can also produce ET-1 (53,54). ET-1 acts *via* the ET_A and ET_B receptors, both of which are G-protein coupled receptors and have the same $G_{q/11}$ signalling pathway (54). ET_A receptors are predominantly expressed in VSMCs, and ET_B receptors are expressed in VSMCs and endothelial cells (54).

When either receptor on the VSMC is activated, phospholipase C (PLC) is stimulated to convert phosphatidylinositol 4,5-bisphosphate (PIP_2) into inositol trisphosphate (IP_3) and diacylglycerol (DAG). DAG activates protein kinase C (PKC), which subsequently phosphorylates myosin light chain kinase (MLCK), resulting in vasoconstriction (Figure 1.3). IP_3 migrates to the sarcoplasmic reticulum and binds to its receptor, causing a release of calcium into the cytosol, which in turn binds to calmodulin and activating calmodulin kinase. In VSMCs, calmodulin kinase phosphorylates MLCK resulting in vasoconstriction and also induces VSMC proliferation (54). Whereas in endothelial cells, calmodulin kinase phosphorylates eNOS, resulting in NO production and vasodilation (Figure 1.3) (55,56).

Multiple studies have shown that PAH patients have increased expression of ET in the lung, which may contribute to the pathophysiology of PAH (52,57,58). These findings led to the use of endothelin-receptor antagonists (ERAs) in the clincal setting to treat PAH to help relieve symptoms and improve survival (59–63).

To date, there are three ERAs used in treating PAH: bosentan, macitentan and ambrisentan (59–63). Bosentan and macitentan are dual ET_A/ET_B antagonists whereas ambrisentan is a selective ET_A antagonist (63,64,65). Bosentan and macitentan compete with ET-1 to bind with the ET_A and ET_B receptors to inhibit the ET-1-induced vasoconstriction in the VSMC. However, since bosentan and macitentan are dual ERAs, they also inhibit the ET-1-induced vasodilation *via* the ET_B receptors in the endothelial cells. Despite this, bosentan has a higher affinity for the ET_A receptor compared to the ET_B receptor, with a relative ET_A: ET_B affinity of 20:1 (67). Ambrisentan selectively inhibits the ET_A receptor, therefore preventing ET-1-induced vasoconstriction whilst preserving the possibility of ET-1-induced vasodilation *via* the ET_B receptors in the endothelial cells (68).

In a cohort of 213 patients with PAH, those treated with bosentan had an improvement in 6-minute walking distance of 44m and the borg dyspnoea index of 0.6, as well as significantly increasing the time until clinical worsening when compared to those without bosentan treatment (63). Ambisentan and macitentan also significantly improved 6-minute walking distance and reduced the time until clinical worsening in PAH patients in

recent clinical trials (61,62). Ambrisentan therapy improved 6-minute walking distance by an average of 39m in 280 PAH patients and macitentan significnatly improved 6-minute walking distance in PAH patients *vs* the placebo group with a mean difference of 21.9m (61,62). However, a recent meta-analysis study revealed some serious adverse effects of the use of ERAs such as hepatic transaminitis, anaemia and peripheral oedema (69).

1.2.3. Targeting prostacyclin signalling to treat PAH

Prostacyclin is mainly synthesised by vascular endothelial cells and acts on its receptor, the prostacyclin IP receptor which is found in the heart, lungs, pulmonary and peripheral arteries and the gastrointestinal system (69,70,71). Activation of the IP receptor in PAH results in vasodilation, inhibition of the proliferation of VSMCs and platelet aggregation (2,72). Homeostasis of vascular tone is maintained through a balance of prostacyclin and thromboxane (TX_{a2}). TX_{a2} is a member of the prostanoid family and is an effective vasoconstrictor, helping balance the vasodilatory effects of prostacyclin (74).

Some prostanoid receptors induce vasodilation when activated (IP, DP, EP_2 and EP_4) whilst others induce vasoconstriction when activated (EP_1, EP_3, FP and TP) (75). The IP receptor is the only receptor able to induce vasodilation within the pulmonary arteries *via* activation of adenylate cyclase, subsequent cyclic adenosine monophosphate (cAMP) synthesis and activation of protein kinase A (PKA) (Figure 1.3) (76). The TP and EP_3 receptors are the receptors that mediate vasoconstriction in the pulmonary arteries (77).

In PAH, there is an imbalance in the synthesis and release of mediators of vasodilation such as prostacyclin, NO and mediators of vasoconstriction such as ET-1 and TX_{a2} (48,58,74,78). Tuder et al found there was reduced expression of prostacyclin synthase and subsequent reduction in prostacyclin release in the pulmonary arteries of PAH patients (78). These findings suggest that the prostacyclin pathway may serve as a therapeutic target for treating PAH and analogues of prostacyclin may have therapeutic potential for the treatment of PAH.

Currently, there are three prostanoids (epoprostenol, iloprost and treprostinil) and one non-prostanoid drug (selexipag) used to treat PAH (79–87). These drugs act primarily *via* activation of the IP receptor, resulting in activation of PKA and subsequent inhibition of proliferation and vasoconstriction (Figure 1.3) (76).

When compared to conventional therapy in clinical trials, epoprostenol treatment has been demonstrated to improve 6-minute walking distance, mPAP, PVR, cardiac output and quality of life in PAH patients (79,80). However, epoprostenol is difficult to administer as it requires a continuous infusion pump and must be refrigerated as it is unstable at room temperature (3). Treprostinil treatment has advantages compared to epoprostenol treatment. Treprostinil is stable at room temperature and has a longer half life compared to epoprostenol, it can also be administered subcuatenously, intravenously, orally or *via* inhalation. Treprostinil treatment has been shown to improve 6-minute walking distance, quality of life, mPAP and PVR compared to the placebo treatment group in PAH patients in multiple clinical trials (81–86). Inhaled iloprost was shown to improve 6-minute walking

distance, dyspnoea, quality of life and the New York Heart Association (NYHA) functional class in PAH patients compared to the placebo treatment group (88). In PAH patients, selexipag treatment has also been demonstrated to improve PVR and reduce the risk of death or a PAH-associated complication (89–91).

Although these treatments are able to alleviate the symptoms of PAH, none of them reverse the pathophysiology of PAH, therefore new treatments are urgently needed. As such, some research groups have attempted to further elucidate other potential targets, such as the metabolic pathways that may potentially reverse the pathophysiology of PAH (92–95). This will be discussed further in Section 1.4.

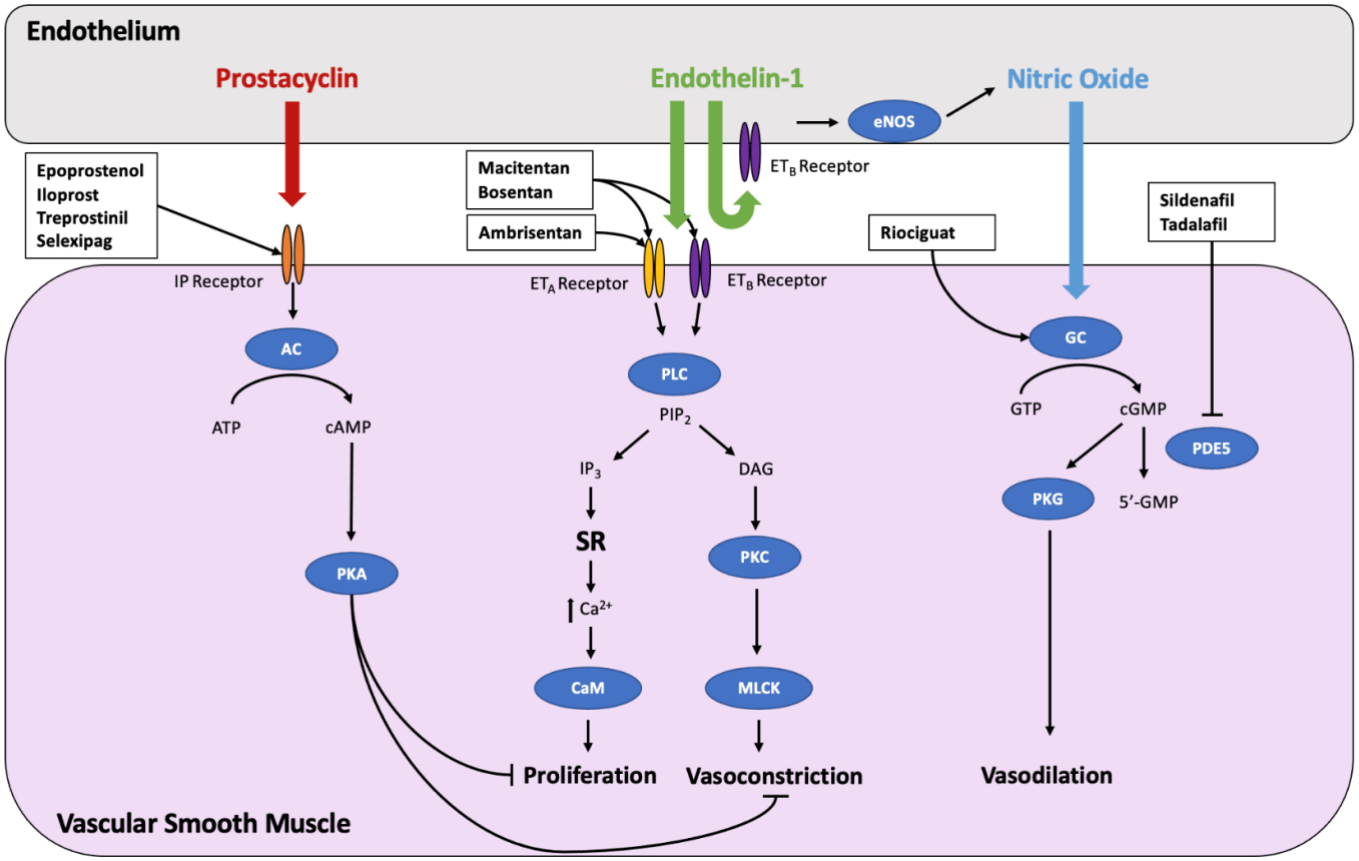

Figure 1.3. A schematic of the Prostacyclin, Endothelin and Nitric Oxide pathways and how they can be targeted with pharmacological agents to treat pulmonary arterial hypertension. Epoprostenol, Iloprost, Treprostinil and Selexipag are all prostacylin analogues. Macitentan and Bosentan are dual ET_A/ET_B antagonists whereas ambrisentan is a selective ET_A antagonist. Riociguat is a soluble guanylate cyclase stimulator. Sildenafil and Tadalafil are PDE5 inhibitors. AC= adenylate cyclase; ATP= adenosine triphosphate; CaM= calmodulin kinase; cAMP= cyclic adenosine monophosphate; cGMP= cyclic guanosine monophosphate; DAG= diacylglycerol; eNOS= endothelial nitric oxide synthase; GC= guanylate cyclase; GTP= guanosine triphosphate; IP_3= inositol triphosphate; MLCK= myosin light chain kinase; PDE5= phosphodiesterase type V; PIP_2= phosphatidylinositol 4,5-bisphosphate; PKA= protein kinase A; PKC= protein kinase C; PKG= protein kinase G; PLC= phospholipase C; SR= sarcoplasmic reticulum. Figure has been adapted from Humbert et al (96).

1.3. Metabolic alterations in PAH

1.3.1. Cellular metabolism in healthy individuals

Mitochondria are essential for life and play a crucial role in cellular respiration to produce the cell's "energy" in the form of adenosine triphosphate (ATP). Glucose oxidation is the main source of ATP during aerobic conditions (97). The glucose oxidation process can be separated into three main pathways: glycolysis, the tricarboxylic acid (TCA) cycle and oxidative phosphorylation. Glycolysis takes place in the cytosol, whereas the TCA cycle and oxidative phosphorylation occur in the mitochondria of the cell (97).

As depicted in Figure 1.4, glycolysis is a series of ten reactions whereby one molecule of glucose is converted into two molecules of pyruvate, two hydrogen ions, two molecules of water and two molecules of ATP (98). Pyruvate dehydrogenase (PDH) then converts pyruvate to acetyl-CoA, which inturn enters the TCA cycle (also known as the Krebs cycle) (99). The TCA cycle describes the oxidation of acetyl-CoA through a series of eight reactions, producing nicotinamide adenine dinucleotide (NADH), flavin adenine dinucleotide ($FADH_2$) and guanosine triphosphate (GTP) (Figure 1.4) (99). The oxidative phosphorylation pathway or the electron transport chain, is where the majority of the ATP is produced in aerobic respiration (100). Utilising O_2 and the NADH and $FADH_2$ produced by the TCA cycle, electrons are transferred in a series of redox reactions. Protons are pumped across the inner mitochondrial membrane using the energy transferred by the flow of electrons which creates a potential energy gradient. The protons then flow back down the potential energy gradient across the inner mitochondrial membrane, through an enzyme called ATP synthase, which uses the energy of the protons flowing through to convert adenosine diphosphate (ADP) and inorganic phosphate (Pi) to ATP (100).

In addition to glucose oxidation, fatty acids can also be used as a substrate for the TCA cycle *via* the β-oxidation pathway (also known as the fatty acid oxidation (FAO) pathway) (101). The β-oxidation pathway describes the oxidation of fatty acids through a series of four reactions, ending in the conversion of fatty acyl CoA to acetyl coenzyme A, which can then enter the TCA cycle (101). The rest of the β-oxidation pathway is the same as the glucose oxidation pathway, with the products of the TCA cycle going to the electron transport chain and producing ATP *via* oxidative phosphorylation (101).

Fatty acid synthase (FAS) is a large multi-enzyme complex that plays a key role in the production of long chain fatty acids from acetyl CoA and malonyl CoA (102). A key enzyme involved in the regulation of FAO is malonyl-CoA decarboxylase (MCD) (103). MCD decarboxylates malonyl-CoA to acetyl CoA and malonyl-CoA inhibits the rate-limiting enzyme for the FAO pathway called carnitine palmitoyltransferase 1 (CPT1) (103). Long chain fatty acids (LCFAs) cannot diffuse freely across the mitochondrial membrane, therefore CPT1/2 transports the LCFAs into the mitochondria *via* the “carnitine shuffle” (104). Therefore, inhibiting MCD increases malonyl-CoA which inhibits CPT1, resulting in activation of PDH and upregulation of glucose oxidation to compensate for the decrease in FAO, this is known as the Randle cycle (104,105). The Randle cycle was first described by Randle and colleagues in 1963 (105), they proposed that glucose and fatty acids competed for their oxidation in muscle and adipose tissue. Randle also showed that FAO inhibited glucose oxidation *via* short-term inhibition of key enzymes involved in glycolysis such as 6-phosphofructo-1-kinase (PFK-1) and PDH (106).

Glucose and fatty acids are not the only molecules that can be oxidised and used as a substrate for the TCA cycle, branched chain amino acids (BCAAs) and ketones can also be oxidised to acetyl CoA to fuel the TCA cycle during periods of limited glucose availability (107–109). L-type amino acid transporters (LATs) transport the BCAAs into the cell (107). Once inside the cell, BCAAs are converted to branched-chain α-keto acids (BCKAs) by branched-chain amino acid transaminases (BCATs), BCATs simultaneously transfer the amino group from BCAAs to α-ketoglutarate (α-KG) to produce glutamate, which is a vital intermediate of the TCA cycle (107). Branched-chain α-keto acid dehydrogenase (BCKDH) converts BCKAs to acetyl Co-A which can then enter the TCA cycle (107). β-hydroxybutyrate is the most prominent ketone body found in the blood (108,109). It is unknown how exactly ketone bodies enter the cell (110), however, once inside the cell, D-β-hydroxybutyrate dehydrogenase (BDH1) catalyses the oxidation of β-hydroxybutyrate to acetoacetate (108,109). Acetyl-CoA is then produced from acetoacetate *via* succinyl-CoA:3-oxoacid-CoA transferase (SCOT) and mitochondrial thiolase (108,109), this acetyl-CoA can then enter the TCA cycle and produce ATP.

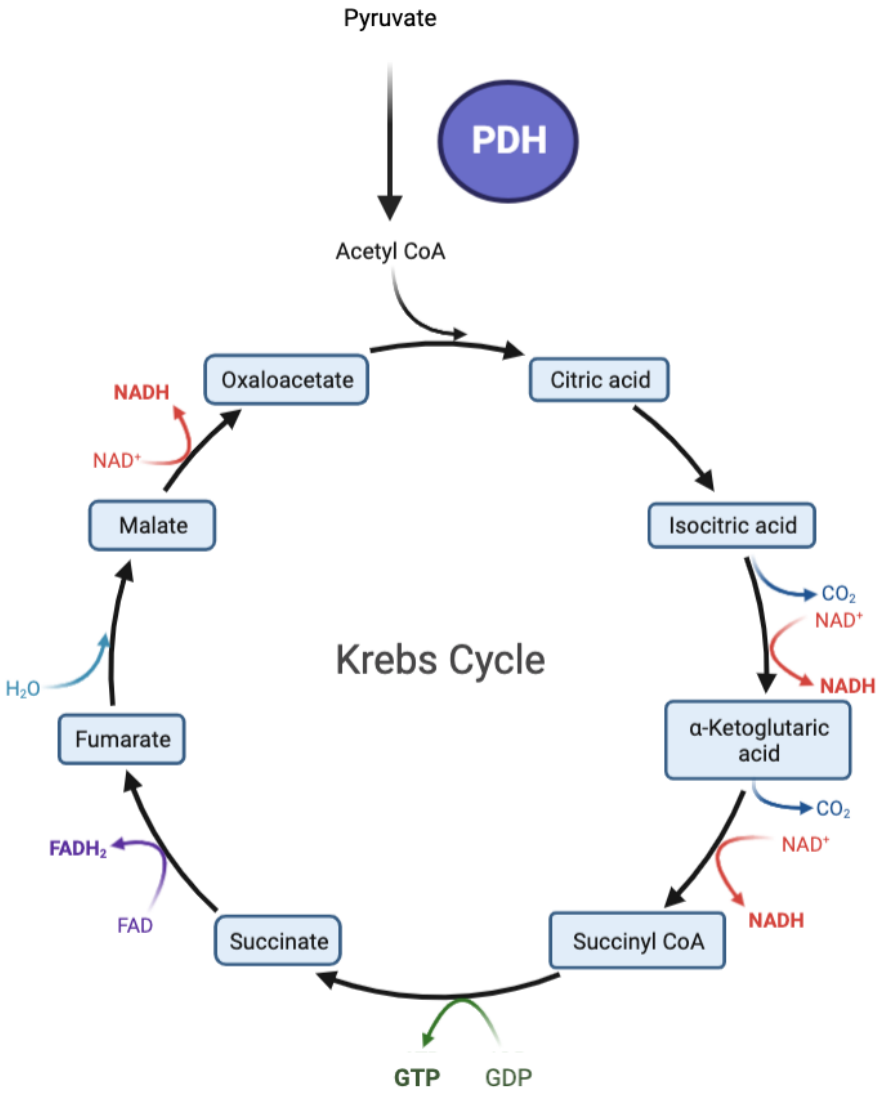

Figure 1.4. A schematic of the TCA cycle. The TCA cycle describes the oxidation of acetyl-CoA through a series of eight reactions, producing nicotinamide adenine dinucleotide (NADH), flavin adenine dinucleotide ($FADH_2$) and guanosine triphosphate (GTP). The NADH and $FADH_2$ generated in the TCA cycle are utilised in the electron transport chain. CO_2= carbon dioxide; FAD= flavin adenine dinucleotide; GDP= guanosine diphosphate; GTP= guanosine triphosphate; H_2O= water; NAD= nicotinamide adenine dinucleotide; PDH= pyruvate dehydrogenase. This figure was created using Biorender.com.

1.3.2. Altered cellular metabolism in PAH

There is a wealth of evidence in the literature demonstrating PAH PASMCs exhibit an abnormal metabolic shift similar to that observed in many cancers, known as the Warburg effect (92,95,111–113). During the Warburg effect in PAH, PASMCs, PAECs and PAfibs reprogram their energy metabolism to utilise glycolysis over oxidative phosphorylation for ATP production, even in the presence of oxygen (114–117). Several experimental studies have suggested that the mechanism of increased proliferation and resistance to apoptosis in PASMCs in PAH is similar to that seen in cancer cells (92,112–114). These findings suggest that the mitochondrial alterations in PAH should be investigated further and may potentially be targeted therapeutically and will be discussed herein.

As mentioned previously, PDH usually converts pyruvate to acetyl-CoA to enter the TCA cycle. Pyruvate dehydrogenase kinase-1 (PDK1) is an enzyme that phosphorylates PDH and inhibits it from converting pyruvate to acetyl CoA. Experimental studies have demonstrated that during PAH, PDK1 is upregulated by the PI3K/AKT/HIF-1α pathway, thus resulting in inhibition of PDH and subsequently attenuating oxidative phosphorylation (118,119) (Figure 1.5). As pyruvate is not able to be converted to acetyl-CoA due to the inhibition of PDH, pyruvate is instead converted to lactate by lactate dehydrogenase (LDH) (Figure 1.5).

Previous studies have demonstrated that platelet-derived growth factor (PDGF) promotes the development of PAH in rats (120,121). Furthermore, it has been shown that PDGF promotes the phenonmenon of the Warburg effect in PASMCs *via* the PI3K/AKT/HIF-1α

pathway (112). This causes an increase in the phosphorylation of PDH and AKT, as well as increased expression of PDK1, HIF-1α and hexokinase-2 (HK-2) when compared to the untreated PASMCs (113).

Futhermore, pre-clinical studies have shown that PAH patients have increased glucose transporter 1 (GLUT1) and hexokinase expression, thus potentiating glucose uptake and increasing the rate of glycolysis (122). Using positron emission tomography (PET) imaging with fluorine-18–labeled 2-fluoro-2-deoxyglucose (^{18}FDG) (122), a fluorescent analogue of glucose, Zhao et al have confirmed the significant increase in glucose uptake in the lungs of PAH patients *vs* control patients (122). Marsboom and colleagues (123) have also demonstrated increased ^{18}FDG uptake in MCT-treated rats and they found that a fall in the ^{18}FDG-PET signal in the lung of the MCT-treated rats corresponded with a decrease in the muclarization of the pulmonary arteries (124). In addition, utilising the MCT-treated rat model of PAH, Chen et al demonstrated by utilising real-time quantative PCR and Western blot analysis, that there was increased expression of LDH, PDK1, GLUT1 and CPT-1 in the lung of the MCT-treated rats compared to the lung of the untreated rats (125).

Another study utilising the MCT-treated rat model of PAH demonstrated that there was increased activity and expression of CPT-1 in the lungs of the MCT-treated rat compared to the untreated rat, and also showed that there was decreased ATP production and downregulation of the AMPK-p53-p21 pathway, a key pathway involved in the regulation of the cell cycle and apoptosis in the MCT-treated mice (126). The same study also

treated isolated rat PASMCs with PDGF to mimic PAH and found that the PDGF-treated PASMCs also exhibited increased CPT-1 expression and activity and demonstrated that treatment with the CPT-1 inhibitor, etomoxir reversed the PDGF-induced increase in proliferation of the PASMCs and partially restored the PDGF-induced downregulation of the AMPK-p53-p21 pathway (126). These results highlight the importance of the alterations in the expression and activity of CPT-1 in rodent and *ex vivo* models of PAH and should be investigated further.

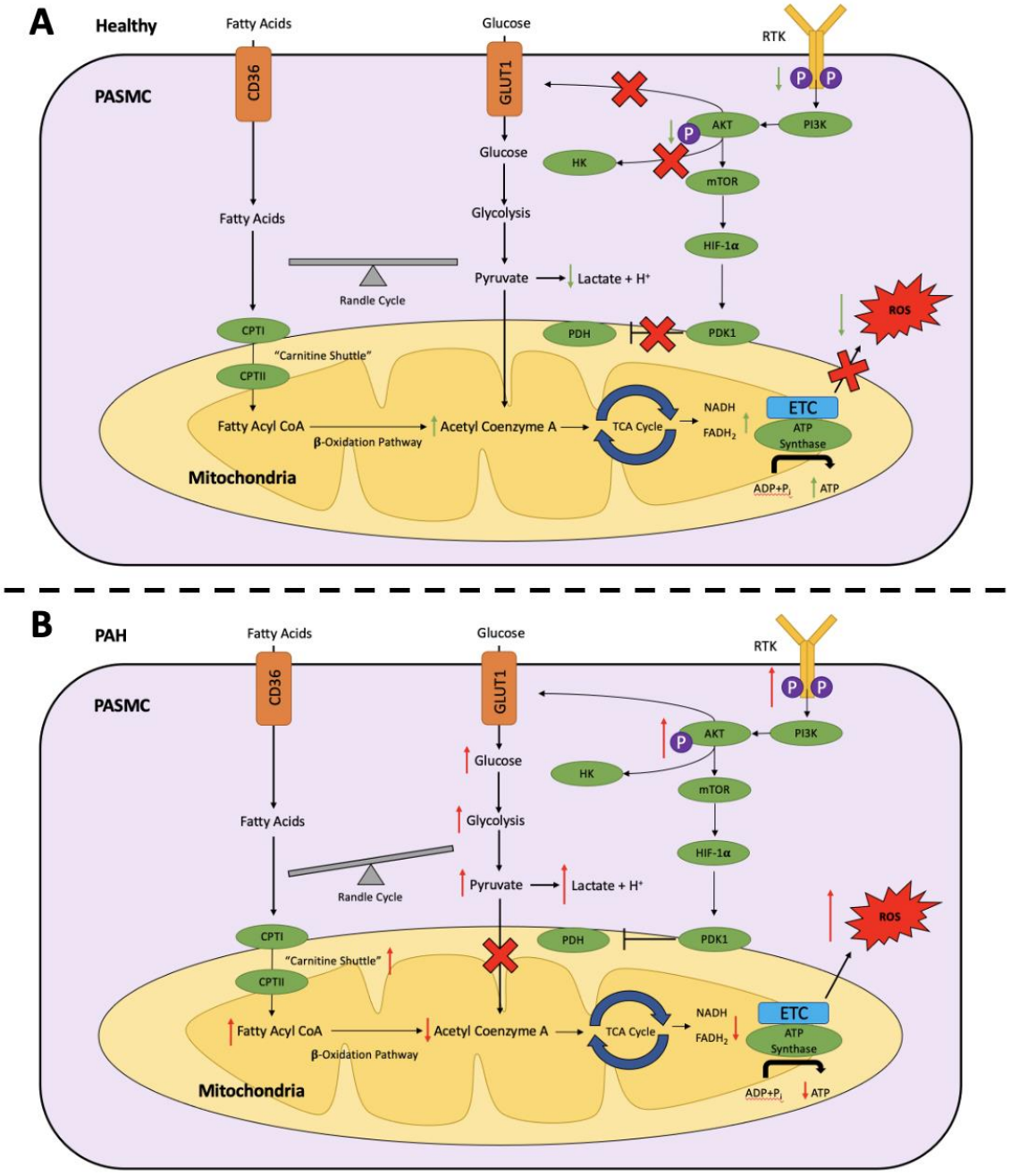

Figure 1.5. A schematic depicting the differences in cellular metabolism between a PASMC from a healthy individual and a PASMC from a PAH patient. Panel A and panel B depict the metabolism of a healthy PASMC and PAH PASMCs respectively. Green arrows indicate a positive difference *vs* the PAH PASMC and red arrows indicate a negative difference *vs* the healthy PASMC. Red "X" indicates inhibition. ADP=Adenosine Diphosphate; AKT=Protein Kinase B; ATP=Adenosine Triphosphate; CPT=Carnitine palmitoyltransferase; ETC=Electron Transport Chain; $FADH_2$= Flavin Adenine Dinucleotide; HIF-1α=Hypoxia Inducible Factor 1 subunit α; HK=Hexokinase; mTOR=Mammalian Target of Rapamycin; NADH=Nicotinamide Adenine Dinucleotide; PI3K=Phosphoinositide 3-Kinase; PDH=Pyruvate Dehydrogenase; PDK1= Pyruvate Dehydrogenase Kinase 1; ROS=Reactive Oxygen Species; RTK=Receptor Tyrosine Kinase; TCA; Tricarboxylic Acid. Figure has been adapted from Peng et al (111).

1.4. Other Potential Mechanisms Underpinning the Increased Proliferation During PAH

1.4.1. The Roles of AKT and ERK in PAH Pathophysiology

In addition to the metabolic alterations that occur during PAH, there are other pathways that have been demonstrated to be upregulated during PAH and implicated in the pathophysiology of PAH. The activation of the PI3K/AKT/ERK pathway has been demonstrated to induce proliferation and apoptosis resistance in PASMCs from multiple models of PAH (127–130), thus reinforces the importance of AKT in the pathophysiology of PAH. Extracellular-signal regulated kinase 1/2 (ERK1/2) are protein kinases downstream of PI3K/AKT, and have also been shown to contribute to the hyperproliferation of PASMCs (131–133). AKT has been demonstrated to be phosphorylated at the Serine 473 residue ($pAKT^{Ser473}$) and ERK has been demonstrated to be phosphorylated at the Threonine 202 and Tyrosine 204 residues ($pERK^{Thr202/Tyr204}$) (112,113,133).

Feng and colleagues (134) stimulated rat PASMCs with high-mobility group box-1 (HMGB1) to mimic PAH as HMGB1 has been identified as a biomarker of PAH pathogenesis (135–137). HMGB1 stimulation induced a dose-dependant increase in the phosphorylation of dynamin-related protein 1 ($Drp1^{Ser616}$; a protein that mediates both physiological and pathological mitochondrial fission (123)) and subsequently altered the mitochondrial morphology (134). The HMGB1 treated PAMSCs had more small spherical mitochondria compared to the usual elongated tubular mitochondria which were observed in the control PASMCs, indicating HMGB1 treatment increases $pDrp^{Ser616}$ and

mitochondrial fragmentation (134). Moreover, HMGB1 treatment induced an increase in the phosphorylation of ERK1/2 and treatment with the ERK1/2 inhibitor U0126 abolished the HMGB1-induced increase in the phosphorylation of Drp1 and restored mitochondrial morphology back to the usual elongated tubular shape (134). This indicates that ERK1/2 plays a crucial role in HMGB1-induced Drp1 phosphorylation and mitochondrial fragmentation in PASMCs. Feng and colleagues then demonstrated that HMGB1 induced PASMC proliferation and migration and treatment with U0126 (ERK1/2 inhibitor) abolished the HMGB1-induced PASMC proliferation and migration, implicating ERK1/2 as a key mediator in HMGB1-induced proliferation and migration (134). Following on from these cellular experiments, the same research group (134) treated rats with MCT to mimic PAH. The authors found that the HMGB1 inhibitor GLY attenuated the increases in mPAP, RVSP, pulmonary arterial wall thickness and PASMC proliferation observed in the MCT-treated rats and GLY treatment prevented vascular remodelling and the development of PAH in MCT-treated rats (134). They also observed an increase in phosphorylation of ERK1/2 and Drp1 in the lungs of the MCT-treated rats but GLY treatment reversed these findings (134). Overall, these findings suggest that ERK1/2 plays a crucial role in MCT-induced PAH *via* the HMGB1 pathway and targeting ERK1/2 or another aspect of the HMGB1 pathway may act as a therapeutic target.

Cheng and colleagues (132) treated rats with MCT to induce PAH and exposed human PASMCs to hypoxia and PDGF to mimic the environment in PAH. The authors then injected the MCT-treated rats with caffeic acid phenethyl ester (CAPE) once a day for two weeks. They found that CAPE treatment significantly reduced vascular remodelling in the

MCT-treated rats by inhibiting HIF-1α expression (132). In addition, it was reported that CAPE treatment reduced hypoxia and PDGF-induced HIF-1α expression through inhibiting the activation of the AKT/ERK pathway and subsequently inhibited the proliferation of the human PASMCs (132). Therefore, the AKT/ERK pathway could act as a therapeutic target to help combat the hyperproliferation in PAH.

1.5. Targeting the metabolic alterations in PAH

1.5.1. The use of DCA to target the altered metabolism in PAH.

Dichloroacetate (DCA) is a selective inhibitor of PDK-1 and is known to indirectly upregulate glucose oxidation and suppress glycolysis (92,94). Previous experimental studies by Michelakis et al have proposed that DCA could be used to treat PAH (92,94). In fact, Michelakis and colleagues have demonstrated DCA to have promising effects in MCT-treated rats (92). The authors revealed that DCA treatment reversed the vascular remodelling, restored the expression and function of K_V channels and increased apoptosis whilst attenuating proliferation in rodent models of PAH (91,92). Down regulation of K_V channels increases the intracellular K^+ levels which inhibits the function of key caspases involved in apoptosis, therefore restoration of the expression and function of the K_V channels decreases intracellular K^+ levels and facilitates apoptosis (139–141). Another study utilised the MCT-rat model of PAH and showed that DCA treatment reduced the phosphorylation of PDH, thus increasing the activity of PDH and subsequently reduced RV fibrosis, RV hypertrophy and improved RV function (118).

In addition, Michelakis and colleagues have also demonstrated that DCA shows promise as a treatment for PAH patients (95). Michelakis and co-workers showed that the expression of PDK1 was increased in the lungs of PAH patients and DCA treatment of peripheral human lung from PAH patients increased PDH activity *via* a decrease in the phosphorylation of PDH by PDK1 and subsequently increased mitochondrial respiration (95). Furthermore, a clinical trial in iPAH patients demonstrated that DCA treatment at concentrations between 3-6.25 mg/kg reduced mPAP, PVR and 6-minute walking distance in genetically susceptible iPAH patients, but DCA treatment in iPAH patients with single-nuceleotide polymorphisms (SNPs) in the genes for SIRT3 or uncoupling protein 2 (UCP2) was not as effective in improving mPAP, PVR or 6-minute walking distance (95). The authors proposed that the lack off effectiveness of DCA in the iPAH patients with SNPs in SIRT3 or UCP2 was due to the inhibition of PDH being less dependant on PDK1 and therefore inhibiting PDK1 did not improve PDH activity or subsequent haemodynamic parameters (95).

Moreover, DCA treatment was shown to attenuate the Warburg effect in PDGF-treated rat PASMCs by increasing PDH activity, thus resulting in a metabolic shift towards glucose oxidation (112). The authors isolated PASMCs from Sprague-Dawley rats and treated the isolated PASMCs with PDGF to mimic PAH (112). PDGF treatment induced the Warburg effect, determined by increased proliferation, glucose consumption, lactate production and the increased expression of LDH and GLUT1 as well as decreased ATP production and expression of PDH (112). DCA treatment of the PDGF-treated PASMCs decreased glucose consumption, lactate production and the expression of LDH and

GLUT1 and increased ATP production and the expression of PDH (112). The authors also showed that PDGF increased cell proliferation and increased the expression of HIF-1α and PDK1 in the isolated rat PASMCs, but DCA treatment significantly reduced the proliferation and reduced the expression of HIF-1α and PDK1 to levels similar to the untreated rat PASMCs (112). These findings suggest that PDGF induces PASMC proliferation by activating HIF-1α, which increases the expression of PDK1 and subsequently decreases the expression of PDH, resulting in a metabolic shift and the Warburg effect.

To investigate the mechanism by which DCA reverses the Warburg effect in PDGF-treated PASMCs, Li and colleagues (113) inhibited the PI3K/AKT/HIF-1α pathway using the PI3K inhibitor LY294002 and found that LY294002 potentiated the pro-apoptotic effect of DCA on human PASMCs. The authors also showed that PDGF increased the expression of PDK1, HIF-1α and hexokinase-2 (HK-2) and increased the phosphorylation of PDH (113). However, DCA treatment (10μM and 20μM) abolished these observations by reducing the expression of PDK1, HIF-1α and HK-2, as well as reducing the phosphorylation of PDH in the PDGF-treated PASMCs, with the concentration of 20μM doing so with greater potency than 10μM for pPDH, PDK1, HIF-1α and HK-2 (113). Moreover, the authors also demonstrated that the increased expression of PDK1 by PDGF was reduced with LY294002 (PI3K inhibitior) treatment in a dose-dependant manner, suggesting that in PDGF-treated human PASMCs, the PI3K/AKT/HIF-1α pathway upregulates PDK1 to inhibit PDH activity and subsequently induces the Warburg effect (113). Overall, this study suggested that combination of DCA treatment and the

inhibition of the PI3K/AKT/HIF-1α pathway could serve as a therapeutic target for the treatment of vascular remodelling in PAH.

Whilst experimental studies in rodent and human models of PAH have revealed promising findings with DCA treatment such as reversal of vascular remodelling, decreased proliferation and increased apoptosis, reduced RV fibrosis, RV hypertrophy and improved RV function and reversal of the Warburg effect (92,93,95,112,113,118), the safety of DCA remains a controversial topic. One study investigated the use of DCA to treat patients with mitochondrial myopathy, encephalopathy, lactic acidosis and stroke-like episodes (MELAS) (142). The MELAS trial showed that DCA at a dose of 25mg/kg/day over a 24 month period led to all of the patients developing peripheral neuropathy, and the trial was withdrawn (142). However, another clinical trial investigating the use of DCA to treat congenital lactic acidosis in children, found that 12.5mg/kg of DCA every 12 hours for 6 months caused no significant neurotoxicity (143). These findings demonstrate that chronic use of DCA at a concentration of 25mg/kg/day induces neurotoxcity, but the neurotoxic effects are not observed with short-term (6 months) DCA treatment at a concentration of 12.5mg/kg every 12 hours. However, the uncertainty around the safety of DCA means that other pathways such as the FAO pathway are being explored to investigate whether they can be targeted to treat PAH.

1.5.2. Inhibiting the FAO pathway to treat PAH

Inhibiting the FAO pathway is also a potential therapy to treat PAH since previous studies have produced promising results (144). For example, Fang et al (144) utilised a

pulmonary artery banding model to induce right ventricular hypertrophy in adult Sprague-Dawley rats. The induction of ventricular hypertrophy caused a metabolic shift from glucose oxidation to glycolysis (144). However, they found that the partial inhibition of FAO, with trimetazidine and ranolazine led to increased glucose oxidation, improved right ventricular function and reduced right ventricular hypertrophy (144). Futhermore, ranolazine has been demonstrated to inhibit FAO and subsequently upregulate PDH in perfused normoxic rat hearts (145). Ranolazine has also been shown to inhibit FAO and upregulate glucose oxidation and subsequently improve cardiac work in rat hearts exposed to ischemia/reperfusion (146). In a randomized controlled trial of a group of 19 patients with idiopathic dilated cardiomyopathy, trimetazidine decreased FAO, increased glucose oxidation and increased ejection fraction (147).

In addition, previous studies have demonstrated that mice lacking the gene coding for MCD (involved in the regulation of FAO) did not develop PAH when exposed to chronic hypoxia (148). It has been demonstrated that the absence of MCD inhibited FAO and upregulated glucose oxidation due to the Randle cycle meaning that the metabolic shift to uncoupled glycolysis that is usually observed after exposure to chronic hypoxia was averted (148–150).

Fatty acid synthase (FAS) has been shown to be upregulated in hypoxic human PASMCs and in MCT-treated rats (151) and FAS is also highly expressed in multiple cancers (152). Inhibition of FAS in human PASMCs following exposure to hypoxia and MCT-treated rats has been demonstrated to increase apoptosis and decrease proliferation (151). Inhibition

of FAS also increased glucose oxidation and decreased glycolysis in the human PASMCs following exposure to hypoxia (151). Overall, these findings imply that the altered FAS activity apparent in PAH contribute to the pathophysiology of PAH and may serve as a potential therapeutic target to treat PAH.

1.6. The use of Perhexiline to treat metabolic diseases

1.6.1 Perhexiline treatment in cardiac metabolic diseases

Perhexiline was first introduced as an anti-anginal drug in the 1970s (153). Perhexiline is thought to act primarily by inhibiting CPT-1, the enzyme responsible for long chain fatty acid uptake into the mitochondria, but can also inhibit CPT-2 less effectively (154–156). Perhexiline has been shown to improve VO_2 max, left ventricular ejection fraction and resting and peak stress myocardial function in chronic heart failure patients (157). Perhexiline increases metabolic efficiency by shifting myocardial metabolism from fatty acid metabolism to carbohydrate consumption (158). Furthermore, perhexiline has also been demonstrated to be beneficial for treating inoperable aortic stenosis (159), acute coronary syndromes (160) and hypertrophic cardiomyopathy (161). Since perhexiline has shown promise in treating other cardiac metabolic diseases (157,161) and the use of FAO inhibitors to treat cardiac metabolic diseases has also demonstrated therapeutic potential (144), the use of perhexiline as a candidate drug to treat PAH, in theory could exhibit similar beneficial effects.

1.6.2. Perhexiline to reverse the Warburg effect in Cancer

Metabolic alterations that stimulate FAO have been linked to increased tumorigenesis and metastasis in several cancers, including colorectal cancer (162). This led to FAO inhibitors becoming a potential therapy for managing cancers (163,164). After observing the beneficial effects perhexiline had on treating cardiac metabolic diseases, Dhakal and colleagues (162) investigated the use of perhexiline in treating colorectal cancer. They found that perhexiline inhibited the growth and induced apoptosis in all five of the colorectal cancer cell lines tested (162). Other studies have shown the beneficial effects of using perhexiline to treat chronic lymphocytic leukaemia (165) and glioblastoma (166). Wang and colleagues found that perhexiline inhibited proliferation and induced apoptosis of both gastric cancer and colorectal cancer cell lines (167). Since perhexiline has been shown to reverse the Warburg effect in cancer (162,165–167), perhexiline could potentially reverse the Warburg effect apparent in PAH.

1.6.3. Perhexiline is toxic and why we need an alternative

Perhexiline has multiple short term side effects such as nausea, vomiting, diarrhoea, dizziness, tremor and insomnia (168). However, there are also long-term, more serious adverse effects, mainly associated with hepatic and neurological toxicity (169–171). By 1983, there had been 80 cases of hepatotoxicity and 131 cases of neurotoxicity in the UK alone (172). The hepatoxicity of perhexiline is linked to its metabolism *via* CYP2D6, which occurs primarily in the liver (173). In patients with slower hepatic metabolism, the CYP2D6 pathway becomes over saturated and perhexiline has a longer plasma half-life. This leads to protonated perhexiline accumulating in the mitochondria, induced uncoupling of

oxidative phosphorylation, inhibition of mitochondrial complexes I and II, decreased ATP synthesis and decreased β-oxidation of long, medium and short-chain fatty acids (173). All these factors contribute to the necrosis of the hepatocytes. There have also been reports of hypoglycaemia and weight loss being associated with long-term perhexiline use (174,175). However, a study investigating the use of perhexiline to treat severe angina pectoris, reported that short-term (18 ± 2 days treatment) perhexiline treatment did not induce hepatotoxicity or neurotoxicity in a patient cohort of 29, but chronic treatment of perhexiline (8.8 ± 1.7 months treatment) induced hepatotoxicity or neurotoxcity in 9 out of 19 severe angina pectoris patients (176). However, a third group of severe angina pectoris patients (n=22) in the same study were treated for 12 ± 2.6 months, with perhexiline dosage being adjusted to ensure plasma perhexiline concentration did not exceed 600ng/ml; 9 of the 22 patients became asymptomatic and none developed hepatotoxicity or neurotoxicity (176). This study demonstrated that if plasma levels of perhexiline are maintained at a safe, therapeutic dose, the associated toxicity with long-term perhexiline treatment could be avoided. Even though perhexiline is an effective metabolic agent to treat cardiac metabolic disease, the uncertainty about the serious hepatic and neurological toxicity associated with long-term perhexiline treatment means an alternative agent with the therapeutic benefits of perhexiline but without the hepatic and neurological toxicity is required to serve as a treatment for PAH.

1.7. FPER-1 as an alternative to treat PAH

Our research group and collaborators investigated synthetic derivatives of perhexiline in the aim to harness the beneficial properties of perhexiline, whilst removing the harmful

effects. Indeed, we developed a novel derivative named fluorinated derivative of perhexilline (FPER-1) (158). By adding fluorine atoms at the sites of metabolism of perhexiline, this derivative is able to successfully bypass CYP2D6 metabolism, the pathway responsible for hepatoxicity seen with perhexiline use (158). Furthermore, it has been demonstrated that this novel derivative of perhexiline exhibited the same potency against CPT-1 as perhexiline (158). Our group also demonstrated FPER-1 increased carbohydrate consumption and myocardial efficiency whilst decreasing fatty acid consumption (158). The promising effects of perhexiline to treat cardiac metabolic disease and of FPER-1 on the murine heart raises the question whether FPER-1 can be used to reverse the pathophysiology of PAH?

1.8. Summary

PAH is a rare, complex disease which is characterised by elevated PAP and PVR due to PASMC proliferation and vascular remodelling. Mitochondrial and metabolic alterations underpin the vascular remodelling, with a shift in cellular metabolism from glucose oxidation to glycolysis. Current treatments aim to alleviate symptoms but are unable to reverse the pathophysiology of the disease. There have been a few attempts to reverse the pathophysiology of cardiac metabolic diseases using metabolic agents such as DCA and perhexiline, which have produced promising results. However, it has later been demonstrated that these drugs were toxic and could not be used in a wider patient population. A synthetic derivative of perhexiline (FPER-1) has recently been synthesised and developed and has been shown to increase carbohydrate consumption and myocardial efficiency, decrease fatty acid consumption without being associated with the

toxicity that perhexiline is (158). Therefore, the main objective of this project is to elucidate the effect of the parent drug perhexiline and FPER-1 in an *in vitro* model of PAH.

1.9. Hypothesis and Aims

Hypothesis:

As a proof-of-concept, FPER-1 and the parent drug perhexiline reduces PAH PASMCs cell proliferation by attenuating the enhanced PI3K/AKT and ERK pathways, and reverses the Warburg effect by improving PDH activity (inhibition of PDH).

Aims:

To assess whether FPER-1, when compared to the parent drug perhexiline attenuates PAH PASMCs cell proliferation, we aimed to test the following in human healthy and PAH PASMCs:

1. Assess whether FPER-1 and/or perhexiline reverses cell proliferation and maintains cell viability.
2. Determine whether FPER-1 and/or perhexiline attenuates the phosphorylation of AKT (p-AKT^{Ser473}) and/or ERK (p-ERK1/2$^{Thr202/Tyr204}$) to reverse cell proliferation in PAH PASMCs.
3. Establish whether FPER-1 and/or perhexiline reverses cell proliferation in PAH PASCMs by re-activating PDH complex (e.g dephosphorylation of p-PDH-E1α^{Ser293}).

2. Methods

2.1. Ethics.

Human distal PASMCs were kindly provided by Professor Nicholas Morrell from the Royal Papworth Hospital Tissue Bank (Cambridge, UK). PASMCs were isolated from patients with primary PAH and from healthy control adults undergoing lung resection for suspected malignancy as previously described (177). This study was approved by the ethical committee of the University of Cambridge and conducted according to the declaration of Helsinki. All subjects signed informed consent.

2.2. Materials.

Unless stated otherwise, all reagents were purchased from Sigma Aldrich (Missouri, USA) or VWR (Pennsylvania, USA).

2.3. Cell Culture.

To study the effects of the metabolic modulators perhexiline and its derivative FPER-1 on PAH, human distal PASMCs were cultured as previously described (177). Briefly, PASMCs were isolated from patients with PAH and from control healthy volunteers undergoing lung resection for suspected malignancy. PASMCs were cultured in Dulbecco's Modified Eagle Media (DMEM; Sigma Aldrich, Missouri, MO) supplemented with 20% of fetal bovine serum (FBS; Sigma-Aldrich), as previously described (177). PASMCs were treated with vehicle control, perhexiline or FPER-1 and assessed for cell viability, proliferation, and Western blotting, respectively.

2.4. The Assessment of Cell Proliferation and Viability.

For the assessment of proliferation and viability, PASMCs were seeded onto 96 well plates (clear or black opaque-walled, respectively) at a density of 1000 cells per well and incubated for 24 hours to allow cells to adhere to the plate. Following 24 hours, the cells were incubated with perhexiline or FPER-1 (0, 1, 2.5, 5.0 or 10.0μM) for 24, 48 or 72 hours, in triplicate.

2.4.1. Cell Proliferation Assay.

Cell proliferation was measured using a CellTiter96® Aqueous One Cell Proliferation Assay (Promega G3580) as per the manufacturer's instructions and as previously described (178). Briefly, prior to proliferation analysis, the CellTiter96® AQueous One Solution Reagent was placed in a water bath at 37°C for 10 minutes to thaw, this was then aliquoted into 1 ml aliquots and stored at -20°C until required.

Following 24, 48 or 72 hours incubation of PASMCs with perhexiline or FPER-1 (0, 1, 2.5, 5.0 or 10.0μM), 20μl of the CellTiter96® AQueous One Solution Reagent was pipetted into each well of 96-well assay plate, containing the samples and placed in the incubator at 37°C for 1 hour in a humidified, 5% CO_2 atmosphere. Control blank wells containing media without cells were used to measure background luminescence. When transporting the plate to and from the incubator/plate reader, it was covered in foil as the CellTiter96® AQueous One Solution Reagent is light-sensitive. Following 1 hour incubation, the plate was taken to the plate reader and the absorbance was measured at 490nm (Software

max pro version 7.1.0). Cell proliferation data was presented as a fold change when compared to the absorbance value collected at time 0 hours.

2.4.2. Cell Viability Assay.

Cell viability was measured using a CellTiter-Glo® Luminescent Cell Viability Assay (Promega G7572) as per the manufacturer's instructions and as previously described (179). Briefly, both the CellTiter-Glo® buffer and CellTiter-Glo® substrate were thawed and allowed to equilibrate at room temperature prior to use. To make the working CellTiter-Glo® reagent, 100ml CellTiter-Glo® buffer was added to the CellTiter-Glo® substrate and the mixture was inverted gently. The stock solution of CellTiter-Glo® reagent was aliquoted into 5ml aliquots, and stored at -20°C until required to prevent freeze/thaw.

Following 24, 48 or 72 hours incubation with perhexiline or FPER-1 (0, 1, 2.5, 5.0 or 10.0μM), the black opaque-walled 96 well plate was removed from the incubator and allowed to equilibrate at room temperature for 30 minutes. After 30 minutes, a black sticker was placed on the bottom of the 96-well plate to limit crosstalk between wells. 100μl CellTiter-Glo® reagent was pipetted into each well of the 96-well plate. Control blank wells containing media without cells were used to measure background luminescence. The plate was covered with foil to protect the CellTiter-Glo® reagent from the light and placed on a shaker for 2 minutes at room temperature to induce cell lysis. The shaker was turned off after 2 minutes and the plate was allowed to incubate at room temperature for 10 minutes to stabilise the luminescent signal. The luminescence was then measured

using Flex station 3, Software max pro version 7.1.0. Cell viability data was presented as a fold change when compared to the absorbance value collected at 0 hours.

2.5. Western Blotting.

For Western blotting experiments, PASMCs were grown until 80% confluent. PASMCs were then incubated with perhexiline or FPER-1 (2.5 and 5.0μM) for 1 hour or 24 hours. The incubation period was ended by adding 9M urea, 40mM Tris HCl, 0.15M β-mercaptoethanol lysis buffer at the desired time point.

2.5.1. Determining the Protein Concentration of Cell Lysates.

Preparing the Protein Standards.

To calculate the protein concentration of each cell lysate for the Western Blotting experiments, a protein assay was carried out. Firstly, 50ml of lysis buffer was made fresh on the day of the protein assay as depicted in Table 2.1. To prepare the protein standards for the standard curve, 10mg of bovine serum albumin (BSA; Europa Bioproducts Ltd) was dissolved in 1ml of lysis buffer to make a stock solution of 10µg/µl. The standard curve was prepared as depicted in Table 2.2.

Reagents	Quantity
100mM Tris Buffer (pH 7.4)	49ml
Sodium Orthovanadate (200mM stock)	500µl (final concentration=2mM)
Sodium Fluoride (500mM stock) (Sigma)	500µl (final concentration=5mM)
Protease inhibitor tablet (Roche applied sciences)	1 whole tablet

Table 2.1. The makeup of the lysis buffer.

BSA Curve (µg/µl)	BSA Stock (10µg/µl)	Lysis Buffer Volume (µl)
0	0	100
0.2	2	98
0.4	4	96
0.6	6	94
0.8	8	92
1.0	10	90

Table 2.2. Preparation of the standard curve solutions.

Conducting the Protein Assay.

Firstly, the cell samples were diluted 1:20 (5µl lysate, 95µl lysis buffer), then vortexed and placed on ice. Bio-rad DC protein assay kit was used to determine protein concentrations of all samples, as per manufacturer's instructions. Briefly, 5µl of protein standards (from 0 to 1.0µg/µl) and diluted cell samples (1:20) were pipetted in triplicate into a 96 well plate. Working reagent A was made by adding 20µl of reagent S to 1ml of reagent A, then 25µl of working reagent A and 200µl of reagent B were pipetted into each well. The plate was covered with foil to protect it from the light as the reagents are light-sensitive and left on the shaker for 15 minutes. After 15 minutes, the plate was put in the plate reader and the absorbance was measured at 750nm (Software max pro version 7.1.0). The protein

standard curve was plotted, and the protein concentration of the PASMC samples required were calculated.

Preparation of Cell Samples.

Following optimisation of the AKT/ERK/PDH antibodies, we decided to use 25μg of protein for Western blot analysis. Firstly, 5% Laemmli buffer with mercaptoethanol was made by mixing 50μl mercaptoethanol with 950μl Laemmli buffer. Samples were prepared for Western blotting using the appropriate volume of Laemmli buffer, lysis buffer and cell lysate to yield the desired final protein concentration. The samples were then vortexed and boiled at 95°C for 5 minutes, centrifuged at room temperature for 30 seconds at 1200 rpm and then immediately loaded onto a gel or stored at -20°C.

2.5.2. SDS Acrylamide Gel Electrophoresis.

Preparation of the Gel System.

To prepare gels for Western blotting, a Mini-PROTEAN Tetra handcast system (BIO-RAD) was used. For each gel, one Mini-PROTEAN spacer plate and one Mini-PROTEAN multi-caster plate were first cleaned using 70% ethanol and placed on top of each other, before being secured into the holder. The system was checked for leaks using ultrapure water before the gel was cast.

Making the Resolving Gel.

A 10% gel was prepared for AKT, ERK and PDH analysis. The 10% resolving gel was made by preparing the resolving gel solution shown in Table 2.3. 10μl tetramethyl

ethylenediamine (TEMED) and then 100µl ammonium persulfate (APS) were added last to initiate the polymerisation reaction. The resolving gel was quickly poured in-between the Mini-PROTEAN spacer plate and the Mini-PROTEAN multi-caster plate and then water saturated Butan-1-ol was pipetted on top of the resolving gel solution to remove any bubbles in the solution. The gel was then allowed to set for 30 minutes.

30% Acrylamide (National Diagnostics)	Deionised Water	1M Tris-HCL pH 8.8	SDS (from 10% stock solution) (Sigma)	TEMED (Sigma)	APS (Sigma)
3.33ml	2.72ml	3.8ml	100µl	10µl	100µl

Table 2.3. The recipe for the 10% resolving gel

Stacking Gel Preparation.

Once the resolving gel was set, the water saturated Butan-1-ol was poured off and the surface was rinsed with distilled water and blotted dry using a paper towel. The stacking gel was prepared as shown in Table 2.4, with 10µl TEMED and 100µl APS added to the stacking gel solution last. The stacking gel solution was pipetted in-between the Mini-PROTEAN spacer plate and the Mini-PROTEAN multi-caster plate, on top of the resolving gel, a comb (10 well Mini-PROTEAN comb (1.0mm)) was inserted immediately to form the sample wells. Once the stacking gel was set, the gels were wrapped in wet paper towels, covered in tin foil, and stored at 4°C overnight.

30% Acrylamide (National Diagnostics)	Deionised Water	1M Tris-HCL pH 6.8	SDS (from 10% stock solution) (Sigma)	TEMED (Sigma)	APS (Sigma)
0.9ml	4ml	720µl	60µl	10µl	100µl

Table 2.4. The recipe for the stacking gel.

Loading Samples and Running the Gel.

On the day of the experiment, the gel was placed into Mini-PROTEAN Tetra electrophoresis tanks and the tanks were filled with 1x running buffer. 10x running buffer was made up of 30g Tris base, 144g Glycine and made up to 1L with ddH_2O (Table 2.5). 1x running buffer was made by adding 100ml 10x running buffer stock, 10ml of 10% sodium dodecyl sulfate (SDS) and made up to 1L with ddH_2O (Table 2.6). The combs were carefully removed from the gel, leaving the sample wells in the gels.

Tris base	Glycine	ddH_2O
30g	144g	Made up to 1L

Table 2.5. The recipe for 10x running buffer.

10x Running buffer stock	10% SDS	ddH_2O
100ml	10ml	Made up to 1L

Table 2.6. The recipe for 1x running buffer.

5µl of protein standard (precision plus protein dual colour standards, BioRad) was loaded onto each gel so that the molecular weight of the proteins could be determined, then 20µl of sample was loaded into each well. The gels were run at 150V for approximately 60 minutes or until the samples had run off the bottom of the gel. Figure 2.1 shows an image of the polyacralymide gel in the tank, with the samples running on the gel.

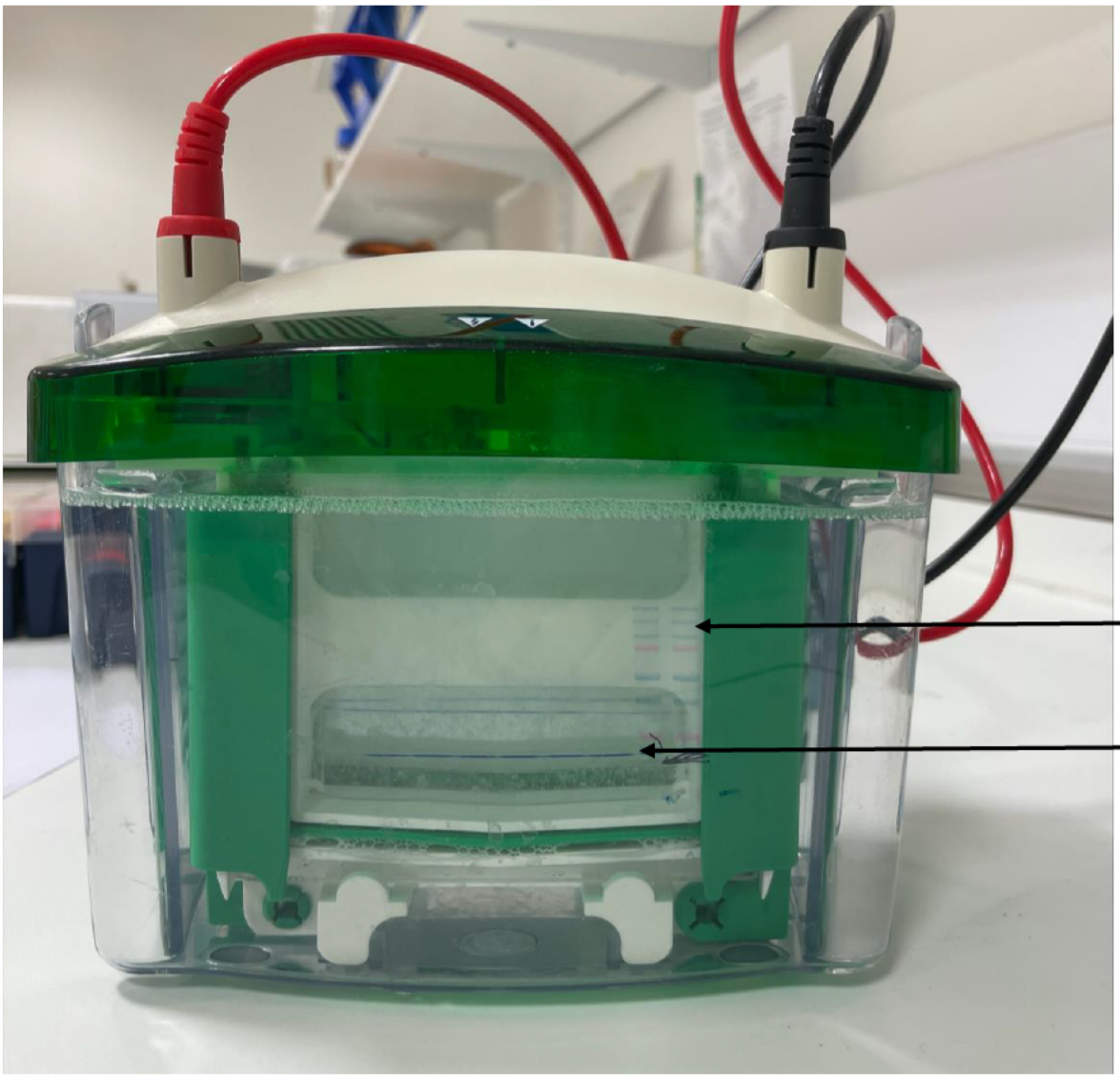

Figure 2.1. Image of the samples running down the polyacrylamide gel.

2.5.3. Wet Transfer Method.

Preparation for the Wet Transfer.

Whilst the gels were running, the transfer buffer was made by mixing 6g Tris Base, 28.8g Glycine, 400ml Methanol and made up to 2L with ultrapure water. Two fibre pads and two sheets of blotting paper, per membrane, were submerged in transfer buffer and stored at 4°C to equilibrate. AmershamTM HybondTM hydrophobic polyvinylidene fluoride (PVDF) membranes were cut into 6.5cm x 9cm sections and then submerged in methanol for 30 minutes for activation. After 30 minutes, the PVDF membranes were placed in transfer buffer and stored at 4°C.

Assembling the Wet Transfer Cassette.

Once the gel had finished running, the two glass plates were then separated using a scraper and the gel was placed in transfer buffer to allow it to equilibrate. The cassette for the wet transfer method was assembled, as depicted in Figure 2.2. The cassette was placed with the grey side down, then one pre-soaked fibre pad was placed on the grey side of the cassette. One pre-soaked sheet of blotting paper was placed on top of the fibre pad and the bubbles were rolled out using a roller. The wells were carefully cut away from the gel, which was then carefully placed onto the blotting paper in the opposite orientation to that in which the gel was loaded (so that the PVDF membrane reads in the same orientation as that in which the gel was originally loaded). The PVDF membrane was then carefully placed on top of the gel and rolled using the roller to eliminate any air bubbles. The second sheet of pre-soaked blotting paper was placed on top of the PVDF membrane and rolled. Finally, the remaining pre-soaked fibre pad was placed on top of

the blotting paper and rolled. The cassette was firmly closed and locked in place using the latch.

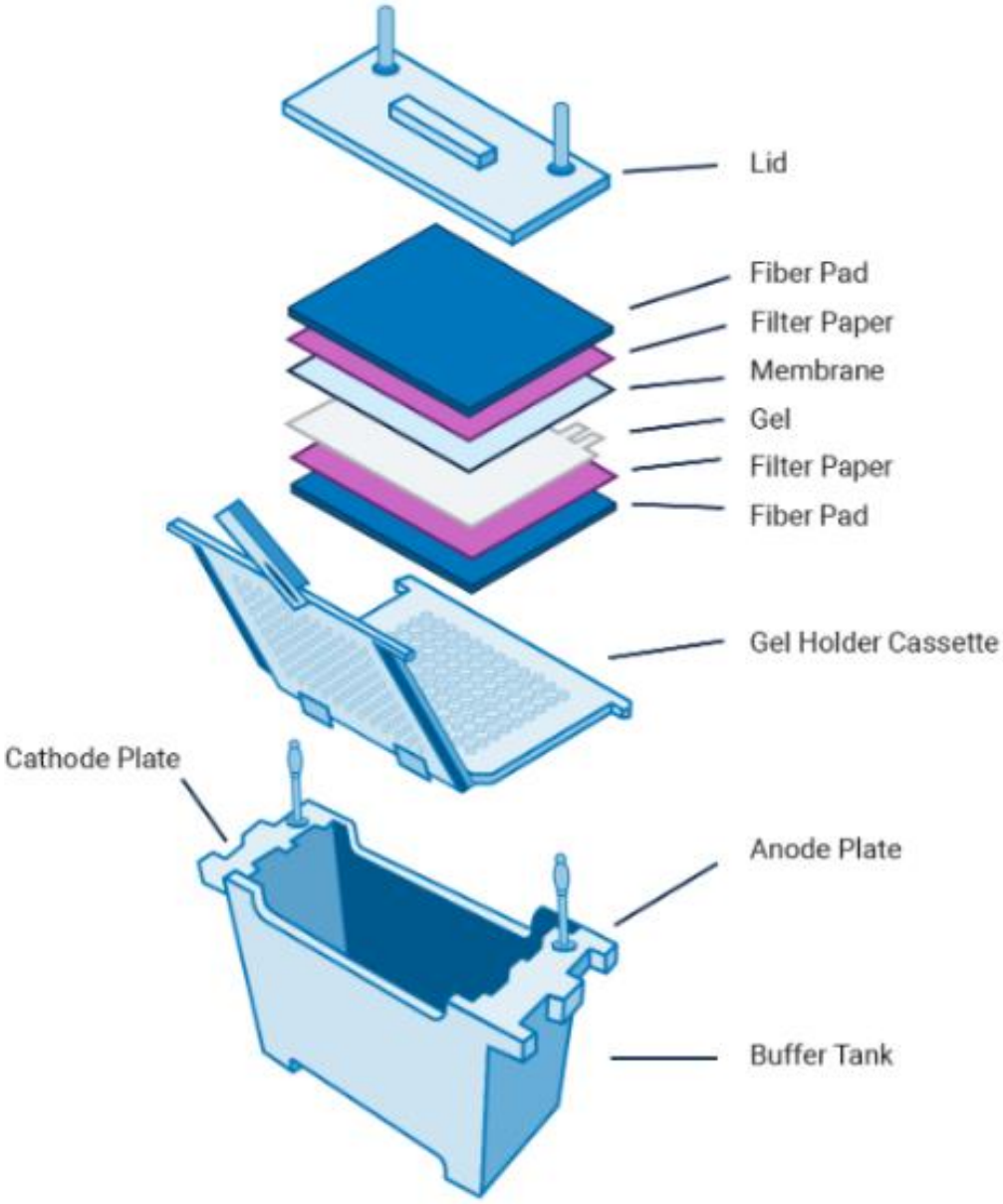

Figure 2.2. Schematic of how the wet transfer cassette is assembled. Taken from Licor.com (180).

Wet Transfer of the Gel to the PVDF membrane.

The cassette was placed in the electrode module in the buffer tank. An ice pack was added to the tank to prevent the buffer from overheating. A magnetic stirrer was added to the tank to help maintain the temperature of the buffer and ion distribution in the tank. The tank was then filled to the “blotting” line with ice cold transfer buffer and the wet transfer was run at 100V for 90 minutes. Once the transfer was complete, the cassette was disassembled and the membrane was placed in a sterile plastic box, ensuring the protein side of the membrane was facing up throughout subsequent steps.

2.5.4. Antibody Exposure and ECL Detection.

Blocking the Membrane and Cutting of the Membrane.

The membrane was blocked using 5% BSA for 1 hour at room temperature. Firstly, a phosphate buffered saline tween (PBST) solution was made (10 tablets of PBS, 2ml tween 20 dissolved in 2L of ultrapure water), then 5% BSA was made up by mixing 1g of BSA with 20 ml PBST. After blocking, the 5% BSA was poured off and the membrane was cut at 50kDa using a sterile scalpel and ruler, this enabled multiple antibodies of different molecular weights to be examined at the same time. The top half of the membrane was used to determine expression of AKT (60kDa) and phosphorylated AKT^{Ser473} ($pAKT^{Ser473}$; 60kDa). The bottom half of the membrane was used to assess the expression of PDH (43kDa) and phosphorylated PDH^{Ser293} ($pPDH^{Ser293}$; 43kDa) or ERK1/2 (42kDa and 44kDa) and phosphorylated ERK ($pERK1/2^{Thr202/Tyr204}$; 42kDa and 44kDa). The respective membranes were placed in separate clean plastic boxes and labelled accordingly.

Preparation and Incubation of Primary Antibodies.

The concentrations of the primary antibodies used are shown in Table 2.7. All primary antibodies were made in 10ml volume. The primary antibodies were poured onto the respective membranes and incubated at 4°C overnight. On the following day, the primary antibodies were poured back into the labelled falcon tubes and stored in the freezer for further use, ensuring to note every time the antibody is used. The primary antibodies were used no more than 3 times.

Primary antibody	Concentration	Blocking agent	Product details
pAKT^{Ser473}	1:1000	5% BSA	(Cell Signalling #4060)
Total AKT	1:1000	5% BSA	(Cell Signalling #9272)
pERK$^{Thr202/Tyr204}$	1:1000	5% BSA	(Cell Signalling #4377)
Total ERK	1:1000	5% BSA	(Cell Signalling #9102)
pPDH^{Ser293}	1:1000	5% BSA	(Cell Signalling #31866)
Total PDH	1:1000	5% BSA	(Cell Signalling #2784)
β-Actin	1:5000	1% Milk	(Sigma A5441)

Table 2.7. Primary antibody concentrations

Washing and Preparation of the Secondary Antibody.

A generous amount of PBST was added to wash the membranes, changing the PBST every 15 minutes for an hour (4x15-minute washes). Thorough washing minimises background when it comes to developing the membranes. The concentration of the secondary antibodies are shown in Table 2.8. The respective secondary antibody for the

protein of interest (shown in Table 2.8.) was added for 1 hour at room temperature. The membranes were then washed with PBST for an hour (4 x 15-minute washes).

Secondary antibody	Concentration	Blocking agent	Product details
pAKT^{Ser473}: Anti-rabbit	1:1000	1% BSA	(Cell signalling #7074)
Total AKT: Anti-rabbit	1:2000	1% BSA	(Cell signalling #7074)
pERK$^{Thr202/Tyr204}$: Anti-rabbit	1:5000	1% BSA	(Cell signalling #7074)
Total ERK: Anti-mouse	1:5000	1% BSA	(Dako P0447)
pPDH^{Ser293}: Anti-rabbit	1:1000	1% BSA	(Cell signalling #7074)
Total PDH: Anti-rabbit	1:1000	1% BSA	(Cell signalling #7074)
β-Actin: Anti-mouse	1:5000	1% BSA	(Dako P0447)

Table 2.8. Secondary antibody concentrations

2.5.5. ECL Detection and Development of the Film

Whilst the membranes were being washed, the developing cassette was prepared for ECL detection. Firstly, the cassette was wiped down with water, allowed to dry and cleaned with 70% ethanol. A plastic wallet was cut in half and the edges cut, so that only one edge was attached, and the plastic wallet was taped to the cassette. A 15ml falcon tube was covered in tin foil to protect the ECL (Thermo Scientific) reagent from the light. A 1:1 ratio of reagent A and reagent B were pipetted into the foil-covered falcon tube, trying to limit light exposure during the pipetting. The falcon tube was inverted to mix the 2 reagents and then 2ml of the working ECL reagent was pipetted onto each membrane, aiming roughly where the respective bands would be. The membranes were placed on the shaker for 3 minutes, excess ECL removed and the membrane placed in the plastic

wallet. The cassette was then closed and taken to the dark room along with a pack of high performance chemiluminescence film (Amersham). In the dark room, the films were taken out of the pack and placed in the cassette on top of the plastic wallet. Once the desired exposure time is reached, the films were taken out the cassette and put into the developer. The exposure times varied depending on the antibody used.

2.5.6. Re-probing the Membranes

To re-probe the AKT, ERK and PDH membranes for control loading analysis, the membranes were blocked with 5% BSA for 1 hour. Then 100μl sodium azide (1g/10ml) was pipetted onto the membranes and incubated for 1 hour. The blots were then quickly washed with PBST to remove any remaining sodium azide. The primary antibody of choice, e.g., a loading control such as β-actin was then added and incubated overnight at 4°C and the process described in section 2.5.4 was repeated.

2.5.7. Densitometry

Once the films had been developed, they were scanned, and the densitometry of the bands were analysed using photoshop (Adobe Photoshop Elements 2021). The mean intensity of the bands were measured by detecting the mean number of photons per pixel in the box. To measure the bands, a box large enough to fit each band in was drawn and the number of pixels inside the box was noted (Figure 2.3.). The background of the film was then measured by moving the box over a space on the film away from the bands.

Once the densitometry for all the bands and the background values had been recorded, the data was normalised. The mean intensity of the background was subtracted from the mean intensity of the band then expression was normalised to β-actin (loading control). In the case of phosphorylated proteins, these were further normalised to total expression of the corresponding protein.

Figure 2.3. Example of densitometry analysis, using photoshop. The box around the band is indicated by the arrow.

2.6. Statistical Analysis

Statistical analysis was performed using GraphPad prism version 9.0 (GraphPad Software, San Diego, CA, USA). All data are presented as mean ± standard error of the mean (SEM), $P \leq 0.05$ was considered significant, as determined using t-test, one-way or two-way analysis of variance (ANOVA), with Bonferroni post hoc tests where appropriate.

3. Results

Perhexiline has shown promise in treating cardiometabolic diseases (157–161) and studies have demonstrated that AKT, PDH and ERK play crucial roles in the pathophysiology of PAH (118,127–133). Therefore, the present study explores whether perhexiline and FPER-1 are able to reduce the proliferation rate of PASMCs from PAH donors using cell proliferation and cell viability assays. The effect of perhexiline and FPER-1 on the expression of AKT, PDH and ERK was also investigated by Western Blotting. All experiments were performed using cultured PASMC from PAH donors or from control healthy volunteers undergoing lung resection for suspected malignancy as described earlier (Section 2.3).

3.1. The Effect of Perhexiline and FPER-1 on the Rate of Proliferation and Viability in PAH PASMCs

3.1.1. PAH PASMCs have a higher rate of proliferation and viability compared to PASMCs from healthy control donors.

To demonstrate that PAH PASMCs were hyperproliferative, cell proliferation and viability assays were performed as described in section 2.4.1 and 2.4.2. Figure 3.1A shows that PASMCs from PAH donors have a significantly higher rate of proliferation than the PASMCs from healthy donors, particularly at 48 hours ($P \leq 0.05$) and 72 hours ($P \leq 0.001$). Figure 3.1B shows that cell viability also increases with time in the PAH PASMCs, with a significant increase in cell viability in the PAH PASMCs *vs* the control PASMCs at 72 hours ($P \leq 0.01$).

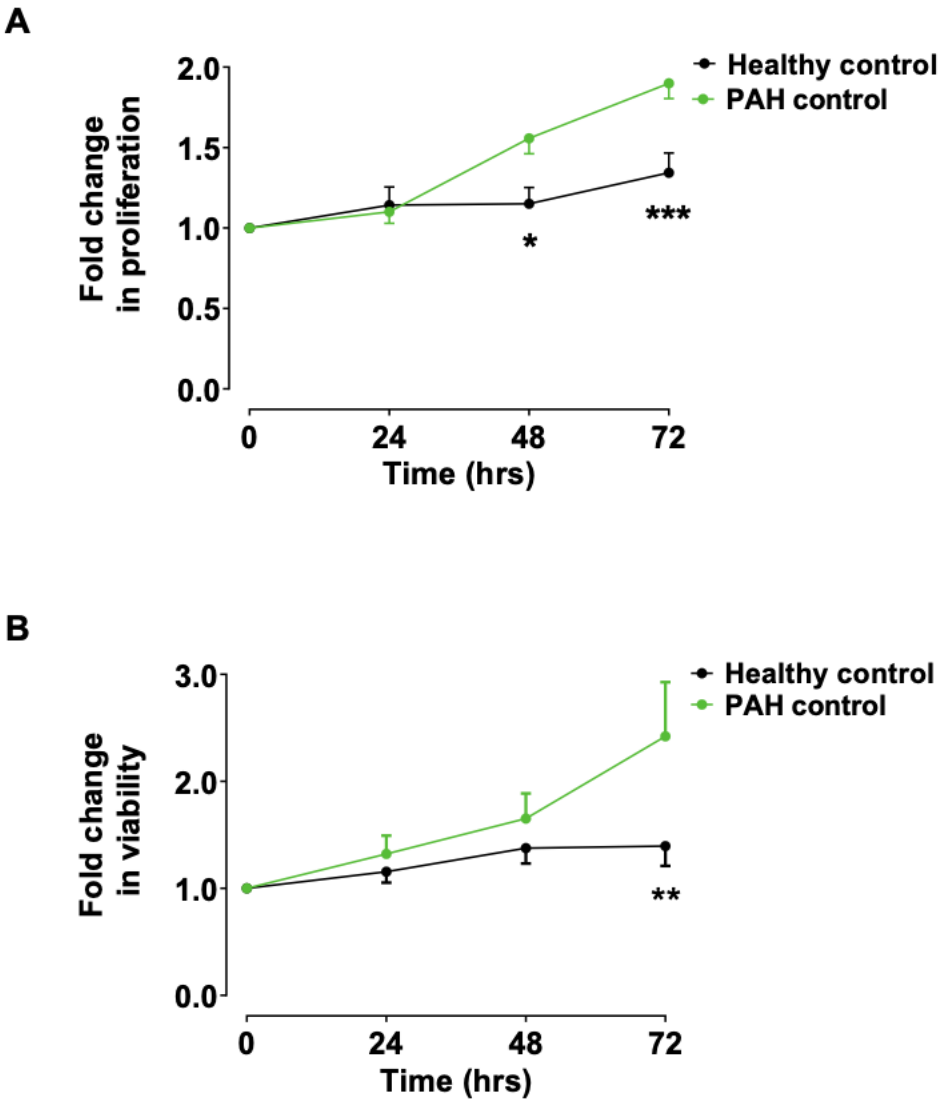

Figure 3.1. PASMCs from PAH donors have an increased rate of proliferation and viability vs PASMCs from healthy control donors. PASMCs from PAH donors and healthy control donors were cultured and assessed for cell proliferation and viability, respectively. The fold change in proliferation **(A)** and the fold change in viability **(B)** were measured at 24, 48 and 72 hours. n=8 healthy and n=6 PAH donors, all experiments were performed in triplicate. Data expressed as mean ± SEM, *P≤0.05, **P≤0.01 and ***P≤0.001, as determined by two-way ANOVA with Bonferroni's test.

3.1.2. Perhexiline and FPER-1 attenuate the rate of proliferation in healthy control PASMCs.

The effect of perhexiline and FPER-1 on the rate of proliferation and viability in healthy PASMCs was also investigated. Figure 3.2A shows that we observed a significant reduction in cell proliferation after 48 hours with 10μM perhexiline ($P \leq 0.05$) when compared to the vehicle treated healthy control PASMCs. Figure 3.2B shows that we also observed significant reductions in cell proliferation with 10μM treatment of FPER-1 after 48 ($P \leq 0.01$) and 72 hours ($P \leq 0.05$) when compared to the vehicle treated healthy control PASMCs. Figure 3.2C shows that 10μM treatment of perhexiline visibly reduced cell viability after 72 hours, although not significant ($P = 0.3843$). Similar results were also observed with FPER-1 treatment (Figure 3.2D) whereby 10μM FPER-1 treatment caused a significant reduction in cell viability after 72 hours ($P \leq 0.05$) when compared to the vehicle treated healthy control PASMCs.

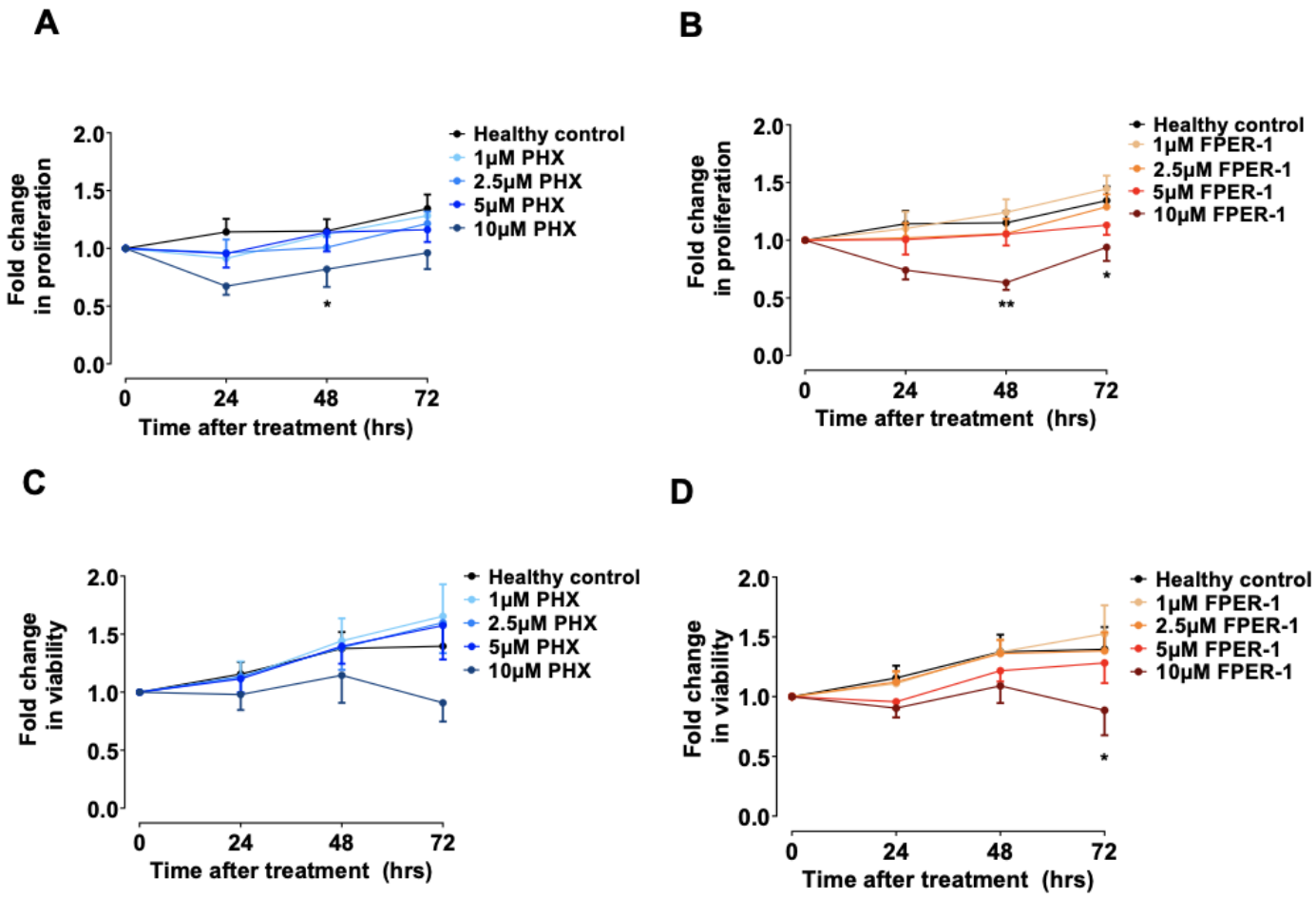

Figure 3.2. The effect of perhexiline (PHX) and FPER-1 on cell proliferation and cell viability in healthy PASMCs. PASMCs from control healthy donors were either treated with vehicle control, 1, 2.5, 5 or 10μM of perhexiline or FPER-1. **(A)** The fold change in proliferation following treatment with perhexiline and **(B)** FPER-1. The fold change in viability following **(C)** perhexiline treatment and **(D)** FPER-1 treatment. Cell proliferation and cell viability were measured at 24, 48 and 72 hours. n=8 healthy donors were all assessed in triplicate. Data expressed as mean ± SEM, *P≤0.05 and **P≤0.01, as determined by two-way ANOVA with Bonferroni's test.

3.1.3. Perhexiline and FPER-1 attenuate the increased rate of proliferation in PAH PASMCs.

To investigate whether perhexiline or FPER-1 could attenuate the hyperproliferation apparent in the PAH donor PASMCs, the PAH donor PASMCs were either treated with vehicle control, 1, 2.5, 5 or 10μM of perhexiline or FPER-1. Figure 3.3A illustrates that perhexiline treatment in PASMCs from PAH donors reduced the rate of proliferation in a concentration-dependent manner compared to the vehicle control PAH PASMCs, with a significant reduction in proliferation with 10μM treatment of perhexiline after 72 hours ($P \leq 0.05$). Figure 3.3B depicts that FPER-1 treatment in PASMCs from PAH donors reduced the rate of proliferation in a concentration-dependent manner compared to the vehicle control PAH PASMCs, with significant reductions in the rate of proliferation after 48 ($P \leq 0.05$) and 72 hours ($P \leq 0.01$) with 5μM FPER-1 and 48 ($P \leq 0.0001$) and 72 hours ($P \leq 0.0001$) with 10μM FPER-1. Figure 3.3C and Figure 3.3D show that perhexiline and FPER-1 did not significantly affect the viability of the PASMCs when compared to the vehicle control PAH PASMCs up to a concentration of 5μM. However, a concentration of 10μM of perhexiline resulted in a visible, although not significant reduction in cell viability after 72 hours (Figure 3.3C), whereas concentration of 10μM of FPER-1 resulted in a significant reduction in cell viability after 72 hours ($P \leq 0.05$) when compared to the untreated PAH PASMCs (Figure 3.3D).

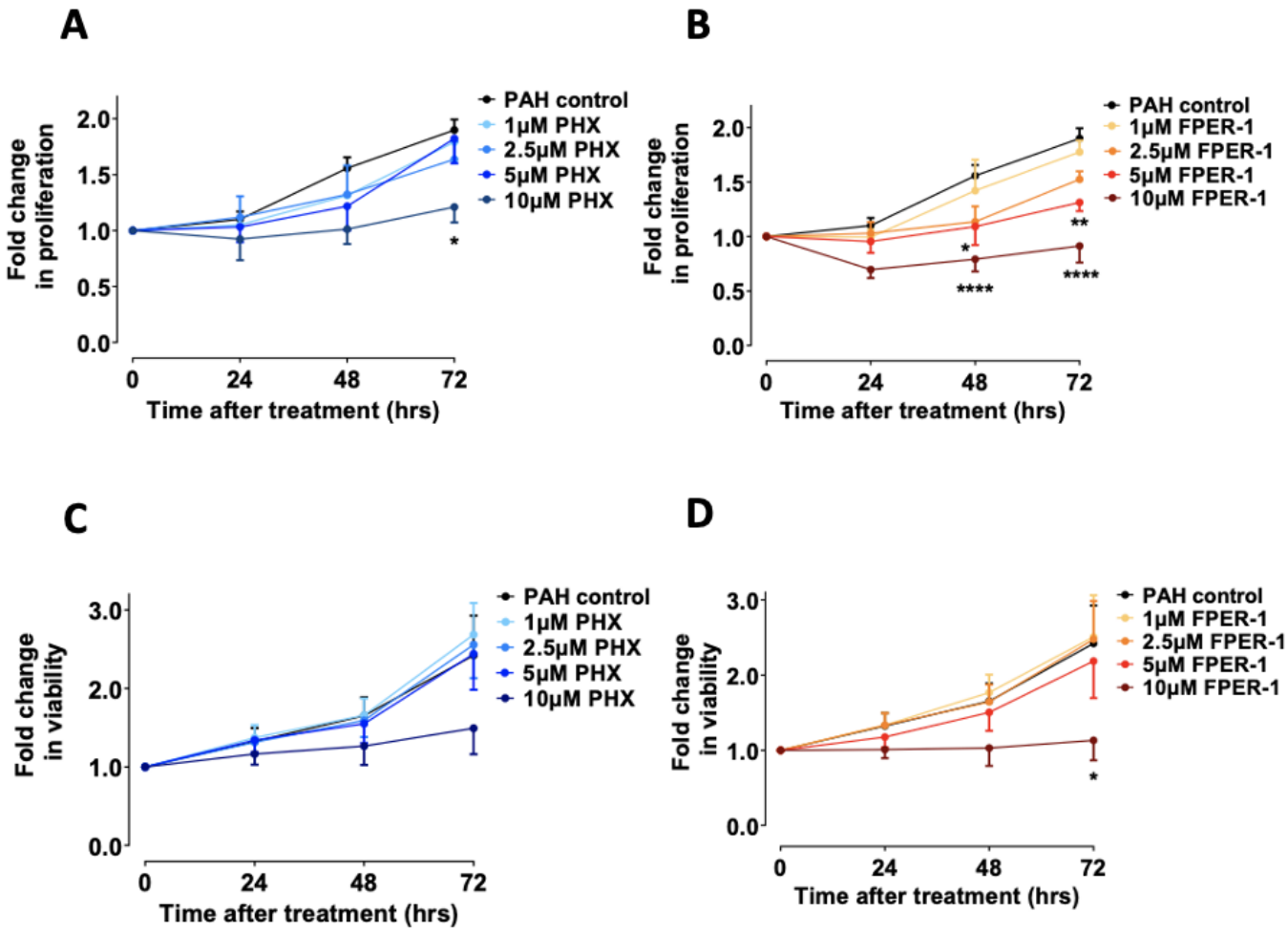

Figure 3.3. The effect of perhexiline (PHX) and FPER-1 on cell proliferation and cell viability in PAH donor PASMCs. PASMCs from PAH donors were treated with vehicle control, 1, 2.5, 5 or 10μM of perhexiline or FPER-1. Cell proliferation and cell viability was assessed. The fold change in proliferation following treatment with **(A)** perhexiline and **(B)** FPER-1. The fold change in viability following **(C)** perhexiline and **(D)** FPER-1 treatment. Cell proliferation and cell viability were measured at 24, 48 and 72 hours. n=6 PAH donors. All experiments were performed in triplicate. Data expressed as mean ± SEM, *P≤0.05, **P≤0.01, ***P≤0.001 and ****P≤0.0001, as determined by two-way ANOVA with Bonferroni's test.

3.2. The Effect of Perhexiline and FPER-1 on AKT in Healthy Control and PAH PASMCs

3.2.1. PAH PASMCs exhibit higher levels of phosphorylated AKT than PASMCs from healthy donors.

Western blot analysis was performed to investigate the expression of phosphorylated AKT^{Ser473} (p-AKT^{Ser473}) and AKT in PASMCs from healthy control (Ctrl) and PAH donors, respectively. Figure 3.4A shows a representative blot of the increased expression of both p-AKT^{Ser473} and AKT in PAH PASMCs compared to Ctrl PASMCs. This effect is further depicted in Figure 3.4B, which shows a significant increase in the phosphorylation of AKT in PAH PASMCs compared to healthy control PASMCs ($P \leq 0.01$).

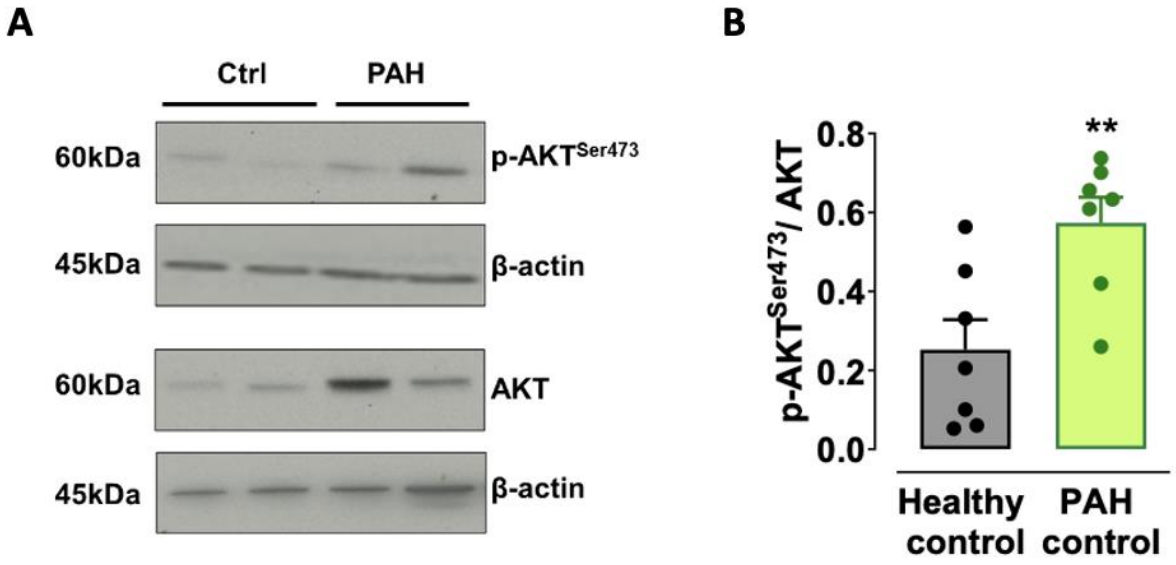

Figure 3.4. The expression of phosphorylated AKT^{Ser473} (p-AKT^{Ser473}) and AKT in PASMCs from healthy control donors and from PAH donors. (A) A representative Western Blot of the expression of p-AKT^{Ser473} and AKT in control (Ctrl) and PAH PASMCs. **(B)** The densitometry data from the Western Blot experiments of p-AKT^{Ser473} and AKT in healthy control and PAH PASMCs, expressed as a ratio of p-AKT^{Ser473}/AKT and normalised to β-actin. n=7 per group. Data expressed as mean ± SEM, **P≤0.01, as determined by an unpaired t-test.

3.2.2. Perhexiline and FPER-1 did not significantly affect the phosphorylation of AKT in control healthy PASMCs.

To determine whether perhexiline and/or FPER-1 affected the phosphorylation status and/or total expression of AKT in healthy control PASMCs, Western blot analysis were performed. As shown in Figure 3.5, neither perhexiline (2.5μM and 5μM) nor FPER-1 (2.5μM and 5μM) treatment for 1- or 24 hours appeared to attenuate the phosphorylation statuts of AKT or affect the expression of AKT in healthy PASMCs (Figure 3.5A and 3.5B) when compared to the vehicle treated healthy control PASMCs ($P>0.05$). Interestingly, treatment with both perhexiline (2.5μM and 5μM) and FPER-1 (2.5μM and 5μM) for 1 hour induced a modest, although not significant increase in the phosphorylation status of AKT in PASMCs from healthy control donors.

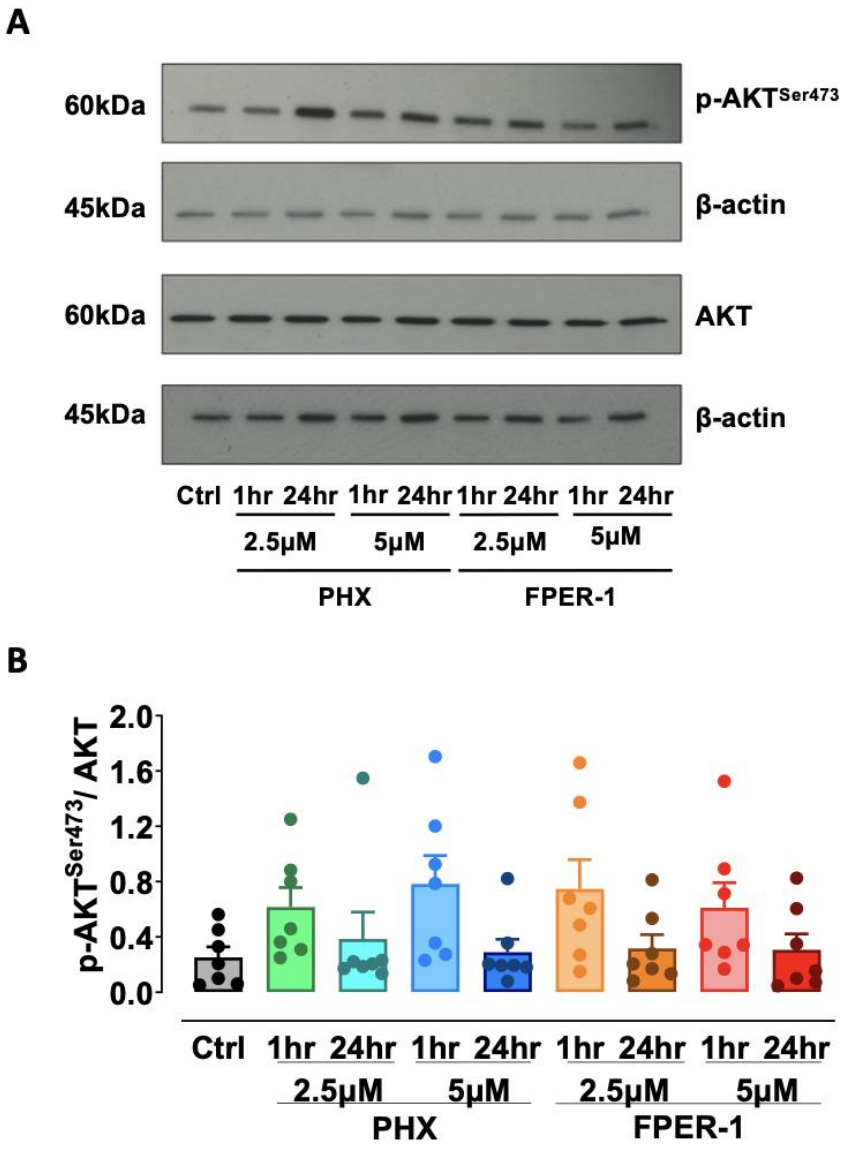

Figure 3.5. The expression of phosphorylated AKT^{Ser473} (p-AKT^{Ser473}) and AKT in PASMCs from healthy control donors in response to perhexiline and FPER-1 treatment. Healthy control PASMCs were treated with vehicle control (ctrl), 2.5 or 5μM of perhexiline or FPER-1 for either 1 hour or 24 hours and were analysed for p-AKT^{Ser473} and AKT expression by Western Blot analysis. **(A)** A representative Western Blot of the expression of p-AKT^{Ser473} and AKT in healthy control PASMCs in response to perhexiline and FPER-1. **(B)** The densitometry data from the Western Blot experiments of p-AKT^{Ser473} and AKT in healthy control PASMCs, expressed as a ratio of p-AKT^{Ser473}/AKT. The densitometry data for p-AKT^{Ser473} and AKT were normalised to β-actin. n=7. Data expressed as mean ± SEM, data analysis by one-way ANOVA with Bonferroni's test (P>0.05).

3.2.3. Perhexiline and FPER-1 attenuate the phosphorylation of AKT in PAH PASMCs.

Next, we investigated the effect of perhexiline and FPER-1 on the phosphorylation status and total expression of AKT in PASMCs from PAH donors. As shown in Figure 3.6, following treatment with perhexiline (2.5μM and 5μM) for 24 hours, there was a significant attenuation in the phosphorylation status of AKT at serine residue 473 (p-AKT^{Ser473}; P≤0.01 and P≤0.05, respectively). A similar trend was also observed with 2.5μM and 5μM FPER-1 (P≤0.05 and P≤0.01, respectively) when compared to the untreated PAH PASMCs (Ctrl). Similar to the healthy PASMCs, we observed a modest increase in the phosphorylation of AKT following treatment with both perhexilne (2.5μM and 5μM) and FPER-1 (2.5μM and 5μM) for 1 hour.

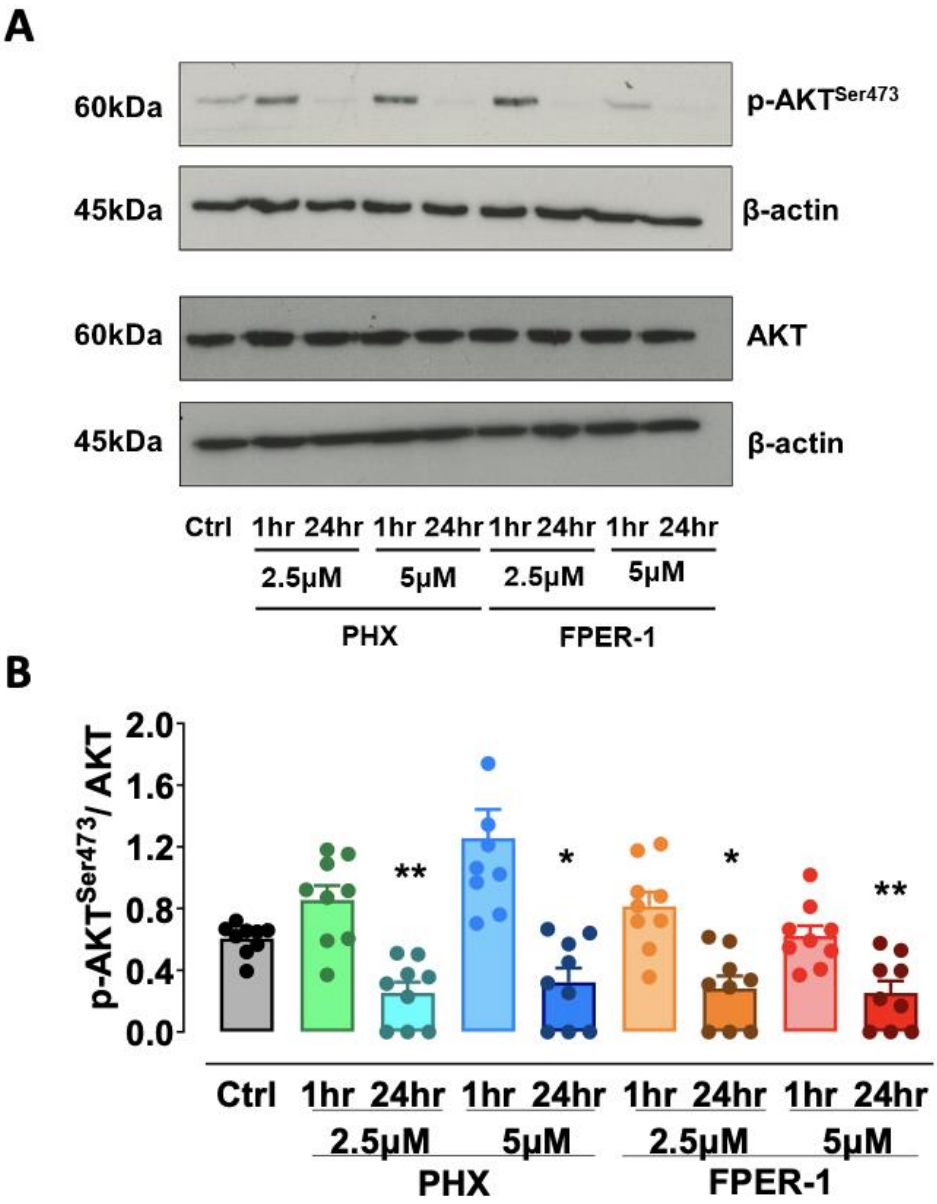

Figure 3.6. The expression of phosphorylated AKT^{Ser473} (p-AKT^{Ser473}) and AKT in PASMCs from PAH donors in response to perhexiline and FPER-1 treatment. PAH PASMCs were treated with vehicle control (ctrl), 2.5 or 5μM of perhexiline (PHX) or FPER-1 for either 1 hour or 24 hours and were analysed for p-AKT^{Ser473} and AKT expression by Western Blot analysis. **(A)** A representative Western Blot of the expression of p-AKT^{Ser473} and AKT in PAH PASMCs in response to perhexiline and FPER-1. **(B)** The densitometry data from the Western Blot experiments of p-AKT^{Ser473} and AKT in PAH PASMCs, expressed as a ratio of p-AKT^{Ser473}/AKT and were normalised to β-actin. n=3 cell lines, ran in triplicate. Data expressed as mean ± SEM, n=9; *P≤0.05 and **P≤0.01 when compared to Ctrl, as determined by one-way ANOVA with Bonferroni's test.

3.3. The Effect of Perhexiline and FPER-1 on ERK1/2 in Healthy Control and PAH PASMCs

3.3.1. PAH PASMCs demonstrate a slight increase in the phosphorylation of ERK1/2 when compared to PASMCs from healthy donors.

Increased phosphorylation of ERK1/2 has been reported to play an essential role in the increased PASMC proliferation during PAH (131,132). We therefore tested whether our experimental model induced an increase in phosphorylation of ERK1/2$^{Thr202/Tyr204}$ (p-ERK1/2$^{Thr202/Tyr204}$) and/or total ERK1/2 expression in PAH PASMCs when compared to healthy control donors. We found that PASMCs from PAH donors caused a modest but not significant increase in p-ERK1/2$^{Thr202/Tyr204}$ and total ERK1/2 expression when compared to PASMCs from healthy control donors (P=0.2912; Figure 3.7A and Figure 3.7B).

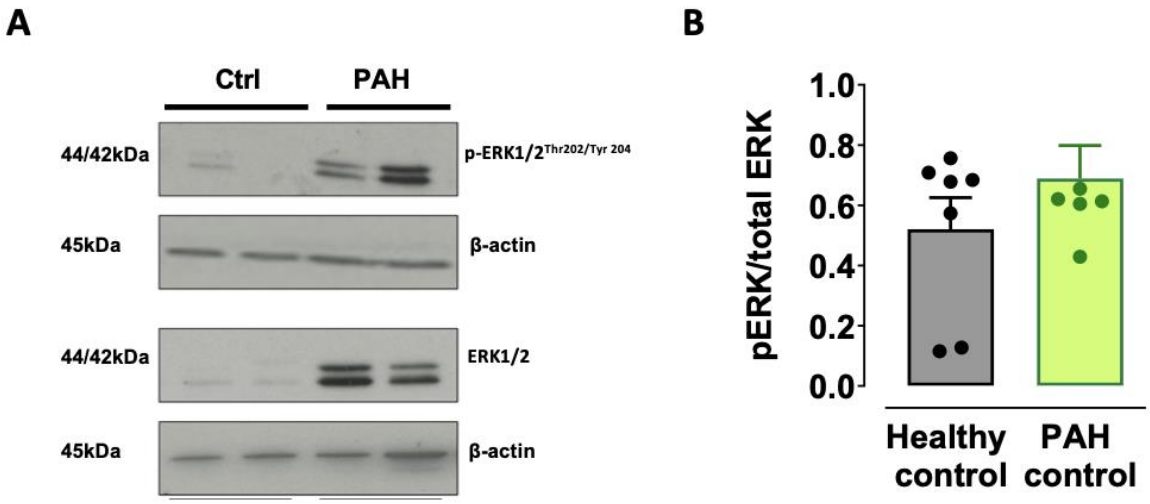

Figure 3.7. The expression of phosphorylated ERK1/2$^{Thr202/Tyr204}$ (p-ERK1/2$^{Thr202/Tyr204}$) and ERK1/2 in PASMCs from healthy control donors and from PAH donors. (A) A representative Western Blot of the expression of p-ERK1/2$^{Thr202/Tyr204}$ and ERK1/2 in control (Ctrl) and PAH PASMCs. **(B)** The densitometry data from the Western Blot experiments of p-ERK1/2$^{Thr202/Tyr204}$ and ERK1/2 in healthy control and PAH PASMCs, expressed as a ratio of p-ERK1/2$^{Thr202/Tyr204}$/ERK1/2. The densitometry data for p-ERK1/2$^{Thr202/Tyr204}$ and ERK1/2 were normalised to β-actin. n=7 Ctrl and n=5 PAH. Data expressed as mean ± SEM, data analysis by an unpaired t-test, P=0.2912.

3.4.2. Perhexiline and FPER-1 treatment did not significantly affect the phosphorylation of ERK1/2 in control healthy PASMCs.

To investigate whether perhexiline and/or FPER-1 altered ERK expression in the healthy donor PASMCs, Western blot experiments were also performed using PAMSCs from healthy control donors. We found that neither perhexiline (2.5μM and 5μM) nor FPER-1 (2.5μM and 5μM) treatment for 24 hours caused a significant effect on either the phosphorylation status of ERK1/2 or total expression of ERK1/2 when compared to the untreated healthy control PASMCs ($P>0.05$) (Figure 3.8A and Figure 3.8B). Although not significant, there was a modest increase in the phosphorylation of ERK1/2 following 1-hour treatment both perhexiline (2.5μM and 5μM) and FPER-1 (2.5μM and 5μM) in healthy control PASMCs compared to untreated healthy control PASMCs.

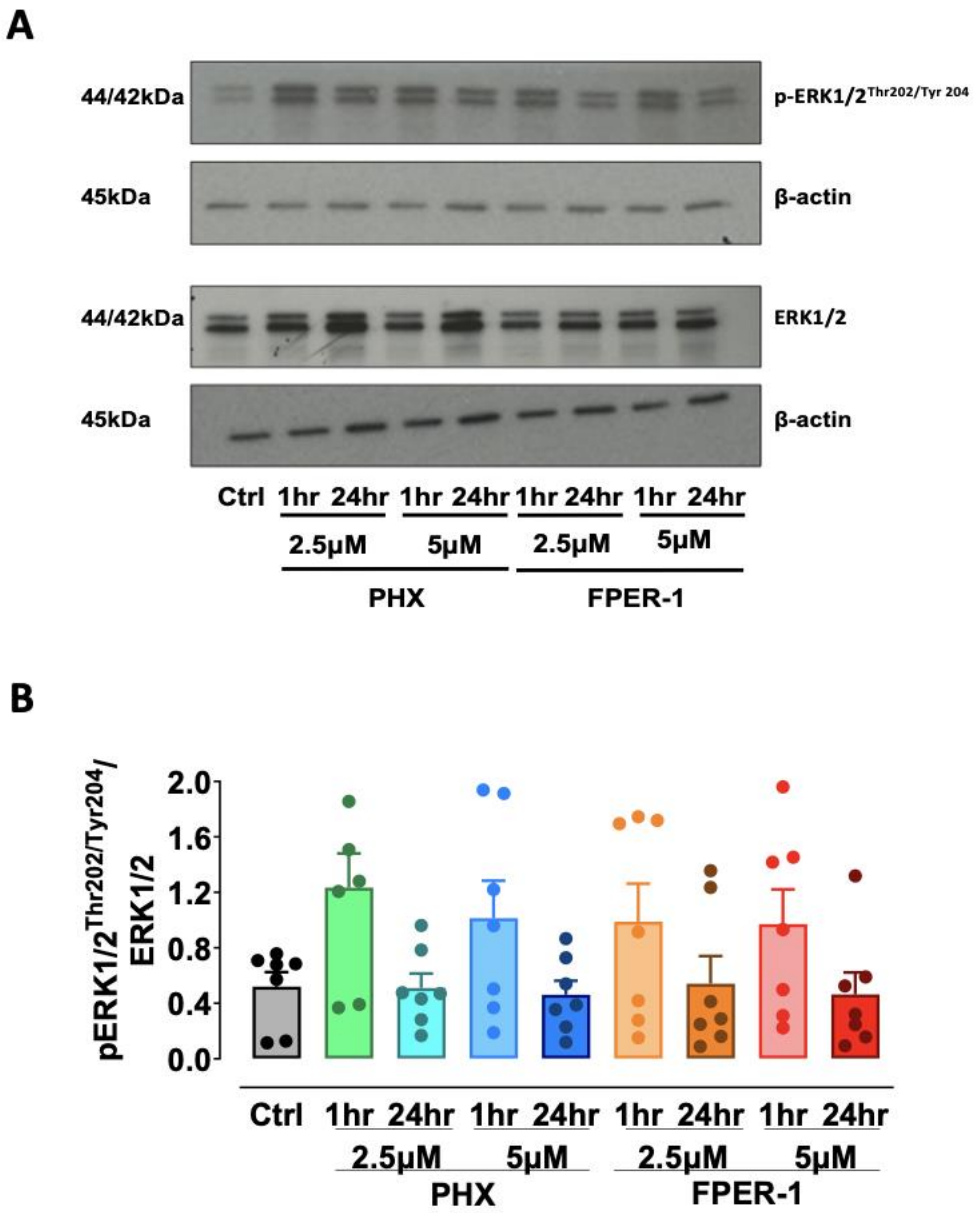

Figure 3.8. The expression of phosphorylated ERK1/2$^{Thr202/Tyr204}$ (p-ERK1/2$^{Thr202/Tyr204}$) and ERK1/2 in PASMCs from healthy control donors in response to perhexiline and FPER-1 treatment. Healthy control PASMCs were treated with vehicle control, 2.5 or 5μM of perhexiline or FPER-1 for either 1 hour or 24 hours and were analysed for p-ERK1/2$^{Thr202/Tyr204}$ and ERK1/2 expression by Western Blot analysis. **(A)** A representative Western Blot of the expression of p-ERK1/2$^{Thr202/Tyr204}$ and ERK1/2 in healthy control PASMCs in response to perhexiline and FPER-1. **(B)** The densitometry data from the Western Blot experiments of p-ERK1/2$^{Thr202/Tyr204}$ and ERK1/2 in healthy control PASMCs, expressed as a ratio of p-ERK1/2$^{Thr202/Tyr204}$/ ERK1/2 and were normalised to β-actin. n=7. Data expressed as mean ± SEM, data analysis by one-way ANOVA with Bonferroni's test.

3.4.3. Perhexiline and FPER-1 treatment did not significantly affect the phosphorylation of ERK1/2 in PAH PASMCs.

Next, we assessed whether perhexiline and/or FPER-1 pre-treatment for 1 or 24 hours reduces the expression of ERK 1/2 in the PAH donors. We found that neither perhexiline (2.5μM and 5μM) nor FPER-1 (2.5μM and 5μM) significantly changed the phosphorylation status of ERK1/2 and total expression of ERK1/2 in PAH PASMCs when compared to untreated PAH PASMCs ($P>0.05$) (Figure 3.9A and Figure 3.9B).

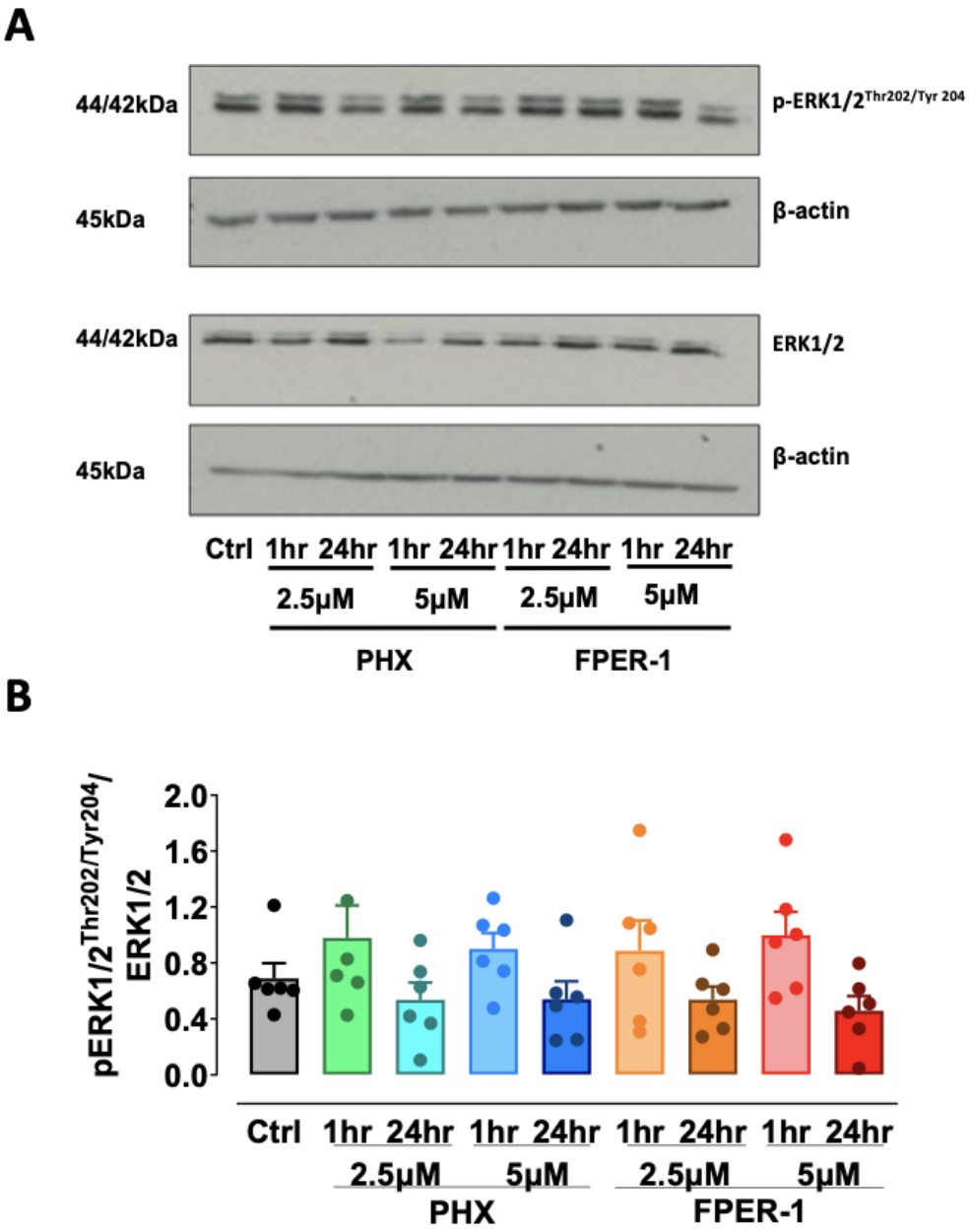

Figure 3.9. The expression of phosphorylated ERK1/2$^{Thr202/Tyr204}$ (p-ERK1/2$^{Thr202/Tyr204}$) and ERK1/2 in PASMCs from PAH donors in response to perhexiline and FPER-1 treatment. PAH PASMCs were treated with vehicle control, 2.5 or 5μM of perhexiline or FPER-1 for either 1 hour or 24 hours and were analysed for p-ERK1/2$^{Thr202/Tyr204}$ and ERK1/2 expression by Western Blot analysis. **(A)** A representative Western Blot of the expression of p-ERK1/2$^{Thr202/Tyr204}$ and ERK1/2 in PAH PASMCs in response to perhexiline and FPER-1. **(B)** The densitometry data from the Western Blot experiments of p-ERK1/2$^{Thr202/Tyr204}$ and ERK1/2 in PAH PASMCs, expressed as a ratio of p-ERK1/2$^{Thr202/Tyr204}$/ERK1/2 and normalised to β-actin. n=6. Data expressed as mean ± SEM, data analysis by one-way ANOVA with Bonferroni's test showed no significance (P>0.05).

3.4. The Effect of Perhexiline and FPER-1 on PDH-E1α in Healthy Control and PAH PASMCs

3.4.1. PAH PASMCs demonstrate higher levels of phosphorylation of PDH-E1α than PASMCs from healthy donors.

To validate whether PAH induces a reduction in PDH activity (e.g increased phosphorylation of PDH) when compared with the healthy donors, phosphorylation status of p-PDH-E1α^{Ser293} and expression of PDH (PDH-E1α) was assessed in PASMCs from PAH and healthy control (Ctrl) donors by Western blotting. We found that there was a significant increase in p-PDH-E1α^{Ser293} in PAH PASMCs compared to Ctrl PASMCs ($P \leq 0.01$; Figure 3.10B). Figure 3.10B shows the densitometry data of the expression of p-PDH-E1α^{Ser293} normalised to the expression of PDH-E1α.

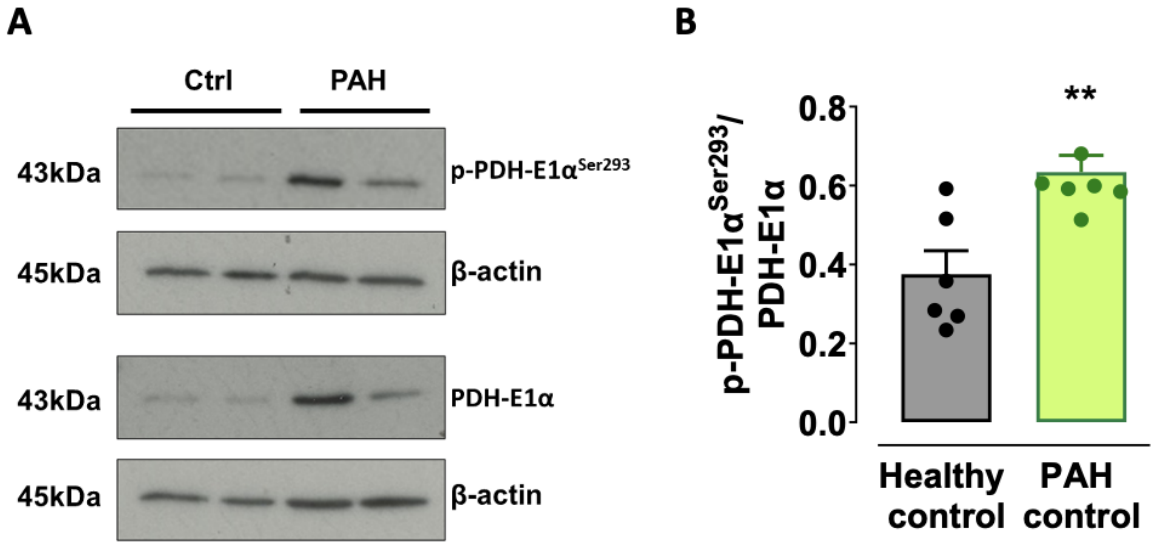

Figure 3.10. The expression of phosphorylated PDH-E1α^{Ser293} (p-PDH-E1α^{Ser293}) and PDH-E1α in PASMCs from healthy control donors and from PAH donors. (A) A representative Western Blot of the expression of p-PDH-E1α^{Ser293} and PDH-E1α in control (Ctrl) and PAH PASMCs. **(B)** The densitometry data from the Western Blot experiments of p-PDH-E1α^{Ser293} and PDH-E1α in healthy control and PAH PASMCs, expressed as a ratio of p-PDH-E1α^{Ser293}/ PDH-E1α. The densitometry data for p-PDH-E1α^{Ser293} and PDH-E1α were normalised to β-actin. n=6 per group. Data expressed as mean ± SEM, **=P≤0.01, as determined by an unpaired t-test.

3.4.2. Perhexiline and FPER-1 did not have a substantial effect on the phosphorylation of PDH-E1α in control healthy PASMCs.

To investigate whether perhexiline and/or FPER-1 altered the phosphorylation status of PDH-E1α in healthy control PASMCs, Western blot experiments were also performed in healthy control PASMCs. Pre-treatment with either perhexiline or FPER-1 did not significantly effect the phosphorylation of PDH-E1α ($P>0.05$) when compared to the vehicle treated healthy control donor PASMCs (Figure 3.11B).

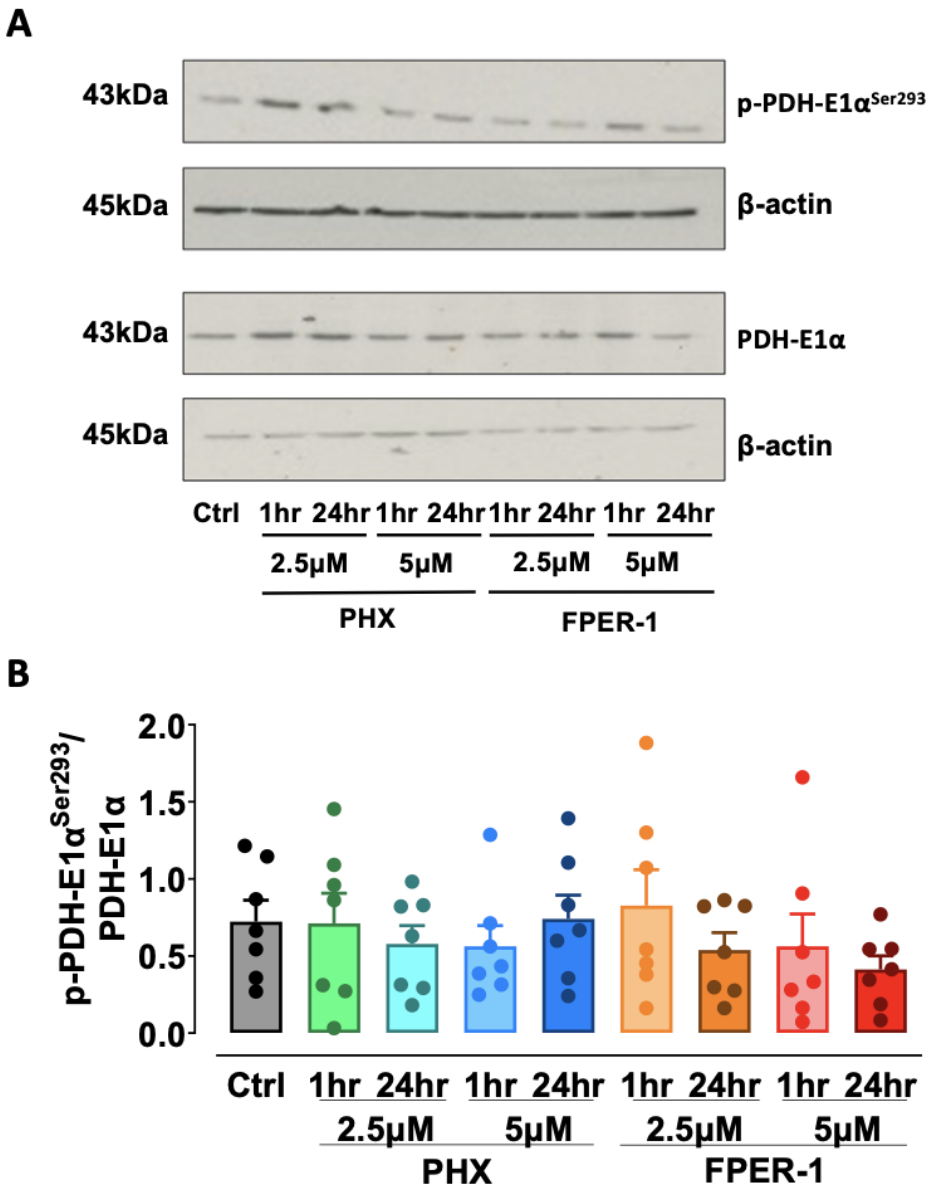

Figure 3.11. The expression of phosphorylated PDH-E1α^{Ser293} (p-PDH-E1α^{Ser293}) and PDH-E1α in PASMCs from healthy control donors in response to perhexiline and FPER-1 treatment. Healthy control PASMCs were treated with either vehicle control (ctrl), 2.5 or 5μM of perhexiline or FPER-1 for either 1 hour or 24 hours and were analysed for p-PDH-E1α^{Ser293} and PDH-E1α expression by Western Blot analysis. **(A)** A representative Western Blot of the expression of p-PDH-E1α^{Ser293} and PDH-E1α in healthy control PASMCs in response to perhexiline and FPER-1. **(B)** The densitometry data from the Western Blot experiments of p-PDH-E1α^{Ser293} and PDH-E1α in healthy control PASMCs, expressed as a ratio of p-PDH-E1α^{Ser293}/PDH-E1α. The densitometry data for p-PDH-E1α^{Ser293} and PDH-E1α were normalised to β-actin. n=7. Data expressed as mean ± SEM, data analysis by one-way ANOVA with Bonferroni's test.

3.4.3. Perhexiline and FPER-1 attenuate the phosphorylation of PDH-E1α in PAH PASMCs.

To determine whether perhexiline and/or FPER-1 improves PDH activity, the phosphorylation status of p-PDH-E1α^{Ser293} and expression of PDH (PDH-E1α) was assessed in PASMCs from PAH donors. As depicted in Figure 3.12, treatment with either perhexiline or FPER-1 for 1 hour significantly reduced the phosphorylation status of PDH-E1α (e.g. increased PDH activity) when compared to the untreated PAH PASMCs. A significant reduction in p-PDH-E1α^{Ser293} was particularly found with 2.5μM (P≤0.05) and 5μM (P≤0.01) perhexiline at 1 hour. In contrast, FPER-1 caused significant reduction in p-PDH-E1α^{Ser293} with 2.5μM (P≤0.01) and 5μM (P≤0.05) at 1hour and also at 24 hours pre-treatment with 5μM (P≤0.05) (Figure 3.12A and Figure 3.12B). Although not significant, there was a slight reduction in the phosphorylation of PDH-E1α with 2.5μM perhexiline, 5μM perhexiline and 2.5μM FPER-1 when treated for 24 hours (Figure 3.12B). Figure 3.12A also shows that neither perhexiline (2.5μM and 5μM) or FPER-1 (2.5μM and 5μM) treatment for 1- or 24 hours had an impact on the total expression of PDH-E1α.

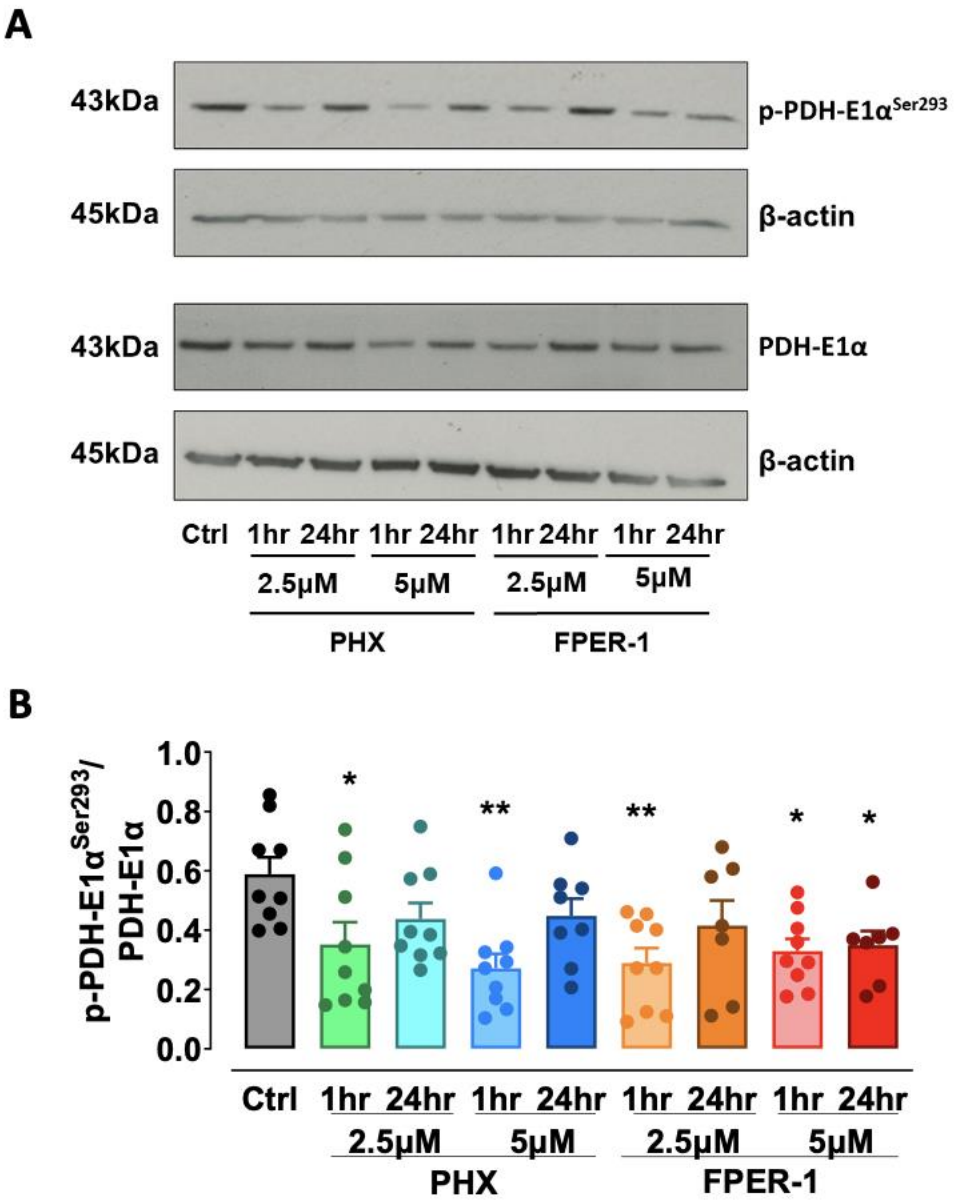

Figure 3.12. The expression of phosphorylated PDH-E1α^{Ser293} (p-PDH-E1α^{Ser293}) and PDH-E1α in PASMCs from PAH donors in response to perhexiline and FPER-1 treatment. PAH PASMCs were treated with vehicle control (ctrl), 2.5 or 5μM of perhexiline or FPER-1 for either 1 hour or 24 hours and were analysed for p-PDH-E1α^{Ser293} and PDH-E1α expression by Western Blot analysis. **(A)** A representative Western Blot of the expression of p-PDH-E1α^{Ser293} and PDH-E1α in PAH PASMCs in response to perhexiline and FPER-1. **(B)** The densitometry data from the Western Blot experiments of p-PDH-E1α^{Ser293} and PDH-E1α in PAH PASMCs, expressed as a ratio of p-PDH-E1α^{Ser293}/PDH-E1α and were normalised to β-actin. n=3 cell lines, ran in triplicate. Data expressed as mean ± SEM, *P≤0.05 and **P≤0.01 when compared to Ctrl, as determined by one-way ANOVA with Bonferroni's test.

4. Discussion

In the present study, we examined whether the parent drug, perhexiline and the novel FPER-1, are able to reduce the rate of proliferation of PASMCs from PAH donors. To the best of our knowledge, this is the first study to show that both perhexiline and FPER-1 are able to attenuate the rate of proliferation of PASMCs from PAH donors by reducing the phosphorylation of AKT^{Ser473}. Furthermore, we show that perhexiline and FPER-1 treatment improves mitochondrial respiration by attenuating the phosphorylation status of PDH^{Ser293} in PASMCs from PAH donors.

There is a growing body of evidence in the literature which supports the notion that PAH exhibits a metabolic phenotype similar to that of cancer cells (92,95,111–113). This cancer like metabolic shift is known as the Warburg effect, whereby PAH PASMCs reprogram their energy metabolism to use glycolysis over oxidative phosphorylation for ATP production (92,95,111–113). Currently, there are no treatments to reverse the pathophysiology of PAH. However, recent attempts at reversing the pathophysiology of PAH using other metabolic agents such as DCA to target the metabolic pathways have shown promise, but resulted in toxic side effects in both preclinical and clinical trials (92–95,112,142). Therefore, new therapies to target the metabolic pathways in PAH PASMCs is urgently required.

The use of perhexiline as a treatment for cardiac diseases such as chronic heart failure, inoperable aortic stenosis, acute coronary syndromes and hypertrophic cardiomyopathy has been shown to improve key indicators of cardiac function such as VO_2 max and left

ventricular ejection fraction (157,159–161). Previous studies have also demonstrated that perhexiline induces its benefits in treating cardiac disease by decreasing mitochondrial fatty acid uptake and increasing carbohydrate metabolism, therefore subsequently improving metabolic efficiency by producing more ATP for a specified oxygen consumption (157,161). Despite these beneficial effects of perhexiline for the treatment of these cardiac diseases, it has been shown that the primary mechanism of perhexiline clearance appears to be *via* the CYP2D6 pathway (173). However, patients with a polymorphic variant of the CYP2D6 gene are known to have poor perhexiline metabolism which leads to hepatotoxicity and neurotoxcity (169–171,176,181,182). Given the fact that perhexiline treatment requires monitoring of plasma concentrations to prevent toxicity (176), our group has designed and synthesised a novel derivitave, FPER-1 that posses a similar therapeutic profile as perhexiline but avoids metabolism *via* CYP2D6 (158). Therefore circumventing the associated toxicities with CYP2D6 metabolism (158).

We have previously demonstrated that FPER-1 has a similar inhibitory potency against rat mitochondrial CPT-1 *in vitro* when compared to the parent drug perhexiline and also has a similar pharmacokinetic profile following *in vivo* rodent pharmacokinetic models (158). In addition, we have shown by utilising the *ex vivo* Langendorff mouse model, that FPER-1 improves cardiac contractility and cardiac relaxation following perfusion with a high fat buffer in a dose-dependant manner (158). Based on these promising findings, we hypothesised that perhexiline and FPER-1 may offer therapeutic effects in PAH.

To test our hypothesis, we first examined the rate of proliferation in both the PASMCs from healthy donors and PAH donors, respectively. In agreement to previously published studies, we found that untreated PAH PASMCs had an increased rate of proliferation when compared to the untreated PASMCs from the healthy donors (183–186). In addition, we found that both perhexiline and FPER-1 could attenuate the PAH PASMC proliferation whilst maintaining the cell viability. These findings corroborate with previous work by Xiao et al (112) and Li et al (113) who assessed the effects of an alternative metabolic agent known as DCA (PDK1 inhibitor). The authors showed that in rat and human PASMCs treated with PDGF to mimic PAH, there was an increased rate of proliferation but DCA treatment significantly attenuated PASMC proliferation (112,113). In addition, another group reported that in isolated rat PASMCs treated with PDGF, treatment with the CPT-1 inhibitor etomoxir reversed the PDGF-induced increase in PASMC proliferation *in vitro* (126). These findings, along with our current data demonstrate that it is possible to modulate the metabolic pathway and attenuate the increased PASMC proliferation that is observed in PAH utilising an *in vitro* cell culture model. However, the mechanism by which perhexiline and/or FPER-1 produce their anti-proliferative effect requires further investigation.

To determine the potential mechanism by which perhexiline and FPER-1 reduces cell proliferation, we next examined the role of the PI3K/AKT and ERK pathways. We chose to focus on these pathways because both the PI3K/AKT and ERK1/2 pathways have both been reported to increase PAH PASMC proliferation (112,113,127–133). In particular, various studies have shown that there is increased phosphorylation of AKT^{Ser473} in

multiple models of PAH, including rat PASMCs treated with PDGF (112,130), human PASMCs treated with PDGF (113,132), rat PASMCs exposed to hypoxia (127), and human PASMCs exposed to hypoxia (128,131,132). There is also evidence of increased phosphorylation of ERK in PAH preclinical models, including human PASMCs exposed to hypoxia (131,132) and treated with PDGF (132). Furthermore, perhexiline has also been shown to inhibit breast cancer cell proliferation *in vitro* by reducing the phosphorylation of AKT and ERK (187). Therefore, these findings suggest that our observed reduction in PASMC proliferation following perhexiline or FPER-1 treatment may potentially occur *via* inhibition of the PI3K/AKT or ERK pathways.

To estabilish whether perhexiline and/or FPER-1 attenuates cell proliferation *via* the AKT and/or ERK pathway, we assessed the phosphorylation status by Western blotting. In the present study, we found that PASMCs from PAH donors had a significant increase in the phosphorylation of AKT compared to PASMCs from healthy donors. These findings supports previous studies that have demonstrated that there is increased phosphorylation of AKT in both rat and human *in vitro* models of PAH (112,113,127,128,130–132). Furthermore, we also found that both perhexiline and FPER-1 significantly reduced the phosphorylation status of AKT^{Ser473} in PASMCs from PAH donors following 24 hours pretreatment, but had no effect on AKT in PASMCs from healthy donors. Our findings corroborate with previous studies, which have demonstrated that treatment with DCA (112) or with the AKT inhibitor LY294002 (113,132) reduces AKT phosphorylation in PDGF-treated PASMCs to mimic PAH. To further support our results, perhexiline has been demonstrated to inhibit the proliferation of MDA-MB-468 breast cancer cells *in vitro*

through reducing the phosphorylation of AKT (187). Overall, these findings, together with our current results, suggest that perhexiline and FPER-1 attenuates cell proliferation *via* the AKT pathway.

Next, we examined the role of ERK in healthy and PAH donor PASMC proliferation. We observed a modest, although not significant increase in the phosphorylation of ERK in the PAH PASMCs when compared to the healthy donor PASMCs. However, our findings contradict work by previous groups. For instance, it has been demonstrated that in human PASMCs exposed to hypoxia or treated with PDGF to mimic PAH, there is a significant increase in ERK phosphorylation (131,132,188). Where as previous work by BelAiba and colleagues have shown that in mouse PASMCs, hypoxia stimulates HIF-1α mRNA expression *via* the PI3K/AKT pathway and independently of ERK1/2 (189), therefore, supporting our results. Despite these findings, it is important to note that these studies were conducted in mouse PASMCs exposed to hypoxia or human PASMCs from healthy donors which were exposed to hypoxia or treated with PDGF to mimic PAH. Whereas our experiments were carried out using PASMCs from patients with PAH. Therefore, there is a possibility of different mechanisms in these experimental designs.

Despite not observing a significant increase in the phosphorylation of ERK1/2 in the PASMCs from PAH donors compared to PASMCs from healthy donors, we next investigated the effect of perhexiline and FPER-1 treatment on the phosphorylation status of ERK1/2 in healthy and PAH donor PASMCs. We found that treatment with perhexiline and FPER-1 did not significantly affect the phosphorylation status of ERK1/2.

Interestingly, there are mixed results in the literature related to the effect of perhexiline on the ERK pathway. For example, previous studies investgating the effect of perhexiline on the ERK pathway in prostate (190) and breast (187) cancer cell lines have shown that perhexiline treatment reduces ERK phosphorylation. On the other hand, Nassar and colleagues have shown that perhexiline treatment did not reduce the phosphorylation of ERK in two different prostate cancer cell lines (190). Furthermore, Ren and colleagues (191) investigated the mechanism in which perhexiline induces hepatotoxicity and showed that perhexiline treatment (25μM for 4 hours) induced cytotoxicity in HepG2 cells, a hepatocarcinoma cell line. However, the authors reported that perhexiline treatment (5-25μM) did not affect the phosphorylation status of ERK in the HepG2 cells (191), therefore supporting our findings.

Although not significant, we did observe that 1-hour pretreatment with perhexiline or FPER-1 caused a modest increase in the phosphorylation of ERK1/2 in PASMCs from PAH and healthy donors compared to the untreated PAH/healthy PASMCs. The reason for the observed modest increase in the phosphorylation of ERK1/2 following perhexiline/FPER-1 treatment is unclear. However, a previous study investigating the effect of saturated fatty acids on ERK signalling in diabetic mice, has demonstrated that palmitate, one of the most common saturated fatty acids in mammals, induced a substantial increase in the phosphorylation of ERK in HepG2 cells (192). Since perhexiline and FPER-1 inhibit CPT-1 and subsequently, fatty acid oxidation, there could be an accumulation of fatty acids which could be causing the observed modest increase in the phosphorylation of ERK following perhexiline and FPER-1 treatment.

To explore the mechanistic pathway for the reduction of PASMCs proliferation further, we next examined the effect of perhexiline and FPER-1 on the phosphorylation status of PDH^{Ser293}. PDH is known to catalyse the decarboxylation of pyruvate to acetyl-CoA, which plays an essential role in linking glycolysis to the TCA cycle. During physiological conditions, PDH is inactivated by PDKs. Previous studies have reported decreased PDH activity (indicated by increased phosphorylation) during PAH, which leads to decreased aerobic glucose metabolism (95,113,118). Furthermore, one study has shown that in lung tissue from PAH patients, the expression of PDK1 is increased and subsequently, the phosphorylation of PDH^{Ser293} is increased which inhibits PDH activity (95). This study suggests that in the lung of the PAH patients, there is indeed reduced PDH activity and therefore decreased aerobic glucose metabolism (95). Moreover, other studies corroborate these findings whereby human PASMCs treated with PDGF and right ventricular fibroblasts derived from MCT-treated rats have been shown to have increased phosphorylation of PDH^{Ser293} (113,118).

Therefore, activation of PDH by inhibiting PDK may lead to metabolic benefits in PAH. To support this notion, previous studies have attempted to reverse the pathophysiology of PAH by using the PDK inhibitor DCA (95,113,118). Michelakis and associates treated PAH patients with DCA with the aim of reducing the inhibition of PDH and subsequently increasing aerobic glucose metabolism (95). The authors found that DCA treatment reduced the phosphorylation of PDH^{Ser293} and subsequently increased PDH activity and mitochondrial respiration (indicated by an increase in the oxygen consumption rate) in the

lungs of the PAH patients, as well as significantly reducing the mPAP and PVR (95). Furthermore, previous studies have shown that DCA treatment decreases the rate of proliferation and the phosphorylation of PDH^{Ser293} in both human PASMCs treated with PDGF and right ventricular fibroblasts derived from MCT-treated rats (113,118). Overall, these findings suggest that DCA may be able to improve PDH activity and mitochondrial respiration and decrease the rate of proliferation in PAH PASMCs. Therefore, further supporting the notion that pehexiline and FPER-1 may potentially have similar therapeutic effects.

To investigate the role of PDH in healthy and PAH PASMC proliferation, we examined the phosphorylation status of PDH^{Ser293} in healthy and PAH PASMCs. We observed a significant increase in the phosphorylation of PDH^{Ser293} in PASMCs from PAH donors compared to PASMCs from healthy donors. Thus, corroborating with previous studies as discussed above (95,113). In the present study, we also assessed the effect of perhexiline and FPER1 pre-treatment on the phosphorylation status of PDH^{Ser293} from both healthy and PAH PASMCs. Our results revealed that both perhexiline and FPER-1 significanlty reduced $pPDH^{Ser293}$ in the PAH PASMCs, but caused no significant reduction in the phosphorylation status of PDH^{Ser293} in the healthy PASMCs donors. Thus, further corroborating with similar findings observed with DCA treatment in various PAH models (95,113). Furthermore, a proteomic study investigating the effect of perhexiline on the heart has suggested that perhexiline may directly increase PDH activity (193). Overall, our results suggest that perhexiline and FPER1 have the ability to improve PDH activity in PAH PASMCs and potentially shift the Warburg effect. However, further studies are

warranted to validate whether these changes observed in the present study improves mitochondrial function by improving aerobic glucose metabolism.

Study Limitations

Whilst we have evaluated the direct effects of perhexiline and FPER-1 on $pPDH^{Ser293}$ it is possible that the PDH activity is augmented indirectly. For example, perhexiline is a CPT-1 inhibitor and may indeed inhibit the FAO pathway. Previous work by Randle and colleagues have shown that glucose and fatty acids compete for their oxidation in muscle and adipose tissue and showed that FAO inhibited glucose oxidation *via* short-term inhibition of key enzymes involved in glycolysis such as 6-phosphofructo-1-kinase (PFK-1) and PDH (106). Therefore, it is plausible that inhibiting the FAO pathway with perhexiline or FPER-1 may indirectly increase PDH activity *via* the Randle cycle. Furthermore, we cannot exclude that perhexiline or FPER-1 may target other molecular pathways. For instance, previous work by Horowitz and colleagues have reported the phenomenon of platelet NO resistance to NO donors in various cardiovascular diseases (CVD) (194–196). The Horowitz group postulated that perhexiline may modulate the NO pathway in patients with type 2 diabetes and CVD (197). The authors showed that perhexiline treatment increased the anti-aggregatory effects of the NO donor, sodium nitroprusside and subsequently improved platelet NO responsiveness (197). Therefore, if perhexiline is able to modulate the NO pathway in patients with type 2 diabetes and CVD, perhaps perhexiline may be able to modulate the NO pathway in PAH patients. Perhexiline could potentially be used in combination with other approved current

treatments targeting the NO pathway such as PDE5 inhibitors, to promote NO-induced vasodilation of the PASMCs.

Another pathway perhexiline could target in PAH is the tyrosine-protein kinase Fyn (FYN) pathway. Previous work by Kant et al has demonstrated that the anti-tumour activity of perhexiline in glioblastoma cells is not through inhibition of the FAO pathway but by increasing the phosphorylation of FYN and therefore increasing FYN activity (166). Furthermore, Kurahara and colleagues have shown that eicosapentaenoic acid (EPA), a long-chain n-3 polyunsaturated fatty acid which has previously been shown to inhibit the proliferation of VSMCs (198), inhibited the increased rate of proliferation in PASMCs derived from idiopathic PAH patients *via* inhibition of FYN (199). The same study investigated the use of EPA in rats treated with MCT to mimic PAH (199). The authors found that EPA treatment improved cardiac function and right ventricular hypertrophy and reversed pulmonary vascular remodelling in the MCT-treated rats (199). Therefore, perhexiline may be able to modulate the FYN pathway and serve as a treatment to reduce the PASMC proliferation and vascular remodelling in PAH patients. In summary, perhexiline is more than just a CPT-1 inhibitor and impacts multiple pathways and we cannot be conclusive of the exact mechanism(s) that it may target in PAH and this should be investigated further in future studies.

Future Direction

Our findings demonstrate that perhexiline and FPER-1 can effectively reduce the rate of proliferation by modulating the AKT pathway and improving PDH activity in PASMCs from

PAH donors. This outcome provides promise that perhexiline/FPER-1 could act as a therapeutic agent to help reverse the vascular remodelling and Warburg metabolism apparent in PAH. However, there are still some questions that need further investigation.

To investigate the efficacy of perhexiline/FPER-1 *in vivo*, future studies could utilise rodent models of PAH such as treating the rodents with MCT, exposing them to hypoxia or pulmonary arterial banding to induce PAH and then treat the rodents with varying concentrations of perhexiline/FPER-1. Following this, haemodynamic changes such as pulmonary vascular resistance, mean arterial pressure and right ventricular thickness could be measured. Additionally, staining for markers of proliferation such as PCNA and Ki67 and markers of apoptosis such as cleaved caspase-3 and TUNEL in the lungs of the MCT-treated rodents could be measured. These outcomes can be compared between control, MCT-treated and MCT-treated+perhexiline/FPER-1 rodents to investigate the effect of perhexiline/FPER-1 in a more realistic whole body, albeit rodent, *in vivo* model of PAH.

To further elucidate the mechanism(s) by which perhexiline and FPER-1 are acting, additional molecular investigations could be performed. For example, PDK1 and HIF-1α are two proteins thought to be associated with the increased phosphorylation of AKT and PDH (95,118,200,201). As discussed earlier, PDK1 phosphorylates PDH and inhibits PDH activity, and previous studies have shown that PAH patients have increased expression of PDK1 in the lung (95). Also, DCA (PDK1 inhibitor) treatment increases PDH activity and mitochondrial respiration in the lung of PAH patients (95). In addition,

experimental studies have shown that in rodent models of PAH, there is normoxic activation of HIF-1α and HIF-1α subsequently activates the gene coding for PDK1 (200,201). Furthermore, HIF-1α has been shown to induce the Warburg effect through increasing PDK1 expression in rats treated with MCT to mimic PAH (118). Therefore, future studies could investigate the expression of PDK1 and HIF-1α in PAH and healthy PASMCs and following that, assess the effect of perhexiline/FPER-1 treatment on the expression of PDK1/ HIF-1α.

To further explore the effect of perhexiline and FPER-1 on PDH activity and cellular metabolism, Seahorse XF analysis could be undertaken. In this experiment the differences between PAH PASMCs and control PASMCs could be used to investigate the effect of perhexiline/FPER-1 on the oxygen consumption rate and extracellular acidification rate in PAH PASMCs to see if perhexiline/FPER-1 are able to reverse the Warburg metabolism apparent in PAH.

Although FPER-1 is able to avoid CYP2D6 metabolism, the pathway responsible for hepatoxicity seen with perhexiline use (158), future studies should investigate the safety of FPER-1 in comparison to perhexiline. For example, pharmacological assessment of acute and chronic effects of FPER1 on hepatoxicity in both *in vitro* and *in vivo* models (158).

Conclusion

In conclusion, this study is the first to report the use of perhexiline and FPER-1 (a novel derivative of perhexiline) as a treatment for attenuating the rate of proliferation in PAH PASMCs whilst maintaining cell viability. We also elucidate the mechanism by which perhexiline and FPER-1 attenuate PAH PASMC proliferation as depicted in Figure 4.1. We propose a novel mechanism of action of perhexiline/FPER-1 in PAH PASMCs whereby both perhexiline and FPER-1 attenuate PAH PASMC proliferation through the modulation of the AKT pathway and also *via* mediating cellular metabolism by improving PDH activity (Figure 4.1). However, we did not observe a significant effect on the phosphorylation status of the ERK pathway following perhexiline or FPER-1 treatment (Figure 4.1.). Our findings demonstrate that FPER-1 shows promise as a novel therapeutic agent for reversing the increased PASMC proliferation apparent in PAH, but additional studies regarding the safety of FPER-1 as a therapy are required.

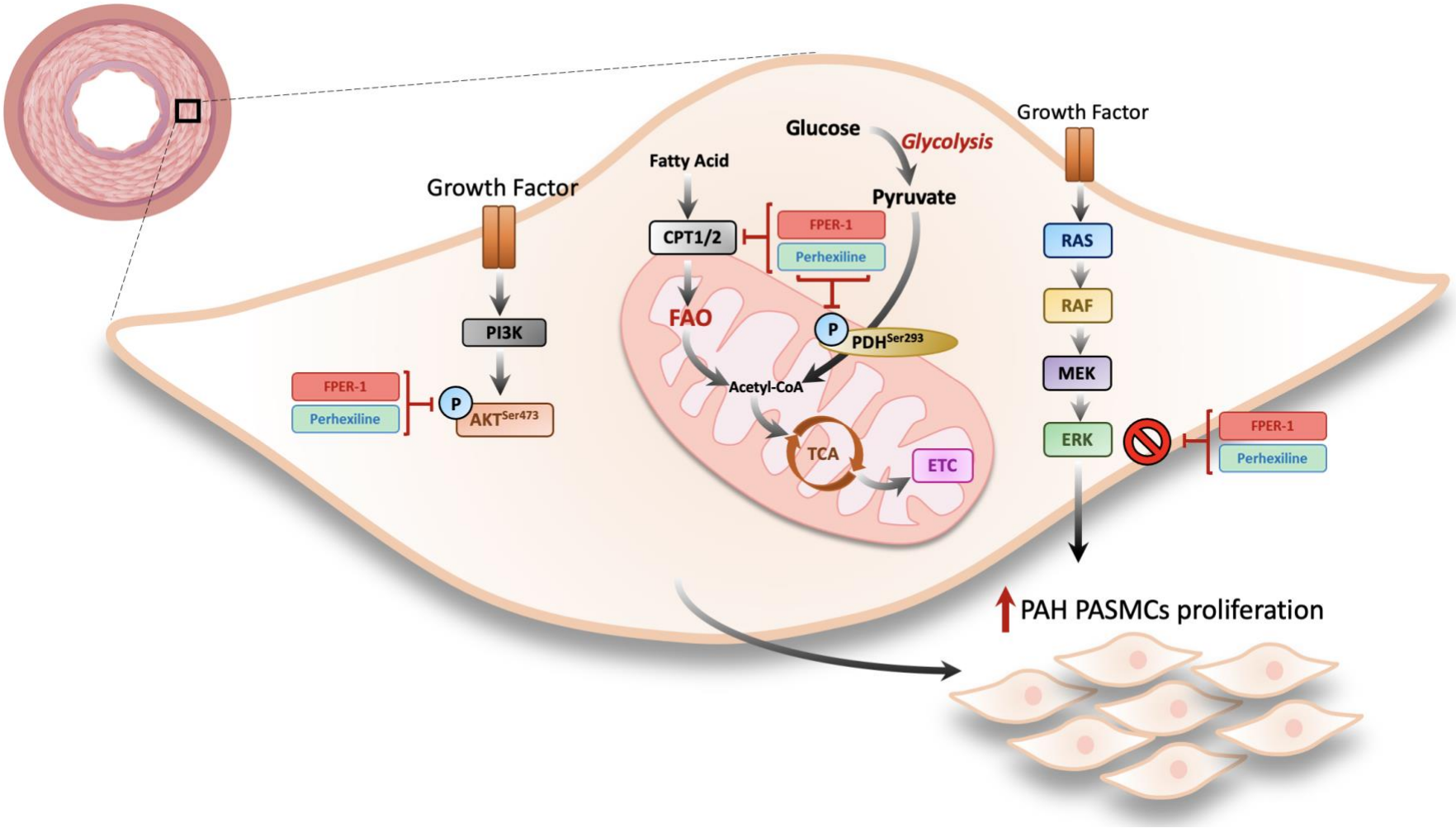

Figure 4.1. A schematic depicting our proposed mechanism of action of perhexiline and FPER-1 in a PAH PASMC. Perhexiline/FPER-1 are able to decrease the augmented phosphorylation of AKT and PDH in PAH PASMCs, resulting in an increase in oxidative glucose metabolism and decreased PASMC proliferation as supported by the findings of the present study. Neither perhexiline or FPER-1 effected the phosphorylation of ERK. This figure was adapted from (202).

References

1. Humbert M, Sitbon O, Simonneau G. Treatment of Pulmonary Arterial Hypertension. N Engl J Med. 2004 Sep 30;351(14):1425–36.

2. Simonneau G, Montani D, Celermajer DS, Denton CP, Gatzoulis MA, Krowka M, et al. Haemodynamic definitions and updated clinical classification of pulmonary hypertension. Eur Respir J [Internet]. 2019 Jan 1 [cited 2022 Mar 9];53(1). Available from: https://erj.ersjournals.com/content/53/1/1801913

3. Thenappan T, Ormiston ML, Ryan JJ, Archer SL. Pulmonary arterial hypertension: pathogenesis and clinical management. The BMJ. 2018 Mar 14;360:j5492.

4. nhs.uk [Internet]. 2017 [cited 2022 Mar 8]. Pulmonary hypertension - Causes. Available from: https://www.nhs.uk/conditions/pulmonary-hypertension/causes/

5. Research into pulmonary hypertension [Internet]. [cited 2022 Jun 29]. Available from: https://www.bhf.org.uk/informationsupport/heart-matters-magazine/research/research-beyond-the-heart/research-into-pulmonary-hypertension

6. Badesch DB, Raskob GE, Elliott CG, Krichman AM, Farber HW, Frost AE, et al. Pulmonary Arterial Hypertension: Baseline Characteristics From the REVEAL Registry. Chest. 2010 Feb 1;137(2):376–87.

7. Exposto F, Hermans R, Nordgren Å, Taylor L, Sikander Rehman S, Ogley R, et al. Burden of pulmonary arterial hypertension in England: retrospective HES database analysis. Ther Adv Respir Dis. 2021 Feb 23;15:1753466621995040.

8. Coons JC, Pogue K, Kolodziej AR, Hirsch GA, George MP. Pulmonary Arterial Hypertension: a Pharmacotherapeutic Update. Curr Cardiol Rep. 2019 Nov 22;21(11):141.

9. Aldred MA, Vijayakrishnan J, James V, Soubrier F, Gomez-Sanchez MA, Martensson G, et al. BMPR2 gene rearrangements account for a significant proportion of mutations in familial and idiopathic pulmonary arterial hypertension. Hum Mutat. 2006 Feb;27(2):212–3.

10. Cogan JD, Vnencak-Jones CL, Phillips JA, Lane KB, Wheeler LA, Robbins IM, et al. Gross BMPR2 gene rearrangements constitute a new cause for primary pulmonary hypertension. Genet Med Off J Am Coll Med Genet. 2005 Mar;7(3):169–74.

11. Cogan JD, Pauciulo MW, Batchman AP, Prince MA, Robbins IM, Hedges LK, et al. High Frequency of BMPR2 Exonic Deletions/Duplications in Familial Pulmonary Arterial Hypertension. Am J Respir Crit Care Med. 2006 Sep 1;174(5):590–8.

12. Thomson J, Machado R, Pauciulo M, Morgan N, Humbert M, Elliott G, et al. Sporadic primary pulmonary hypertension is associated with germline mutations of the gene encoding BMPR-II, a receptor member of the TGF-β family. J Med Genet. 2000 Oct;37(10):741–5.

13. Trembath RC, Thomson JR, Machado RD, Morgan NV, Atkinson C, Winship I, et al. Clinical and molecular genetic features of pulmonary hypertension in patients with hereditary hemorrhagic telangiectasia. N Engl J Med. 2001 Aug 2;345(5):325–34.

14. Chaouat A, Coulet F, Favre C, Simonneau G, Weitzenblum E, Soubrier F, et al. Endoglin germline mutation in a patient with hereditary haemorrhagic telangiectasia and dexfenfluramine associated pulmonary arterial hypertension. Thorax. 2004 May;59(5):446–8.

15. Zamanian RT, Hedlin H, Greuenwald P, Wilson DM, Segal JI, Jorden M, et al. Features and Outcomes of Methamphetamine-associated Pulmonary Arterial Hypertension. Am J Respir Crit Care Med. 2018 Mar 15;197(6):788–800.

16. Ruopp NF, Cockrill BA. Diagnosis and Treatment of Pulmonary Arterial Hypertension: A Review. JAMA. 2022 Apr 12;327(14):1379–91.

17. Hachulla E, Gressin V, Guillevin L, Carpentier P, Diot E, Sibilia J, et al. Early detection of pulmonary arterial hypertension in systemic sclerosis: a French nationwide prospective multicenter study. Arthritis Rheum. 2005 Dec;52(12):3792–800.

18. Mukerjee D, St George D, Coleiro B, Knight C, Denton CP, Davar J, et al. Prevalence and outcome in systemic sclerosis associated pulmonary arterial hypertension: application of a registry approach. Ann Rheum Dis. 2003 Nov;62(11):1088–93.

19. Humbert M, Sitbon O, Chaouat A, Bertocchi M, Habib G, Gressin V, et al. Pulmonary Arterial Hypertension in France. Am J Respir Crit Care Med. 2006 May;173(9):1023–30.

20. McGoon MD, Benza RL, Escribano-Subias P, Jiang X, Miller DP, Peacock AJ, et al. Pulmonary arterial hypertension: epidemiology and registries. J Am Coll Cardiol. 2013 Dec 24;62(25 Suppl):D51-59.

21. Sitbon O, Lascoux-Combe C, Delfraissy JF, Yeni PG, Raffi F, De Zuttere D, et al. Prevalence of HIV-related pulmonary arterial hypertension in the current antiretroviral therapy era. Am J Respir Crit Care Med. 2008 Jan 1;177(1):108–13.

22. Le Pavec J, Souza R, Herve P, Lebrec D, Savale L, Tcherakian C, et al. Portopulmonary hypertension: survival and prognostic factors. Am J Respir Crit Care Med. 2008 Sep 15;178(6):637–43.

23. Krowka MJ, Swanson KL, Frantz RP, McGoon MD, Wiesner RH. Portopulmonary hypertension: Results from a 10-year screening algorithm. Hepatol Baltim Md. 2006 Dec;44(6):1502–10.

24. Galiè N, Humbert M, Vachiery JL, Gibbs S, Lang I, Torbicki A, et al. 2015 ESC/ERS Guidelines for the diagnosis and treatment of pulmonary hypertension: The Joint Task Force for the Diagnosis and Treatment of Pulmonary Hypertension of the European Society of Cardiology (ESC) and the European Respiratory Society (ERS): Endorsed by: Association for European Paediatric and Congenital Cardiology (AEPC), International Society for Heart and Lung Transplantation (ISHLT). Eur Heart J. 2016 Jan 1;37(1):67–119.

25. Manes A, Palazzini M, Leci E, Bacchi Reggiani ML, Branzi A, Galiè N. Current era survival of patients with pulmonary arterial hypertension associated with congenital heart disease: a comparison between clinical subgroups. Eur Heart J. 2014 Mar;35(11):716–24.

26. nhs.uk [Internet]. 2017 [cited 2022 Aug 8]. Schistosomiasis (bilharzia). Available from: https://www.nhs.uk/conditions/schistosomiasis/

27. King CH. PARASITES AND POVERTY: THE CASE OF SCHISTOSOMIASIS. Acta Trop. 2010 Feb;113(2):95–104.

28. Mickael CS, Graham BB. The Role of Type 2 Inflammation in Schistosoma-Induced Pulmonary Hypertension. Front Immunol. 2019 Jan 24;10:27.

29. Pinsky MR. The right ventricle: interaction with the pulmonary circulation. Crit Care. 2016 Sep 10;20(1):266.

30. Kovacs G, Berghold A, Scheidl S, Olschewski H. Pulmonary arterial pressure during rest and exercise in healthy subjects: a systematic review. Eur Respir J. 2009 Oct;34(4):888–94.

31. Nair R, Lamaa N. Pulmonary Capillary Wedge Pressure. In: StatPearls [Internet]. Treasure Island (FL): StatPearls Publishing; 2022 [cited 2022 Oct 18]. Available from: http://www.ncbi.nlm.nih.gov/books/NBK557748/

32. Widrich J, Shetty M. Physiology, Pulmonary Vascular Resistance. In: StatPearls [Internet]. Treasure Island (FL): StatPearls Publishing; 2022 [cited 2022 Oct 18]. Available from: http://www.ncbi.nlm.nih.gov/books/NBK554380/

33. Madden JA, Dawson CA, Harder DR. Hypoxia-induced activation in small isolated pulmonary arteries from the cat. J Appl Physiol Bethesda Md 1985. 1985 Jul;59(1):113–8.

34. Rounds S, McMurtry IF. Inhibitors of oxidative ATP production cause transient vasoconstriction and block subsequent pressor responses in rat lungs. Circ Res. 1981 Mar;48(3):393–400.

35. Michelakis ED, Thébaud B, Weir EK, Archer SL. Hypoxic pulmonary vasoconstriction: redox regulation of O2-sensitive K+ channels by a mitochondrial O2-sensor in resistance artery smooth muscle cells. J Mol Cell Cardiol. 2004 Dec;37(6):1119–36.

36. Wu D, Dasgupta A, Read AD, Bentley RET, Motamed M, Chen KH, et al. Oxygen sensing, mitochondrial biology and experimental therapeutics for pulmonary hypertension and cancer. Free Radic Biol Med. 2021 Jul 1;170:150–78.

37. Amsallem M, Bagherzadeh SP, Boulate D, Sweatt AJ, Kudelko KT, Sung YK, et al. Hemodynamic trajectories and outcomes in patients with pulmonary arterial hypertension. Pulm Circ. 2020 Dec 6;10(4):2045894020941343.

38. Vonk Noordegraaf A, Chin KM, Haddad F, Hassoun PM, Hemnes AR, Hopkins SR, et al. Pathophysiology of the right ventricle and of the pulmonary circulation in pulmonary hypertension: an update. Eur Respir J. 2019 Jan;53(1):1801900.

39. Sommer N, Ghofrani HA, Pak O, Bonnet S, Provencher S, Sitbon O, et al. Current and future treatments of pulmonary arterial hypertension. Br J Pharmacol. 2021;178(1):6–30.

40. nhs.uk [Internet]. 2017 [cited 2022 Apr 26]. Pulmonary hypertension - Treatment. Available from: https://www.nhs.uk/conditions/pulmonary-hypertension/treatment/

41. Klinger JR, Elliott CG, Levine DJ, Bossone E, Duvall L, Fagan K, et al. Therapy for Pulmonary Arterial Hypertension in Adults: Update of the CHEST Guideline and Expert Panel Report. Chest. 2019 Mar;155(3):565–86.

42. Korde Choudhari S, Chaudhary M, Bagde S, Gadbail AR, Joshi V. Nitric oxide and cancer: a review. World J Surg Oncol. 2013 May 30;11:118.

43. Galiè N, Ghofrani HA, Torbicki A, Barst RJ, Rubin LJ, Badesch D, et al. Sildenafil citrate therapy for pulmonary arterial hypertension. N Engl J Med. 2005 Nov 17;353(20):2148–57.

44. Galiè N, Brundage BH, Ghofrani HA, Oudiz RJ, Simonneau G, Safdar Z, et al. Tadalafil therapy for pulmonary arterial hypertension. Circulation. 2009 Jun 9;119(22):2894–903.

45. Poch DS. Case report: a patient with pulmonary arterial hypertension transitioning from a PDE-5 inhibitor to Riociguat. BMC Pulm Med. 2016 May 18;16:82.

46. Black SM, Sanchez LS, Mata-Greenwood E, Bekker JM, Steinhorn RH, Fineman JR. sGC and PDE5 are elevated in lambs with increased pulmonary blood flow and

pulmonary hypertension. Am J Physiol Lung Cell Mol Physiol. 2001 Nov;281(5):L1051-1057.

47. Murray F, MacLean MR, Pyne NJ. Increased expression of the cGMP-inhibited cAMP-specific (PDE3) and cGMP binding cGMP-specific (PDE5) phosphodiesterases in models of pulmonary hypertension. Br J Pharmacol. 2002 Dec;137(8):1187–94.

48. Giaid A, Saleh D. Reduced expression of endothelial nitric oxide synthase in the lungs of patients with pulmonary hypertension. N Engl J Med. 1995 Jul 27;333(4):214–21.

49. Wharton J, Strange JW, Møller GMO, Growcott EJ, Ren X, Franklyn AP, et al. Antiproliferative effects of phosphodiesterase type 5 inhibition in human pulmonary artery cells. Am J Respir Crit Care Med. 2005 Jul 1;172(1):105–13.

50. Corbin JD. Mechanisms of action of PDE5 inhibition in erectile dysfunction. Int J Impot Res. 2004 Jun;16(1):S4–7.

51. Hassoun PM, Thappa V, Landman MJ, Fanburg BL. Endothelin 1: mitogenic activity on pulmonary artery smooth muscle cells and release from hypoxic endothelial cells. Proc Soc Exp Biol Med Soc Exp Biol Med N Y N. 1992 Feb;199(2):165–70.

52. Stelzner TJ, O'Brien RF, Yanagisawa M, Sakurai T, Sato K, Webb S, et al. Increased lung endothelin-1 production in rats with idiopathic pulmonary hypertension. Am J Physiol. 1992 May;262(5 Pt 1):L614-620.

53. KOHAN DE, ROSSI NF, INSCHO EW, POLLOCK DM. Regulation of Blood Pressure and Salt Homeostasis by Endothelin. Physiol Rev. 2011 Jan;91(1):1–77.

54. Enevoldsen FC, Sahana J, Wehland M, Grimm D, Infanger M, Krüger M. Endothelin Receptor Antagonists: Status Quo and Future Perspectives for Targeted Therapy. J Clin Med. 2020 Mar 18;9(3):824.

55. Nasser SA, El-Mas MM. Endothelin ETA receptor antagonism in cardiovascular disease. Eur J Pharmacol. 2014 Aug 15;737:210–3.

56. Houde M, Desbiens L, D'Orléans-Juste P. Endothelin-1: Biosynthesis, Signaling and Vasoreactivity. Adv Pharmacol San Diego Calif. 2016;77:143–75.

57. Allen SW, Chatfield BA, Koppenhafer SA, Schaffer MS, Wolfe RR, Abman SH. Circulating immunoreactive endothelin-1 in children with pulmonary hypertension. Association with acute hypoxic pulmonary vasoreactivity. Am Rev Respir Dis. 1993 Aug;148(2):519–22.

58. Giaid A, Yanagisawa M, Langleben D, Michel RP, Levy R, Shennib H, et al. Expression of endothelin-1 in the lungs of patients with pulmonary hypertension. N Engl J Med. 1993 Jun 17;328(24):1732–9.

59. Channick RN, Simonneau G, Sitbon O, Robbins IM, Frost A, Tapson VF, et al. Effects of the dual endothelin-receptor antagonist bosentan in patients with pulmonary hypertension: a randomised placebo-controlled study. Lancet Lond Engl. 2001 Oct 6;358(9288):1119–23.

60. Galiè N, Barberà JA, Frost AE, Ghofrani HA, Hoeper MM, McLaughlin VV, et al. Initial Use of Ambrisentan plus Tadalafil in Pulmonary Arterial Hypertension. N Engl J Med. 2015 Aug 27;373(9):834–44.

61. Pulido T, Adzerikho I, Channick RN, Delcroix M, Galiè N, Ghofrani HA, et al. Macitentan and morbidity and mortality in pulmonary arterial hypertension. N Engl J Med. 2013 Aug 29;369(9):809–18.

62. Galiè N, Olschewski H, Oudiz RJ, Torres F, Frost A, Ghofrani HA, et al. Ambrisentan for the treatment of pulmonary arterial hypertension: results of the ambrisentan in pulmonary arterial hypertension, randomized, double-blind, placebo-controlled, multicenter, efficacy (ARIES) study 1 and 2. Circulation. 2008 Jun 10;117(23):3010–9.

63. Rubin LJ, Badesch DB, Barst RJ, Galie N, Black CM, Keogh A, et al. Bosentan therapy for pulmonary arterial hypertension. N Engl J Med. 2002 Mar 21;346(12):896–903.

64. Mathier MA, Ishizawar D. Bosentan. Expert Opin Pharmacother. 2010 Apr;11(6):1023–34.

65. Peacock AJ, Zamboni W, Vizza CD. Ambrisentan for the treatment of adults with pulmonary arterial hypertension: a review. Curr Med Res Opin. 2015;31(9):1793–807.

66. Sidharta PN, Krähenbühl S, Dingemanse J. Pharmacokinetic and pharmacodynamic evaluation of macitentan , a novel endothelin receptor antagonist for the treatment of pulmonary arterial hypertension. Expert Opin Drug Metab Toxicol. 2015 Mar;11(3):437–49.

67. Dingemanse J, van Giersbergen PLM. Clinical pharmacology of bosentan, a dual endothelin receptor antagonist. Clin Pharmacokinet. 2004;43(15):1089–115.

68. Chaumais MC, Guignabert C, Savale L, Jaïs X, Boucly A, Montani D, et al. Clinical pharmacology of endothelin receptor antagonists used in the treatment of pulmonary arterial hypertension. Am J Cardiovasc Drugs Drugs Devices Interv. 2015 Feb;15(1):13–26.

69. Wei A, Gu Z, Li J, Liu X, Wu X, Han Y, et al. Clinical Adverse Effects of Endothelin Receptor Antagonists: Insights From the Meta-Analysis of 4894 Patients From 24 Randomized Double-Blind Placebo-Controlled Clinical Trials. J Am Heart Assoc Cardiovasc Cerebrovasc Dis. 2016 Oct 26;5(11):e003896.

70. Dey I, Lejeune M, Chadee K. Prostaglandin E2 receptor distribution and function in the gastrointestinal tract. Br J Pharmacol. 2006 Nov;149(6):611–23.

71. Narumiya S. Physiology and pathophysiology of prostanoid receptors. Proc Jpn Acad Ser B Phys Biol Sci. 2007 Dec;83(9–10):296–319.

72. Oida H, Namba T, Sugimoto Y, Ushikubi F, Ohishi H, Ichikawa A, et al. In situ hybridization studies of prostacyclin receptor mRNA expression in various mouse organs. Br J Pharmacol. 1995 Dec;116(7):2828–37.

73. Fetalvero KM, Martin KA, Hwa J. Cardioprotective prostacyclin signaling in vascular smooth muscle. Prostaglandins Other Lipid Mediat. 2007 Jan 1;82(1):109–18.

74. Christman BW, McPherson CD, Newman JH, King GA, Bernard GR, Groves BM, et al. An imbalance between the excretion of thromboxane and prostacyclin metabolites in pulmonary hypertension. N Engl J Med. 1992 Jul 9;327(2):70–5.

75. Alfranca A, Iñiguez MA, Fresno M, Redondo JM. Prostanoid signal transduction and gene expression in the endothelium: Role in cardiovascular diseases. Cardiovasc Res. 2006 Jun 1;70(3):446–56.

76. Lindegaard Pedersen M, Krüger M, Grimm D, Infanger M, Wehland M. The prostacyclin analogue treprostinil in the treatment of pulmonary arterial hypertension. Basic Clin Pharmacol Toxicol. 2019 Aug 12;

77. Lang IM, Gaine SP. Recent advances in targeting the prostacyclin pathway in pulmonary arterial hypertension. Eur Respir Rev. 2015 Dec 1;24(138):630–41.

78. Tuder RM, Cool CD, Geraci MW, Wang J, Abman SH, Wright L, et al. Prostacyclin synthase expression is decreased in lungs from patients with severe pulmonary hypertension. Am J Respir Crit Care Med. 1999 Jun;159(6):1925–32.

79. Barst RJ, Rubin LJ, Long WA, McGoon MD, Rich S, Badesch DB, et al. A comparison of continuous intravenous epoprostenol (prostacyclin) with conventional therapy for primary pulmonary hypertension. N Engl J Med. 1996 Feb 1;334(5):296–301.

80. Badesch DB, Tapson VF, McGoon MD, Brundage BH, Rubin LJ, Wigley FM, et al. Continuous intravenous epoprostenol for pulmonary hypertension due to the scleroderma spectrum of disease. A randomized, controlled trial. Ann Intern Med. 2000 Mar 21;132(6):425–34.

81. Simonneau G, Barst RJ, Galie N, Naeije R, Rich S, Bourge RC, et al. Continuous subcutaneous infusion of treprostinil, a prostacyclin analogue, in patients with pulmonary arterial hypertension: a double-blind, randomized, placebo-controlled trial. Am J Respir Crit Care Med. 2002 Mar 15;165(6):800–4.

82. Benza RL, Tapson VF, Gomberg-Maitland M, Poms A, Barst RJ, McLaughlin VV. One-year experience with intravenous treprostinil for pulmonary arterial hypertension. J Heart Lung Transplant Off Publ Int Soc Heart Transplant. 2013 Sep;32(9):889–96.

83. McLaughlin VV, Benza RL, Rubin LJ, Channick RN, Voswinckel R, Tapson VF, et al. Addition of inhaled treprostinil to oral therapy for pulmonary arterial hypertension: a randomized controlled clinical trial. J Am Coll Cardiol. 2010 May 4;55(18):1915–22.

84. Hatton N, Ryan JJ. Sex differences in response to pulmonary arterial hypertension therapy: is what's good for the goose, good for the gander? Chest. 2014 Jun;145(6):1184–6.

85. Jing ZC, Parikh K, Pulido T, Jerjes-Sanchez C, White RJ, Allen R, et al. Efficacy and safety of oral treprostinil monotherapy for the treatment of pulmonary arterial hypertension: a randomized, controlled trial. Circulation. 2013 Feb 5;127(5):624–33.

86. Tapson VF, Jing ZC, Xu KF, Pan L, Feldman J, Kiely DG, et al. Oral treprostinil for the treatment of pulmonary arterial hypertension in patients receiving background endothelin receptor antagonist and phosphodiesterase type 5 inhibitor therapy (the FREEDOM-C2 study): a randomized controlled trial. Chest. 2013 Sep;144(3):952–8.

87. McLaughlin VV, Channick R, Chin K, Frey A, Gaine S, Ghofrani A, et al. EFFECT OF SELEXIPAG ON MORBIDITY/MORTALITY IN PULMONARY ARTERIAL HYPERTENSION: RESULTS OF THE GRIPHON STUDY. J Am Coll Cardiol. 2015 Mar 17;65(10, Supplement):A1538.

88. Olschewski H, Simonneau G, Galiè N, Higenbottam T, Naeije R, Rubin LJ, et al. Inhaled Iloprost for Severe Pulmonary Hypertension. N Engl J Med. 2002 Aug;347(5):322–9.

89. Simonneau G, Torbicki A, Hoeper MM, Delcroix M, Karlócai K, Galiè N, et al. Selexipag: an oral, selective prostacyclin receptor agonist for the treatment of pulmonary arterial hypertension. Eur Respir J. 2012 Oct 1;40(4):874–80.

90. Sitbon O, Channick R, Chin KM, Frey A, Gaine S, Galiè N, et al. Selexipag for the Treatment of Pulmonary Arterial Hypertension. N Engl J Med. 2015 Dec 24;373(26):2522–33.

91. Coghlan JG, Channick R, Chin K, Di Scala L, Galiè N, Ghofrani HA, et al. Targeting the Prostacyclin Pathway with Selexipag in Patients with Pulmonary Arterial Hypertension Receiving Double Combination Therapy: Insights from the Randomized Controlled GRIPHON Study. Am J Cardiovasc Drugs. 2018;18(1):37–47.

92. McMurtry MS, Bonnet S, Wu X, Dyck JRB, Haromy A, Hashimoto K, et al. Dichloroacetate Prevents and Reverses Pulmonary Hypertension by Inducing

Pulmonary Artery Smooth Muscle Cell Apoptosis. Circ Res. 2004 Oct 15;95(8):830–40.

93. Guignabert C, Tu L, Izikki M, Dewachter L, Zadigue P, Humbert M, et al. Dichloroacetate treatment partially regresses established pulmonary hypertension in mice with SM22alpha-targeted overexpression of the serotonin transporter. FASEB J Off Publ Fed Am Soc Exp Biol. 2009 Dec;23(12):4135–47.

94. Michelakis ED, McMurtry MS, Wu XC, Dyck JRB, Moudgil R, Hopkins TA, et al. Dichloroacetate, a Metabolic Modulator, Prevents and Reverses Chronic Hypoxic Pulmonary Hypertension in Rats. Circulation. 2002 Jan 15;105(2):244–50.

95. Michelakis ED, Gurtu V, Webster L, Barnes G, Watson G, Howard L, et al. Inhibition of pyruvate dehydrogenase kinase improves pulmonary arterial hypertension in genetically susceptible patients. Sci Transl Med. 2017 Oct 25;9(413):eaao4583.

96. Humbert M, Kovacs G, Hoeper MM, Badagliacca R, Berger RMF, Brida M, et al. 2022 ESC/ERS Guidelines for the diagnosis and treatment of pulmonary hypertension: Developed by the task force for the diagnosis and treatment of pulmonary hypertension of the European Society of Cardiology (ESC) and the European Respiratory Society (ERS). Endorsed by the International Society for Heart and Lung Transplantation (ISHLT) and the European Reference Network on rare respiratory diseases (ERN-LUNG). Eur Heart J. 2022 Oct 7;43(38):3618–731.

97. Annesley SJ, Fisher PR. Mitochondria in Health and Disease. Cells. 2019 Jul 5;8(7):680.

98. Judge A, Dodd MS. Metabolism. Essays Biochem. 2020 Oct;64(4):607–47.

99. Martínez-Reyes I, Chandel NS. Mitochondrial TCA cycle metabolites control physiology and disease. Nat Commun. 2020 Jan 3;11:102.

100. Wilson DF. Oxidative phosphorylation: regulation and role in cellular and tissue metabolism. J Physiol. 2017 Dec 1;595(23):7023–38.

101. Bartlett K, Eaton S. Mitochondrial beta-oxidation. Eur J Biochem. 2004 Feb;271(3):462–9.

102. Flavin R, Peluso S, Nguyen PL, Loda M. Fatty acid synthase as a potential therapeutic target in cancer. Future Oncol Lond Engl. 2010 Apr;6(4):551–62.

103. Dyck JRB, Barr AJ, Barr RL, Kolattukudy PE, Lopaschuk GD. Characterization of cardiac malonyl-CoA decarboxylase and its putative role in regulating fatty acid oxidation. Am J Physiol-Heart Circ Physiol. 1998 Dec;275(6):H2122–9.

104. McGarry JD, Woeltje KF, Kuwajima M, Foster DW. Regulation of ketogenesis and the renaissance of carnitine palmitoyltransferase. Diabetes Metab Rev. 1989;5(3):271–84.

105. Randle PJ, Garland PB, Hales CN, Newsholme EA. The glucose fatty-acid cycle. Its role in insulin sensitivity and the metabolic disturbances of diabetes mellitus. Lancet Lond Engl. 1963 Apr 13;1(7285):785–9.

106. Randle PJ. Regulatory interactions between lipids and carbohydrates: the glucose fatty acid cycle after 35 years. Diabetes Metab Rev. 1998 Dec;14(4):263–83.

107. Peng H, Wang Y, Luo W. Multifaceted role of branched-chain amino acid metabolism in cancer. Oncogene. 2020 Oct;39(44):6747–56.

108. Weis E, Puchalska P, Nelson AB, Taylor J, Moll I, Hasan SS, et al. Ketone body oxidation increases cardiac endothelial cell proliferation. EMBO Mol Med. 2022 Feb 18;14(4):e14753.

109. Cotter DG, Schugar RC, Crawford PA. Ketone body metabolism and cardiovascular disease. Am J Physiol - Heart Circ Physiol. 2013 Apr 15;304(8):H1060–76.

110. Puchalska P, Crawford PA. Multi-dimensional roles of ketone bodies in fuel metabolism, signaling, and therapeutics. Cell Metab. 2017 Feb 7;25(2):262–84.

111. Peng H, Xiao Y, Deng X, Luo J, Hong C, Qin X. The Warburg effect: A new story in pulmonary arterial hypertension. Clin Chim Acta Int J Clin Chem. 2016 Oct 1;461:53–8.

112. Xiao Y, Peng H, Hong C, Chen Z, Deng X, Wang A, et al. PDGF Promotes the Warburg Effect in Pulmonary Arterial Smooth Muscle Cells via Activation of the PI3K/AKT/mTOR/HIF-1α Signaling Pathway. Cell Physiol Biochem Int J Exp Cell Physiol Biochem Pharmacol. 2017;42(4):1603–13.

113. Li B, Zhu Y, Sun Q, Yu C, Chen L, Tian Y, et al. Reversal of the Warburg effect with DCA in PDGF-treated human PASMC is potentiated by pyruvate dehydrogenase kinase-1 inhibition mediated through blocking Akt/GSK-3β signalling. Int J Mol Med. 2018 Sep;42(3):1391–400.

114. Archer SL, Marsboom G, Kim GH, Zhang HJ, Toth PT, Svensson EC, et al. Epigenetic Attenuation of Mitochondrial Superoxide Dismutase 2 (SOD2) in Pulmonary Arterial Hypertension. Circulation. 2010 Jun 22;121(24):2661–71.

115. Archer SL, Gomberg-Maitland M, Maitland ML, Rich S, Garcia JGN, Weir EK. Mitochondrial metabolism, redox signaling, and fusion: a mitochondria-ROS-HIF-1alpha-Kv1.5 O2-sensing pathway at the intersection of pulmonary hypertension and cancer. Am J Physiol Heart Circ Physiol. 2008 Feb;294(2):H570-578.

116. Caruso P, Dunmore BJ, Schlosser K, Schoors S, Santos CD, Perez-Iratxeta C, et al. Identification of miR-124 as a major regulator of enhanced endothelial cell

glycolysis in pulmonary arterial hypertension via PTBP1 and PKM2. Circulation. 2017 Dec 19;136(25):2451–67.

117. Zhang H, Wang D, Li M, Plecitá-Hlavatá L, D'Alessandro A, Tauber J, et al. The Metabolic and Proliferative State of Vascular Adventitial Fibroblasts in Pulmonary Hypertension is Regulated through a MiR-124/PTBP1/PKM Axis. Circulation. 2017 Dec 19;136(25):2468–85.

118. Tian L, Wu D, Dasgupta A, Chen KH, Mewburn J, Potus F, et al. Epigenetic Metabolic Reprogramming of Right Ventricular Fibroblasts in Pulmonary Arterial Hypertension: A Pyruvate Dehydrogenase Kinase-Dependent Shift in Mitochondrial Metabolism Promotes Right Ventricular Fibrosis. Circ Res. 2020 Jun 5;126(12):1723–45.

119. Dasgupta A, Wu D, Tian L, Xiong PY, Dunham-Snary KJ, Chen K, et al. Mitochondria in the Pulmonary Vasculature in Health and Disease: Oxygen-Sensing, Metabolism, and Dynamics. In: Terjung R, editor. Comprehensive Physiology [Internet]. 1st ed. Wiley; 2020 [cited 2022 Mar 25]. p. 713–65. Available from: https://onlinelibrary.wiley.com/doi/10.1002/cphy.c190027

120. Schermuly RT, Dony E, Ghofrani HA, Pullamsetti S, Savai R, Roth M, et al. Reversal of experimental pulmonary hypertension by PDGF inhibition. J Clin Invest. 2005 Oct 10;115(10):2811.

121. Berghausen E, ten Freyhaus H, Rosenkranz S. Targeting of platelet-derived growth factor signaling in pulmonary arterial hypertension. Handb Exp Pharmacol. 2013;218:381–408.

122. Zhao L, Ashek A, Wang L, Fang W, Dabral S, Dubois O, et al. Heterogeneity in lung (18)FDG uptake in pulmonary arterial hypertension: potential of dynamic (18)FDG positron emission tomography with kinetic analysis as a bridging biomarker for pulmonary vascular remodeling targeted treatments. Circulation. 2013 Sep 1;128(11):1214–24.

123. Marsboom G, Toth PT, RyaN JJ, Hong Z, Wu X, Fang YH, et al. Dynamin-Related Protein 1 (DRP1)-Mediated Mitochondrial Mitotic Fission Permits Hyperproliferation of Vascular Smooth Muscle Cells and Offers a Novel Therapeutic Target in Pulmonary Hypertension. Circ Res. 2012 May 25;110(11):1484–97.

124. Marsboom G, Wietholt C, Haney CR, Toth PT, Ryan JJ, Morrow E, et al. Lung 18F-Fluorodeoxyglucose Positron Emission Tomography for Diagnosis and Monitoring of Pulmonary Arterial Hypertension. Am J Respir Crit Care Med. 2012 Mar 15;185(6):670–9.

125. Chen C, Luo F, Wu P, Huang Y, Das A, Chen S, et al. Metabolomics reveals metabolite changes of patients with pulmonary arterial hypertension in China. J Cell Mol Med. 2020 Feb;24(4):2484–96.

126. Zhuang W, Lian G, Huang B, Du A, Gong J, Xiao G, et al. CPT1 regulates the proliferation of pulmonary artery smooth muscle cells through the AMPK-p53-p21 pathway in pulmonary arterial hypertension. Mol Cell Biochem. 2019 May;455(1–2):169–83.

127. Wu J, Yu Z, Su D. BMP4 Protects Rat Pulmonary Arterial Smooth Muscle Cells from Apoptosis by PI3K/AKT/Smad1/5/8 Signaling. Int J Mol Sci. 2014 Aug;15(8):13738–54.

128. Chen B, Xue J, Meng X, Slutzky JL, Calvert AE, Chicoine LG. Resveratrol prevents hypoxia-induced arginase II expression and proliferation of human pulmonary artery smooth muscle cells via Akt-dependent signaling. Am J Physiol-Lung Cell Mol Physiol. 2014 Aug 15;307(4):L317–25.

129. Zhang H, Gong Y, Wang Z, Jiang L, Chen R, Fan X, et al. Apelin inhibits the proliferation and migration of rat PASMCs via the activation of PI3K/Akt/mTOR signal and the inhibition of autophagy under hypoxia. J Cell Mol Med. 2014;18(3):542–53.

130. Cantoni S, Galletti M, Zambelli F, Valente S, Ponti F, Tassinari R, et al. Sodium butyrate inhibits platelet-derived growth factor-induced proliferation and migration in pulmonary artery smooth muscle cells through Akt inhibition. FEBS J. 2013;280(9):2042–55.

131. Wei C, Li HZ, Wang YH, Peng X, Shao HJ, Li HX, et al. Exogenous spermine inhibits the proliferation of human pulmonary artery smooth muscle cells caused by chemically-induced hypoxia via the suppression of the ERK1/2- and PI3K/AKT-associated pathways. Int J Mol Med. 2016 Jan 1;37(1):39–46.

132. Cheng CC, Chi PL, Shen MC, Shu CW, Wann SR, Liu CP, et al. Caffeic Acid Phenethyl Ester Rescues Pulmonary Arterial Hypertension through the Inhibition of AKT/ERK-Dependent PDGF/HIF-1α In Vitro and In Vivo. Int J Mol Sci. 2019 Jan;20(6):1468.

133. Zhang S, Wang J, Qi X, Tao X, Xie W, Wan J, et al. Plasminogen activator Inhibitor-2 inhibits pulmonary arterial smooth muscle cell proliferation in pulmonary arterial hypertension via PI3K/Akt and ERK signaling. Exp Cell Res. 2021 Jan 1;398(1):112392.

134. Feng W, Wang J, Yan X, Zhang Q, Chai L, Wang Q, et al. ERK/Drp1-dependent mitochondrial fission contributes to HMGB1-induced autophagy in pulmonary arterial hypertension. Cell Prolif. 2021 May 4;54(6):e13048.

135. Suzuki S, Nakazato K, Sugimoto K, Yoshihisa A, Yamaki T, Kunii H, et al. Plasma Levels of Receptor for Advanced Glycation End-Products and High-Mobility Group Box 1 in Patients With Pulmonary Hypertension. Int Heart J. 2016;57(2):234–40.

136. Huang YY, Su W, Zhu ZW, Tang L, Hu XQ, Zhou SH, et al. Elevated serum HMGB1 in pulmonary arterial hypertension secondary to congenital heart disease. Vascul Pharmacol. 2016 Oct;85:66–72.

137. Goldenberg NM, Hu Y, Hu X, Volchuk A, Zhao YD, Kucherenko MM, et al. Therapeutic Targeting of High-Mobility Group Box-1 in Pulmonary Arterial Hypertension. Am J Respir Crit Care Med. 2019 Jun 15;199(12):1566–9.

138. Guignabert C, Dorfmuller P. Pathology and pathobiology of pulmonary hypertension. Semin Respir Crit Care Med. 2013 Oct;34(5):551–9.

139. Krick S, Platoshyn O, Sweeney M, Kim H, Yuan JXJ. Activation of K+ channels induces apoptosis in vascular smooth muscle cells. Am J Physiol-Cell Physiol. 2001 Apr;280(4):C970–9.

140. Krick S, Platoshyn O, Sweeney M, McDaniel SS, Zhang S, Rubin LJ, et al. Nitric oxide induces apoptosis by activating K+ channels in pulmonary vascular smooth muscle cells. Am J Physiol-Heart Circ Physiol. 2002 Jan;282(1):H184–93.

141. Remillard CV, Yuan JXJ. Activation of K+ channels: an essential pathway in programmed cell death. Am J Physiol-Lung Cell Mol Physiol. 2004 Jan;286(1):L49–67.

142. Kaufmann P, Engelstad K, Wei Y, Jhung S, Sano MC, Shungu DC, et al. Dichloroacetate causes toxic neuropathy in MELAS: A randomized, controlled clinical trial. Neurology. 2006 Feb 14;66(3):324–30.

143. Stacpoole PW, Kerr DS, Barnes C, Bunch ST, Carney PR, Fennell EM, et al. Controlled clinical trial of dichloroacetate for treatment of congenital lactic acidosis in children. Pediatrics. 2006 May;117(5):1519–31.

144. Fang YH, Piao L, Hong Z, Toth PT, Marsboom G, Bache-Wiig P, et al. Therapeutic inhibition of fatty acid oxidation in right ventricular hypertrophy: exploiting Randle's cycle. J Mol Med Berl Ger. 2012 Jan;90(1):31–43.

145. Clarke B, Wyatt KM, McCormack JG. Ranolazine increases active pyruvate dehydrogenase in perfused normoxic rat hearts: evidence for an indirect mechanism. J Mol Cell Cardiol. 1996 Feb;28(2):341–50.

146. McCormack JG, Barr RL, Wolff AA, Lopaschuk GD. Ranolazine stimulates glucose oxidation in normoxic, ischemic, and reperfused ischemic rat hearts. Circulation. 1996 Jan 1;93(1):135–42.

147. Tuunanen H, Engblom E, Naum A, Någren K, Scheinin M, Hesse B, et al. Trimetazidine, a metabolic modulator, has cardiac and extracardiac benefits in idiopathic dilated cardiomyopathy. Circulation. 2008 Sep 16;118(12):1250–8.

148. Sutendra G, Bonnet S, Rochefort G, Haromy A, Folmes KD, Lopaschuk GD, et al. Fatty acid oxidation and malonyl-CoA decarboxylase in the vascular remodeling of pulmonary hypertension. Sci Transl Med. 2010 Aug 11;2(44):44ra58.

149. Dyck JRB, Hopkins TA, Bonnet S, Michelakis ED, Young ME, Watanabe M, et al. Absence of malonyl coenzyme A decarboxylase in mice increases cardiac glucose oxidation and protects the heart from ischemic injury. Circulation. 2006 Oct 17;114(16):1721–8.

150. Dyck JRB, Cheng JF, Stanley WC, Barr R, Chandler MP, Brown S, et al. Malonyl coenzyme a decarboxylase inhibition protects the ischemic heart by inhibiting fatty acid oxidation and stimulating glucose oxidation. Circ Res. 2004 May 14;94(9):e78-84.

151. Singh N, Manhas A, Kaur G, Jagavelu K, Hanif K. Inhibition of fatty acid synthase is protective in pulmonary hypertension. Br J Pharmacol. 2016 Jun;173(12):2030–45.

152. Menendez JA, Lupu R. Fatty acid synthase and the lipogenic phenotype in cancer pathogenesis. Nat Rev Cancer. 2007 Oct;7(10):763–77.

153. Singlas E, Goujet MA, Simon P. Pharmacokinetics of perhexiline maleate in anginal patients with and without peripheral neuropathy. Eur J Clin Pharmacol. 1978 Nov 1;14(3):195–201.

154. Lee L, Horowitz J, Frenneaux M. Metabolic manipulation in ischaemic heart disease, a novel approach to treatment. Eur Heart J. 2004 Apr 1;25(8):634–41.

155. Kennedy JA, Unger SA, Horowitz JD. Inhibition of carnitine palmitoyltransferase-1 in rat heart and liver by perhexiline and amiodarone. Biochem Pharmacol. 1996 Jul 26;52(2):273–80.

156. Kennedy JA, Kiosoglous AJ, Murphy GA, Pelle MA, Horowitz JD. Effect of perhexiline and oxfenicine on myocardial function and metabolism during low-flow ischemia/reperfusion in the isolated rat heart. J Cardiovasc Pharmacol. 2000 Dec;36(6):794–801.

157. Lee L, Campbell R, Scheuermann-Freestone M, Taylor R, Gunaruwan P, Williams L, et al. Metabolic Modulation With Perhexiline in Chronic Heart Failure. Circulation. 2005 Nov 22;112(21):3280–8.

158. Tseng CC, Noordali H, Sani M, Madhani M, Grant DM, Frenneaux MP, et al. Development of Fluorinated Analogues of Perhexiline with Improved Pharmacokinetic Properties and Retained Efficacy. J Med Chem. 2017 Apr 13;60(7):2780–9.

159. Unger SA, Robinson MA, Horowitz JD. Perhexiline improves symptomatic status in elderly patients with severe aortic stenosis. Aust N Z J Med. 1997 Feb;27(1):24–8.

160. Willoughby SR, Stewart S, Chirkov YY, Kennedy JA, Holmes AS, Horowitz JD. Beneficial clinical effects of perhexiline in patients with stable angina pectoris and acute coronary syndromes are associated with potentiation of platelet responsiveness to nitric oxide. Eur Heart J. 2002 Dec;23(24):1946–54.

161. Abozguia K, Elliott P, McKenna W, Phan TT, Nallur-Shivu G, Ahmed I, et al. Metabolic Modulator Perhexiline Corrects Energy Deficiency and Improves Exercise Capacity in Symptomatic Hypertrophic Cardiomyopathy. Circulation. 2010 Oct 19;122(16):1562–9.

162. Dhakal B, Li CMY, Li R, Yeo K, Wright JA, Gieniec KA, et al. The Antianginal Drug Perhexiline Displays Cytotoxicity against Colorectal Cancer Cells In Vitro: A Potential for Drug Repurposing. Cancers. 2022 Feb 18;14(4):1043.

163. Mozolewska P, Duzowska K, Pakiet A, Mika A, ŚledziŃski T. Inhibitors of Fatty Acid Synthesis and Oxidation as Potential Anticancer Agents in Colorectal Cancer Treatment. Anticancer Res. 2020 Sep;40(9):4843–56.

164. Koundouros N, Poulogiannis G. Reprogramming of fatty acid metabolism in cancer. Br J Cancer. 2020 Jan 7;122(1):4–22.

165. Liu P pan, Liu J, Jiang W qi, Carew JS, Ogasawara MA, Pelicano H, et al. Elimination of Chronic Lymphocytic Leukemia Cells in Stromal Microenvironment by Targeting CPT with an Anti-Angina Drug Perhexiline. Oncogene. 2016 Oct 27;35(43):5663–73.

166. Kant S, Kesarwani P, Guastella AR, Kumar P, Graham SF, Buelow KL, et al. Perhexiline demonstrates FYN-mediated anti-tumor activity in glioblastoma. Mol Cancer Ther. 2020 Jul;19(7):1415–22.

167. Wang Y, Lu JH, Wang F, Wang YN, He MM, Wu QN, et al. Inhibition of fatty acid catabolism augments the efficacy of oxaliplatin-based chemotherapy in gastrointestinal cancers. Cancer Lett. 2020 Mar 31;473:74–89.

168. Ashrafian H, Horowitz JD, Frenneaux MP. Perhexiline. Cardiovasc Drug Rev. 2007;25(1):76–97.

169. Laplane D, Bousser MG. Polyneuropathy during perhexiline maleate therapy. Int J Neurol. 1981;15(3–4):293–300.

170. Paliard P, Vitrey D, Fournier G, Belhadjali J, Patricot L, Berger F. Perhexiline maleate-induced hepatitis. Digestion. 1978;17(5):419–27.

171. Shah RR. Drug-induced hepatotoxicity: pharmacokinetic perspectives and strategies for risk reduction. Adverse Drug React Toxicol Rev. 1999 Nov;18(4):181–233.

172. Shah RR. http://dx.doi.org/10.2217/14622416.7.6.889. Future Medicine Ltd London, UK; 2006 [cited 2022 May 5]. Can pharmacogenetics help rescue drugs withdrawn from the market? Available from: https://www.futuremedicine.com/doi/epub/10.2217/14622416.7.6.889

173. Ren Z, Chen S, Qin X, Li F, Guo L. Study of the roles of cytochrome P450 (CYPs) in the metabolism and cytotoxicity of perhexiline. Arch Toxicol. 2022 Dec;96(12):3219–31.

174. Dally S, Lagier G, Assan R, Gaultier M. [Hypoglycemia in 2 patients treated with perhexiline maleate]. Nouv Presse Med. 1977 May 7;6(19):1643–4, 1649.

175. Myers JB, Ronthal M. Perhexiline maleate neurotoxicity and weight loss. Med J Aust. 1978 Nov 4;2(10):465–6.

176. Horowitz JD, Sia ST, Macdonald PS, Goble AJ, Louis WJ. Perhexiline maleate treatment for severe angina pectoris--correlations with pharmacokinetics. Int J Cardiol. 1986 Nov;13(2):219–29.

177. Wharton J, Davie N, Upton PD, Yacoub MH, Polak JM, Morrell NW. Prostacyclin Analogues Differentially Inhibit Growth of Distal and Proximal Human Pulmonary Artery Smooth Muscle Cells. Circulation. 2000 Dec 19;102(25):3130–6.

178. Endo H, Owada S, Inagaki Y, Shida Y, Tatemichi M. Glucose starvation induces LKB1-AMPK-mediated MMP-9 expression in cancer cells. Sci Rep. 2018 Jul 4;8:10122.

179. Ourahmane A, Sauer A, Nixon DE, Murphy C, Mondello M, Douglass E, et al. A Guinea Pig Cytomegalovirus Resistant to the DNA Maturation Inhibitor BDCRB. Antiviral Res. 2018 Jun;154:44–50.

180. Choosing the Right Western Blot Transfer Method [Internet]. [cited 2023 Dec 14]. Available from: https://www.licor.com/bio/blog/choosing-the-right-western-blot-transfer-method

181. Davies BJ, Coller JK, James HM, Somogyi AA, Horowitz JD, Sallustio BC. The influence of CYP2D6 genotype on trough plasma perhexiline and cis-OH-perhexiline concentrations following a standard loading regimen in patients with myocardial ischaemia. Br J Clin Pharmacol. 2006 Mar;61(3):321–5.

182. Cooper RG, Evans DA, Whibley EJ. Polymorphic hydroxylation of perhexiline maleate in man. J Med Genet. 1984 Feb;21(1):27–33.

183. Goncharov DA, Kudryashova TV, Ziai H, Ihida-Stansbury K, DeLisser H, Krymskaya VP, et al. Mammalian Target of Rapamycin Complex 2 (mTORC2) Coordinates Pulmonary Artery Smooth Muscle Cell Metabolism, Proliferation, and Survival in Pulmonary Arterial Hypertension. Circulation. 2014 Feb 25;129(8):864–74.

184. Izikki M, Guignabert C, Fadel E, Humbert M, Tu L, Zadigue P, et al. Endothelial-derived FGF2 contributes to the progression of pulmonary hypertension in humans and rodents. J Clin Invest. 2009 Mar 2;119(3):512–23.

185. Li X, Zhang X, Leathers R, Makino A, Huang C, Parsa P, et al. Notch3 signaling promotes the development of pulmonary arterial hypertension. Nat Med. 2009 Nov;15(11):1289–97.

186. Savai R, Al-Tamari HM, Sedding D, Kojonazarov B, Muecke C, Teske R, et al. Pro-proliferative and inflammatory signaling converge on FoxO1 transcription factor in pulmonary hypertension. Nat Med. 2014 Nov;20(11):1289–300.

187. Ren XR, Wang J, Osada T, Mook RA, Morse MA, Barak LS, et al. Perhexiline promotes HER3 ablation through receptor internalization and inhibits tumor growth. Breast Cancer Res BCR. 2015;17(1):20.

188. Hansmann G, de Jesus Perez VA, Alastalo TP, Alvira CM, Guignabert C, Bekker JM, et al. An antiproliferative BMP-2/PPARγ/apoE axis in human and murine SMCs and its role in pulmonary hypertension. J Clin Invest. 2008 May 1;118(5):1846–57.

189. BelAiba RS, Bonello S, Zähringer C, Schmidt S, Hess J, Kietzmann T, et al. Hypoxia Up-Regulates Hypoxia-Inducible Factor-1α Transcription by Involving Phosphatidylinositol 3-Kinase and Nuclear Factor κB in Pulmonary Artery Smooth Muscle Cells. Mol Biol Cell. 2007 Dec;18(12):4691–7.

190. Nassar ZD, Mah CY, Centenera MM, Irani S, Sadowski MC, Scott JS, et al. Fatty Acid Oxidation Is an Adaptive Survival Pathway Induced in Prostate Tumors by HSP90 Inhibition. Mol Cancer Res. 2020 Oct 2;18(10):1500–11.

191. Ren Z, Chen S, Pak S, Guo L. A mechanism of perhexiline's cytotoxicity in hepatic cells involves endoplasmic reticulum stress and p38 signaling pathway. Chem Biol Interact. 2021 Jan 25;334:109353.

192. Bi L, Chiang JYL, Ding WX, Dunn W, Roberts B, Li T. Saturated fatty acids activate ERK signaling to downregulate hepatic sortilin 1 in obese and diabetic mice[S]. J Lipid Res. 2013 Oct 1;54(10):2754–62.

193. Yin X, Dwyer J, Langley SR, Mayr U, Xing Q, Drozdov I, et al. Effects of perhexiline-induced fuel switch on the cardiac proteome and metabolome. J Mol Cell Cardiol. 2013 Feb;55:27–30.

194. Willoughby SR, Stewart S, Holmes AS, Chirkov YY, Horowitz JD. Platelet nitric oxide responsiveness: a novel prognostic marker in acute coronary syndromes. Arterioscler Thromb Vasc Biol. 2005 Dec;25(12):2661–6.

195. Worthley MI, Holmes AS, Willoughby SR, Kucia AM, Heresztyn T, Stewart S, et al. The deleterious effects of hyperglycemia on platelet function in diabetic patients with acute coronary syndromes mediation by superoxide production, resolution with intensive insulin administration. J Am Coll Cardiol. 2007 Jan 23;49(3):304–10.

196. Chirkov YY, Horowitz JD. Impaired tissue responsiveness to organic nitrates and nitric oxide: a new therapeutic frontier? Pharmacol Ther. 2007 Nov;116(2):287–305.

197. Chong CR, Liu S, Imam H, Heresztyn T, Sallustio BC, Chirkov YY, et al. Perhexiline Therapy in Patients with Type 2 Diabetes: Incremental Insulin Resistance despite Potentiation of Nitric Oxide Signaling. Biomedicines. 2022 Sep 23;10(10):2381.

198. Hirafuji M, Machida T, Hamaue N, Minami M. Cardiovascular protective effects of n-3 polyunsaturated fatty acids with special emphasis on docosahexaenoic acid. J Pharmacol Sci. 2003 Aug;92(4):308–16.

199. Kurahara LH, Hiraishi K, Yamamura A, Zhang Y, Abe K, Yahiro E, et al. Eicosapentaenoic acid ameliorates pulmonary hypertension via inhibition of tyrosine kinase Fyn. J Mol Cell Cardiol. 2020 Nov 1;148:50–62.

200. Bonnet S, Michelakis ED, Porter CJ, Andrade-Navarro MA, Thébaud B, Bonnet S, et al. An abnormal mitochondrial-hypoxia inducible factor-1alpha-Kv channel pathway disrupts oxygen sensing and triggers pulmonary arterial hypertension in fawn hooded rats: similarities to human pulmonary arterial hypertension. Circulation. 2006 Jun 6;113(22):2630–41.

201. Kim J whan, Tchernyshyov I, Semenza GL, Dang CV. HIF-1-mediated expression of pyruvate dehydrogenase kinase: a metabolic switch required for cellular adaptation to hypoxia. Cell Metab. 2006 Mar;3(3):177–85.

202. Griffiths K, Grand RJ, Horan I, Certo M, Keeler RC, Mauro C, Tseng C, Grieg I, Morrell NW, Zanda M, Frenneaux MP, Madhani M. Fluorinated Perhexiline Derivative Attenuates Vascular Proliferation in Pulmonary Arterial Hypertension Smooth Muscle Cells. Manuscript Currently Re-Submitted Vasc Pharmacol.